NONLINEAR STRESSES IN THIN SHELLS OF REVOLUTION

by

Wilbur David Birchler

A Dissertation Submitted to the Faculty of the

DEPARTMENT OF CIVIL ENGINEERING AND ENGINEERING MECHANICS

In Partial Fulfillment of the Requirements
For the Degree of

DOCTOR OF PHILOSOPHY
WITH A MAJOR IN CIVIL ENGINEERING

In the Graduate College

THE UNIVERSITY OF ARIZONA

1 9 7 0

THE UNIVERSITY OF ARIZONA

GRADUATE COLLEGE

I hereby recommend that this dissertation prepared under my direction by Wilbur David Birchler

entitled Nonlinear Stresses in Thin Shells of Revolution

be accepted as fulfilling the dissertation requirement of the degree of Doctor of Philosophy

Ralph M Richard — 9 July 1970
Dissertation Director — Date

After inspection of the final copy of the dissertation, the following members of the Final Examination Committee concur in its approval and recommend its acceptance:*

Ralph M Richard	9 July 1970
Allan J Mahrer	10 July 1970
Haaren A. Smithofsky	13 July 1970
R C Neff	15 July 70
D A Da Deppe	15 July 70

*This approval and acceptance is contingent on the candidate's adequate performance and defense of this dissertation at the final oral examination. The inclusion of this sheet bound into the library copy of the dissertation is evidence of satisfactory performance at the final examination.

STATEMENT BY AUTHOR

This dissertation has been submitted in partial fulfillment of requirements for an advanced degree at the University of Arizona and is deposited in the University Library to be made available to borrowers under rules of the Library.

Brief quotations from this dissertation are allowable without special permission, provided that accurate acknowledgment of source is made. Requests for permission for extended quotation from or reproduction of this manuscript in whole or in part may be granted by the copyright holder.

SIGNED: Wilbur D. Birchler

ACKNOWLEDGMENT

The author wishes to express his sincere appreciation to his dissertation adviser, Professor Ralph M. Richard, Ph.D., for his guidance and assistance in the completion of this dissertation.

Appreciation is extended to all the faculty members of the Civil Engineering and Engineering Mechanics Department whose instruction and assistance ultimately made this dissertation possible. In particular, sincere thanks to Professor Quentin Mees for providing the teaching associateships which made the author's graduate work possible.

Also, the author would like to thank his fellow graduate students, Melvin Callabresi and Conrad Huss, for the many rewarding discussions we had about this topic.

The author furthermore wishes to thank his wife, Kathy, for her cooperation and assistance in typing this manuscript and David Yeung for drawing the figures.

TABLE OF CONTENTS

		Page
	LIST OF ILLUSTRATIONS	vii
	LIST OF TABLES	ix
	ABSTRACT	x
1.	INTRODUCTION	1
2.	DEVELOPMENT OF THE SHELL EQUATIONS	5
	Plastic Stress-Strain Relations	6
	Equations of Equilibrium	12
	Strain-Displacement Relations	22
	Stress Resultant-Displacement Relations	25
	Governing Differential Equations	29
3.	SHELL EQUATIONS FOR CONSTANT CURVATURE ELEMENTS	33
	Toroidal Element	33
	Conical Element	38
4.	METHOD OF SOLUTION	43
	Differential Displacement Method	44
	Differential Element Stiffness Matrix	49
	Element Fixed End Forces	55
	Coordinate Transformations	55
	Stiffness Terms	57
	Numerical Methods	57
5.	NUMERICAL RESULTS	61
	Empirical Equation for Uniaxial Stress-Strain Curve	61
	Thick-Walled Cylinders	65
	Thin-Walled Cylinder	66
	Flat Circular Plate	71
	Torispherical Shell	80
6.	SUMMARY AND CONCLUSION	90

TABLE OF CONTENTS--Continued

Page

APPENDIX A: AN EXAMINATION OF THE SINGULAR TERMS 92

Spherical Element 92
Flat Plate Element 99

REFERENCES 101

LIST OF ILLUSTRATIONS

Figure		Page
1.	Shell Geometry and the Differential Shell Element	13
2.	Stress Resultants at the Middle Surface	14
3.	Stress Resultants at State P	18
4.	Stress Resultants at State P + dP	19
5.	Stress Rate Resultants at State dP	21
6.	Displacement Sign Convention - Positive Values	24
7.	Toroidal Element and Associated Geometry	34
8.	Conical Element and Associated Geometry	39
9.	Positive Element End Forces and Displacements - Reference Coordinate System	46
10.	Positive Element End Forces and Displacements - Local Coordinate System	50
11.	Nondimensional Stress-Strain Relationships	63
12.	Nonlinear Parameter n	64
13.	Thick-Walled Cylinder - Hoop Strains on Outside Surface	67
14.	Thick-Walled Cylinder - Radial Stress Distributions	68
15.	Thick-Walled Cylinder - Hoop Stress Distributions	69
16.	Thin-Walled Cylinder	70
17.	Flat Plate - Normal Displacements	74
18.	Flat Plate - Radial Moment Distributions	75
19.	Flat Plate - Hoop Moment Distributions	76
20.	Flat Plate - Variables Changing with Pressure	77

LIST OF ILLUSTRATIONS--Continued

Figure		Page
21.	Flat Plate - Stress Distributions at 10.0 Inches	78
22.	Flat Plate - Stress Distributions at 11.5 Inches	79
23.	Torispherical Shell - Geometry and Elements	81
24.	Torispherical Shell - Displacements at Apex	82
25.	Torispherical Shell - Normal Displacements	84
26.	Torispherical Shell - Meridional Moment Distributions	85
27.	Torispherical Shell - Hoop Force Distributions	86
28.	Torispherical Shell - Stress Paths	87
29.	Torispherical Shell - Stress and Strain Distributions at $\phi = 58.955°$	88
30.	Torispherical Shell - Stress and Strain Distributions at $\phi = 25.186°$	89

LIST OF TABLES

Table Page

1. Comparison of Results 72

ABSTRACT

A numerical procedure is presented for obtaining the nonlinear (material) stresses, strains, internal forces, and displacements of arbitrarily-shaped shells of revolution by integrating the derived differential equations. These equations are developed from the differential shell element at two states of loading and from the differential stress-strain relations. The major assumptions are thinness, small strains and displacements, the Kirchhoff hypothesis, strain-hardening materials, and axisymmetric loading conditions.

CHAPTER I

INTRODUCTION

The stress analysis of thin shells of revolution loaded beyond the elastic limit has received considerable attention in recent years. Much of the work pertains to limit analysis methods (Hodge 1963, Ellyin and Sherbourne 1965, Olszak and Sawczuk 1967, Olszak, Mroz, and Perzyna 1963). Other methods of analysis which are employed are the method of successive elastic solutions (Olszak and Sawczuk 1967, Olszak, Mroz, and Perzyna 1963, Spera 1963, Mendelson and Manson 1959), a differential method (Marcal and Turner 1963), and a finite element method (Khojesteh-Bakht and Popov 1970).

The purpose of the limit analysis method is to predict the collapse load of a shell structure caused by the formation of plastic hinge lines and mechanisms. Analytical yield surfaces have been developed for elastic-perfectly plastic materials and the Tresca yield condition. The yield surfaces for strain-hardening material and the von Mises yield condition are nonlinear (Olszak and Sawczuk 1967). Two restrictive assumptions exist in the reported limit analysis method. First, the hoop moment is neglected in the development of the yield surfaces, and second, the meridional and hoop moments are neglected in the equilibrium equations (Drucker and Shield 1959, Khojesteh-Bakht and Popov 1970).

Closely related to the limit analysis method is the complete analysis method in which the internal force and moment distributions and displacements are determined in addition to the collapse load. Exact solutions have been obtained for special cases of conical shells using the exact yield surfaces derived from the Tresca yield condition. Solutions for other shell shapes have been obtained by using approximate yield surfaces (Thorn and Lee 1964, Flugge and Nakamura 1965).

The method of successive elastic solutions initiated by Ilyushin is used by several investigators (Olszak and Sawczuk 1967, Olszak, Mroz, and Perzyna 1963, Spera 1963, Mendelson and Manson 1959) to obtain the stresses, strains, and displacements in thin shells of revolution. The first solution is an elastic one from which the stresses, strains, internal forces and moments, and displacements can be determined. Plastic strains are estimated from the calculated strains using the deformation theory of plasticity. Fictitious loads, which are assumed to represent the plastic effects, are calculated from the plastic strains and are applied to the shells in the next elastic solution through the equilibrium equations. The procedure is repeated until the plastic components of strain have converged sufficiently. The deformation theory of plasticity is based in part on the assumption that at every point in a structure the loading is proportional (Lin 1968) which is not always the case in nonlinear shell structures.

Marcal and Turner (1963) present a differential method for analyzing shells of revolution loaded symmetrically with respect to

the axis of revolution. The shell material is taken to be elastic-perfectly plastic and the Tresca yield condition is employed. The equilibrium equations and the strain-displacement equations are differentiated implicitly to obtain the governing differential equations. These equations are rewritten as a set of first order differential equations and are numerically integrated by a Runge integrating procedure. A searching procedure is used to find the initial starting values.

Linear stress analysis of shells of revolution have been obtained by the classical finite element methods (Grafton and Strome 1963, Jones and Strome 1966). Khojesteh-Bakht and Popov (1970) have extended the linear finite element method for analyzing shells of revolution into the nonlinear range by what they call the tangent stiffness method. In this method the master stiffness matrix is written as a function of the loading and is always changing. In the finite element method, the displacement functions of the element are assumed. In the nonlinear example problem presented by Khojesteh-Bakht and Popov, the shell material is assumed to be elastic-perfectly plastic, and the von Mises yield condition is used.

Only limited research has been done in thin shell analysis in which a strain-hardening material and an incremental theory of plasticity is employed. The purpose of this dissertation is to develop a method for analyzing thin shells of revolution using an incremental theory of plasticity for strain-hardening materials. The quantities to be calculated are the stresses, strains, internal forces and

moments, and displacements of the shell. The shell is to be thin (say $r/t > 10$), the loading condition is to be symmetric with respect to the axis of revolution, the material is to be initially isotropic and homogeneous, and the analysis is to be limited to small strains and displacements. Creep and temperature strains and time effects are not included. Any other assumptions or restrictions imposed are described when used.

CHAPTER 2

DEVELOPMENT OF THE SHELL EQUATIONS

A close similarity exists between the development of the differential equations for thin linearly elastic shells and the differential equations for thin strain-hardening shells. Stress-strain relations, equilibrium conditions, and strain-displacement relations are needed to derive the governing differential equations for shells modeled by both types of materials.

The literature (Olszak and Sawczuk 1967, Lin 1968) shows that many of the relations derived for thin elastic shells are valid for the analysis of thin nonlinear (material) shells. Two examples of these relations are the equilibrium conditions and the strain-displacement relations. The derivations of the equilibrium conditions and the strain-displacement relations are presented in texts on thin shells (Timoshenko and Woinowsky-Krieger 1959, Flugge 1966, Kraus 1967) and are used without being rederived. Justification for neglecting the effects of the shearing strain on deformation and the dropping of the z/r term from the stress resultant and strain-displacement relations are discussed in the literature (Olszak and Sawczuk 1967, Lin 1968) and these discussions are assumed to be valid for this study. The concepts of strain-hardening materials, expanding yield surfaces, plastic stress and strain increments, no plastic dilatation, deviatoric stresses and strains, hydrostatic stresses, effective stress and strain

and stress and strain invariants are presented in texts on plasticity (Lin 1968, Hill 1950, Mendelson 1968) and are used as required.

Plastic Stress-Strain Relations

In the analysis of thin shells of revolution with axisymmetric loading conditions, two components of stress and of strain play a significant role in the solution. The stress components are σ_ϕ and σ_θ, and the strain components are ε_ϕ and ε_θ. The subscripts ϕ and θ refer to the meridional and hoop directions, respectively. The other components of stress and strain are either zero or small and are set to zero to facilitate the development of the governing equations.

The stresses, σ_ϕ and σ_θ, and the strains, ε_ϕ and ε_θ, for a linearly elastic material are related by the modulus of elasticity, E, and Poisson's ratio, ν.

$$\varepsilon_\phi = \frac{1}{E}\{\sigma_\phi - \nu\sigma_\theta\} \qquad \varepsilon_\theta = \frac{1}{E}\{-\nu\sigma_\phi - \sigma_\theta\} \tag{2.1}$$

$$\sigma_\phi = \frac{E}{(1-\nu^2)}\{\varepsilon_\phi + \nu\varepsilon_\theta\} \qquad \sigma_\theta = \frac{E}{(1-\nu^2)}\{\nu\varepsilon_\phi + \varepsilon_\theta\} \tag{2.2}$$

Equations (2.1) and (2.2) are used in the derivation of the governing differential equations for thin linearly elastic shells.

Callabresi (1970) presented a set of three dimensional plastic stress-strain relations. These relations were based on the incremental theory of plasticity for strain-hardening materials. The plastic stress-strain relations are reduced to a biaxial state of stress and are

$$\frac{d\varepsilon_\phi}{dP} = \left[\frac{1}{E} + \frac{(2\sigma_\phi - \sigma_\theta)^2}{4H'\sigma_e^2}\right]\frac{d\sigma_\phi}{dP} + \left[-\frac{\nu}{E} + \frac{(2\sigma_\phi - \sigma_\theta)(2\sigma_\theta - \sigma_\phi)}{4H'\sigma_e^2}\right]\frac{d\sigma_\theta}{dP} \tag{2.3}$$

$$\frac{d\varepsilon_\theta}{dP} = \left[-\frac{\nu}{E} + \frac{(2\sigma_\phi - \sigma_\theta)(2\sigma_\theta - \sigma_\phi)}{4H'\sigma_e^2}\right]\frac{d\sigma_\phi}{dP} + \left[\frac{1}{E} + \frac{(2\sigma_\theta - \sigma_\phi)^2}{4H'\sigma_e^2}\right]\frac{d\sigma_\theta}{dP} \tag{2.4}$$

$$\frac{d\sigma_\phi}{dP} = \frac{1}{D}\left[\frac{1}{E} + \frac{(2\sigma_\theta - \sigma_\phi)^2}{4H'\sigma_e^2}\right]\frac{d\varepsilon_\phi}{dP} - \frac{1}{D}\left[\frac{-\nu}{E} + \frac{(2\sigma_\phi - \sigma_\theta)(2\sigma_\theta - \sigma_\phi)}{4H'\sigma_e^2}\right]\frac{d\varepsilon_\theta}{dP} \tag{2.5}$$

$$\frac{d\sigma_\theta}{dP} = \frac{-1}{D}\left[\frac{-\nu}{E} + \frac{(2\sigma_\phi - \sigma_\theta)(2\sigma_\theta - \sigma_\phi)}{4H'\sigma_e^2}\right]\frac{d\varepsilon_\phi}{dP} + \frac{1}{D}\left[\frac{1}{E} + \frac{(2\sigma_\phi - \sigma_\theta)^2}{4H'\sigma_e^2}\right]\frac{d\varepsilon_\theta}{dP} \tag{2.6}$$

where

$$D = \left[\frac{1}{E} + \frac{(2\sigma_\phi - \sigma_\theta)^2}{4H'\sigma_e^2}\right]\left[\frac{1}{E} + \frac{(2\sigma_\theta - \sigma_\phi)^2}{4H'\sigma_e^2}\right] - \left[\frac{-\nu}{E} + \frac{(2\sigma_\phi - \sigma_\theta)(2\sigma_\theta - \sigma_\phi)}{4H'\sigma_e^2}\right]^2$$

Equations (2.1) and (2.2) are algebraic equations. Equations (2.3) through (2.6) are differential equations and are referred to as the differential stress-strain relations or plastic stress-strain relations.

The terms $d\sigma_\phi/dP$ and $d\sigma_\theta/dP$ in Equations (2.3) through (2.6) are referred to as stress rates, and the terms $d\varepsilon_\phi/dP$ and $d\varepsilon_\theta/dP$ are called strain rates. The independent variable, P, in the stress rate and strain rate terms is the applied loading. Effective stress is defined as

$$\sigma_e = \{\sigma_\phi^2 - \sigma_\phi\sigma_\theta + \sigma_\theta^2\}^{1/2} \tag{2.7}$$

where subscript e denotes effective for this study. The effective stress squared is equal to three times the second invariant of the deviatoric stress tensor, J_2.

$$\sigma_e^2 = 3J_2 \tag{2.8}$$

H' is the slope of an effective stress-effective plastic strain diagram. The effective plastic strain is defined as

$$\varepsilon_e^p = \frac{2}{\sqrt{3}}\{\varepsilon_\phi^p\varepsilon_\phi^p + \varepsilon_\phi^p\varepsilon_\theta^p + \varepsilon_\theta^p\varepsilon_\theta^p\}^{1/2} \tag{2.9}$$

where the superscript p denotes the plastic components of strain. Empirical equations for the effective stress-effective strain diagram are discussed in detail in Chapter 5.

The assumptions used to derive Equations (2.3) and (2.4) are discussed in articles on plasticity (Hill 1950, Lin 1968, Mendelson 1968, Callabresi 1970) and are presented below to explain the

development of the plastic stress-strain relations. The Prandtl-Reuss flow rule states that the plastic strain increments ($d\varepsilon_\phi^p/dP$ and $d\varepsilon_\theta^p/dP$) are proportional to their deviatoric stresses (S_ϕ and S_θ).

$$\frac{1}{S_\phi}\frac{d\varepsilon_\phi^p}{dP} = \frac{1}{S_\theta}\frac{d\varepsilon_\theta^p}{dP} = \frac{dK}{dP} \tag{2.10}$$

The derivative dK/dP is an instantaneous positive constant of proportionality which may vary throughout the loading process. The deviatoric stresses are

$$S_\phi = \frac{2\sigma_\phi - \sigma_\theta}{3} \qquad S_\theta = \frac{2\sigma_\theta - \sigma_\phi}{3} \tag{2.11}$$

The condition of no plastic dilatation is satisfied by Equation (2.10). Another assumption is that the effective stress and effective plastic strain can be related by a single valued function of the form

$$\sigma_e = H(\varepsilon_e^p) \tag{2.12}$$

The function H has the same shape in tension as compression.

The constant of proportionality, dK/dP, is determined by considering a uniaxial state of stress. The following relations are satisfied when σ_θ is set to zero.

$$\sigma_e = \sigma_\phi = \frac{3}{2} S_\phi$$

$$\varepsilon_e^p = \varepsilon_\phi^p \qquad \frac{d\varepsilon_e^p}{dP} = \frac{d\varepsilon_\phi^p}{dP}$$

and $$\frac{1}{S_\phi} \frac{d\varepsilon_\phi^p}{dP} = \frac{3}{2\sigma_\phi} \frac{d\varepsilon_\phi^p}{dP} = \frac{3}{2\sigma_e} \frac{d\varepsilon_e^p}{dP} = \frac{dK}{dP}$$

or $$\frac{dK}{dP} = \frac{3}{2\sigma_e} \frac{d\varepsilon_e^p}{d\sigma_e} \frac{d\sigma_e}{dP} = \frac{3}{2H'\sigma_e} \frac{d\sigma_e}{dP} \tag{2.13}$$

where $$H' = \frac{d\sigma_e}{d\varepsilon_e^p} \tag{2.14}$$

The quantity H' is the slope of a uniaxial stress-plastic strain diagram, and $d\sigma_e/dP$ is determined by differentiating Equation (2.7) with respect to the independent variable P.

$$\frac{d\sigma_e}{dP} = \frac{1}{2\sigma_e} \{ (2\sigma_\phi - \sigma_\theta) \frac{d\sigma_\phi}{dP} + (2\sigma_\theta - \sigma_\phi) \frac{d\sigma_\theta}{dP} \} \tag{2.15}$$

The total strain increments are the sums of the elastic and plastic parts. The elastic parts of the strains are obtained by differentiating Equation (2.1) with respect to the independent variable P.

$$\frac{d\varepsilon_\phi^e}{dP} = \frac{1}{E}\left\{\frac{d\sigma_\phi}{dP} - \frac{\nu d\sigma_\theta}{dP}\right\} \qquad \frac{d\varepsilon_\theta^e}{dP} = \frac{1}{E}\left\{-\frac{\nu d\sigma_\phi}{dP} + \frac{d\sigma_\theta}{dP}\right\} \tag{2.16}$$

The superscript e denotes the elastic components of strain. The plastic parts of the strains are given by Equation (2.10) and may be written as

$$\frac{d\varepsilon_\phi^p}{dP} = S_\phi \frac{dK}{dP} \qquad \frac{d\varepsilon_\theta^p}{dP} = S_\theta \frac{dK}{dP} \tag{2.17}$$

By combining the elastic and plastic parts of the strain increments and making the required substitutions for S_ϕ, S_θ, dK/dP, and $d\sigma_e/dP$, the results given by Equations (2.3) and (2.4) are obtained.

Some additional comments need to be made about the plastic stress-strain relations. The original material is assumed to be free of all residual stresses and strains. The size of plastic strains are assumed to be of the same order of magnitude as the elastic strains. If σ_y, the yield stress in uniaxial tension, is substituted for σ_e in Equation (2.8), the result is

$$J_2 = \sigma_y^2/3$$

which is the von Mises yield condition. Therefore, the initial yield surface is the von Mises ellipse. Since σ_e can be greater than σ_y for strain-hardening materials, the subsequent yield surfaces are the same

shape as the initial yield surface but are larger. This is the concept of expanding yield surfaces. Loading and unloading depends upon whether σ_e increases or decreases during the loading process. If σ_e decreases, unloading occurs, dK/dP is equal to zero, and the unloading is elastic. The Bauschinger effect and load reversals beyond the elastic range are not included in these plastic stress-strain relations. The direction of the incremental plastic strain, $d\varepsilon_e^p/dP$, is normal to the yield surface and depends on the existing stresses, but not on the stress increments.

Equations of Equilibrium

A differential element is defined and used in the derivation of the equations of equilibrium for thin shells. The element is cut from a shell by two adjacent meridional planes and two sections perpendicular to the meridians. The geometry of the shell and the element are shown in Figure 1. Timoshenko and Wolnowsky-Krieger's (1959) sign conventions are used throughout this dissertation.

The stresses acting on the sides of the element can be reduced to resultant forces and resultant moments acting at the middle surface of the element shown in Figure 2. The stress resultants are defined as

$$N_\phi \equiv \int_{-h/2}^{h/2} \sigma_\phi(z)dz \qquad N_\theta \equiv \int_{-h/2}^{h/2} \sigma_\theta(z)dz$$

$$M_\phi \equiv \int_{-h/2}^{h/2} \sigma_\phi(z)zdz \qquad M_\theta \equiv \int_{-h/2}^{h/2} \sigma_\theta(z)zdz$$

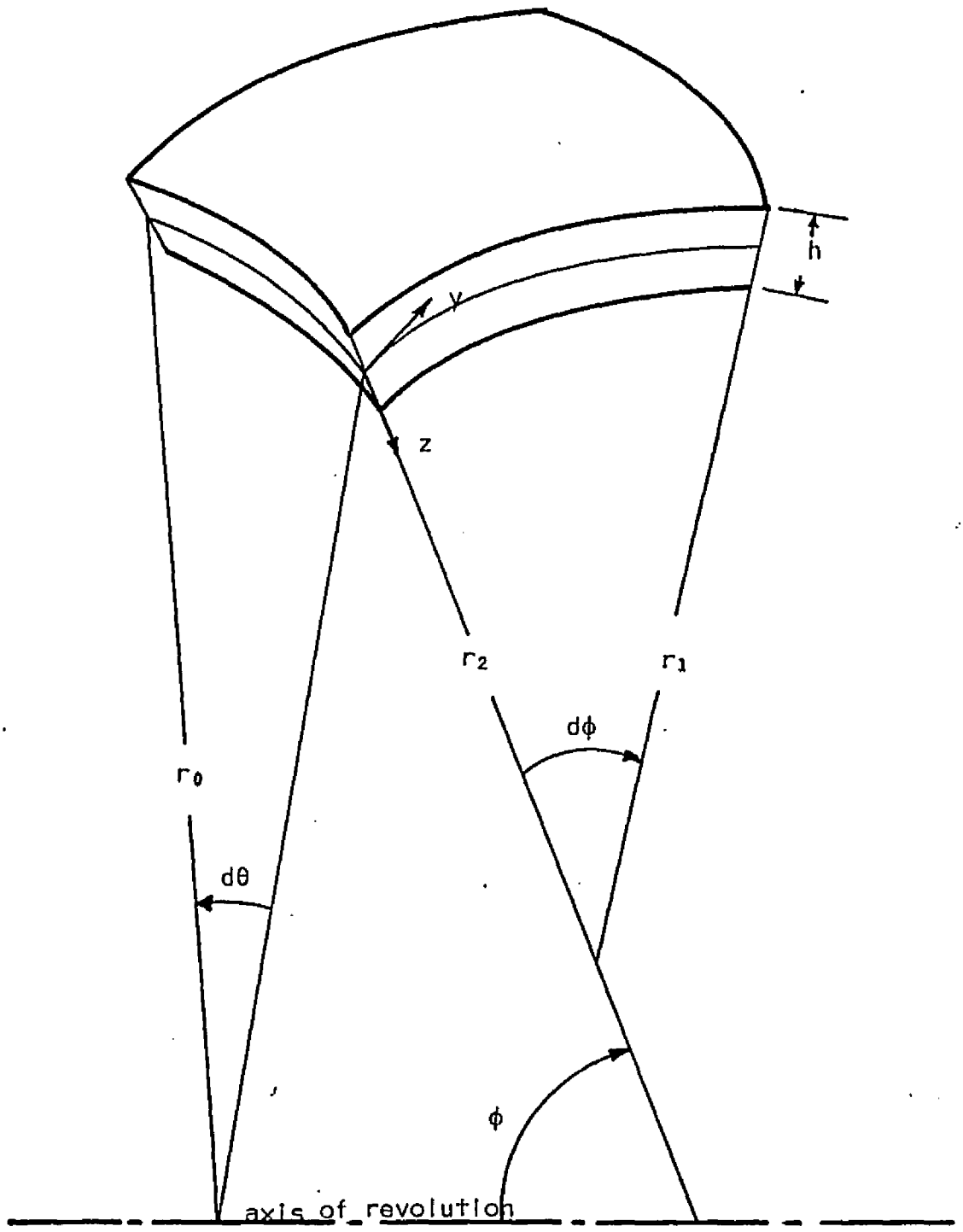

Figure 1. Shell Geometry and the Differential Shell Element

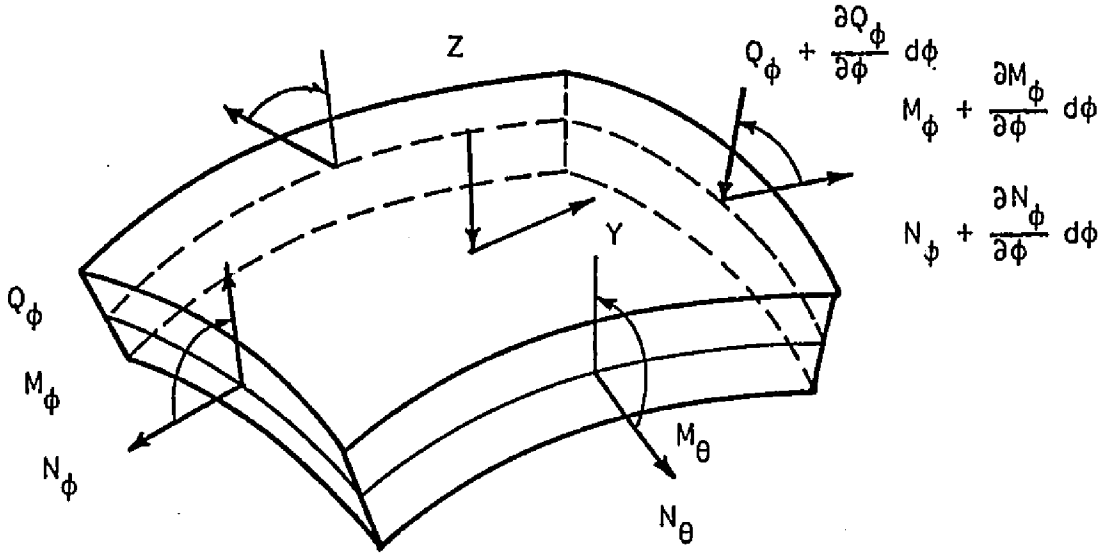

axis of revolution

Figure 2. Stress Resultants at the Middle Surface

$$Q_\phi \equiv \int_{-h/2}^{h/2} \tau_{\phi z}(z)dz \tag{2.18}$$

The force resultants have the dimensions of force per unit length, and the moment resultants have dimensions of force times length per unit length. The z/r terms are not included in the above definitions of the stress resultants. The thickness of the shell is denoted by h. Y and Z are the external pressures acting on the middle surface and are positive in the directions of the positive y and z axes.

The equations of equilibrium are presented in texts on thin shells (Timoshenko and Woinowsky-Krieger 1959, Flugge 1966, Kraus 1967) and are

$$\frac{d(N_\phi r_0)}{d\phi} - N_\phi r_1 \cos\phi - r_0 Q_\phi + r_0 r_1 Y = 0$$

$$N_\phi r_0 + N_\theta r_1 \sin\phi + \frac{d(Q_\phi r_0)}{d\phi} + r_0 r_1 Z = 0$$

$$\frac{d(M_\phi r_0)}{d\phi} - M_\theta r_1 \cos\phi - r_0 r_1 Q_\phi = 0 \tag{2.19}$$

The above equations are independent of material properties, and therefore, are valid for both linear and strain-hardening materials.

However, for strain-hardening materials only rate relationships exist between the stresses and strains, and therefore, the equations of equilibrium must be derived in terms of stress rate resultants. To accomplish this derivation, the stress resultants are considered at two loading states, P and P + dP. The stress resultants at state P + dP are increased by an amount $(\partial F_i/\partial P)dP$ over the corresponding values at state P. The F_i's are defined as

$$F_1 = N_\phi \qquad F_2 = N_\phi + \frac{\partial N_\phi}{\partial \phi} d\phi$$

$$F_3 = Q_\phi \qquad F_4 = Q_\phi + \frac{\partial Q_\phi}{\partial \phi} d\phi$$

$$F_5 = M_\phi \qquad F_6 = M_\phi + \frac{\partial M_\phi}{\partial \phi} d\phi$$

$$F_7 = N_\theta \qquad F_8 = M_\theta \tag{2.20}$$

Figures 3 and 4 show the element and the stress resultants at states P and P + dP, respectively. The expansions of the terms $(\partial F_i/\partial P)dP$ are

$$\frac{\partial F_1}{\partial P} dP = \frac{\partial N_\phi}{\partial P} dP \equiv \dot{N}_\phi dP$$

$$\frac{\partial F_2}{\partial P} dP = \frac{\partial N_\phi}{\partial P} dP + \frac{\partial^2 N_\phi}{\partial P \partial \phi} d\phi dP \equiv \dot{N}_\phi dP + \frac{d\dot{N}_\phi}{d\phi} d\phi dP$$

$$\frac{\partial F_3}{\partial P}\,dP = \frac{\partial Q_\phi}{\partial P}\,dP \equiv \dot{Q}_\phi\,dP$$

$$\frac{\partial F_4}{\partial P}\,dP = \frac{\partial Q_\phi}{\partial P}\,dP + \frac{\partial^2 Q_\phi}{\partial P \partial \phi}\,d\phi dP \equiv \dot{Q}_\phi\,dP + \frac{d\dot{Q}_\phi}{d\phi}\,d\phi dP$$

$$\frac{\partial F_5}{\partial P}\,dP = \frac{\partial M_\phi}{\partial P}\,dP \equiv \dot{M}_\phi\,dP$$

$$\frac{\partial F_6}{\partial P}\,dP = \frac{\partial M_\phi}{\partial P}\,dP + \frac{\partial^2 M_\phi}{\partial P \partial \phi}\,d\phi dP \equiv \dot{M}_\phi\,dP + \frac{d\dot{M}_\phi}{d\phi}\,d\phi dP$$

$$\frac{\partial F_7}{\partial P}\,dP = \frac{\partial N_\theta}{\partial P}\,dP \equiv \dot{N}_\theta\,dP$$

$$\frac{\partial F_8}{\partial P}\,dP = \frac{\partial M_\theta}{\partial P}\,dP \equiv \dot{M}_\theta\,dP$$

$$\frac{\partial Y}{\partial P}\,dP \equiv \dot{Y}\,dP$$

$$\frac{\partial Z}{\partial P}\,dP \equiv \dot{Z}\,dP$$

$$\frac{\partial (d\phi)}{\partial P}\,dP \equiv 0$$

(2.21)

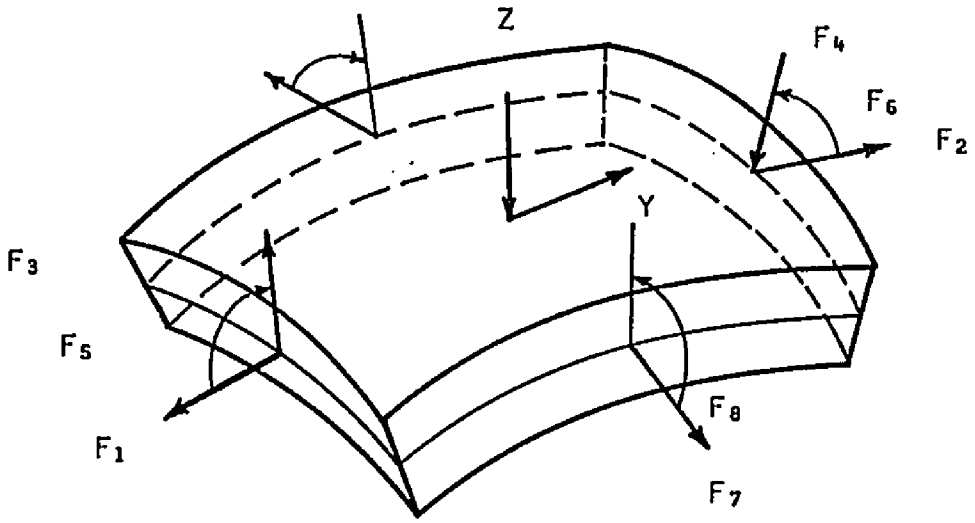

axis of revolution

Figure 3. Stress Resultants at State P

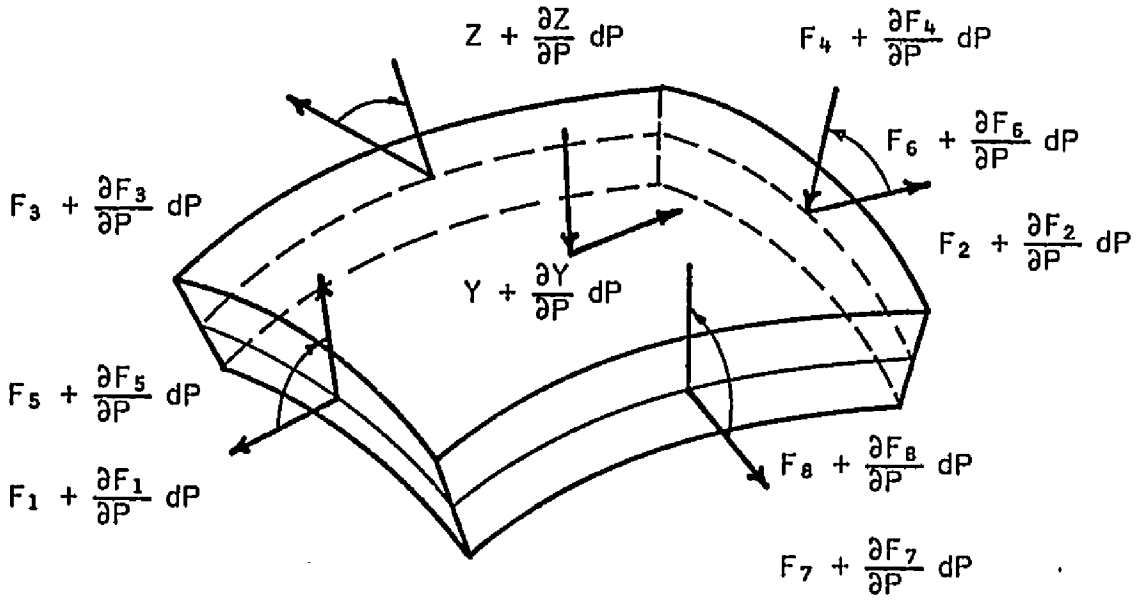

Figure 4. Stress Resultants at State P + dP

The stress resultants are assumed to be continuous functions of ϕ and P and to have continuous derivatives of ϕ and P which implies that the order of differentiation is immaterial. Also, the assumption is made that the shape of the shell does not change significantly with respect to the loading variable, P (small deflection theory).

The state dP is obtained by subtracting state P from state P + dP and dividing the difference by dP. State dP is shown in Figure 5. The only difference between state P and state dP is that the total stress resultants of state P are replaced by the stress rate resultants at state dP. Therefore, the equations of equilibrium for the state dP can be derived by replacing the total stress resultants in Equation (2.19) by the stress rate resultants.

$$\frac{d(\dot{N}_\phi r_0)}{d\phi} - \dot{N}_\phi r_1 \cos\phi - r_0\dot{Q}_\phi + r_0 r_1 \dot{Y} = 0$$

$$\dot{N}_\phi r_0 + \dot{N}_\theta r_1 \sin\phi + \frac{d(\dot{Q}_\phi r_0)}{d\phi} + r_0 r_1 \dot{Z} = 0$$

$$\frac{d(\dot{M}_\phi r_0)}{d\phi} - \dot{M}_\theta r_0 \cos\phi - r_0 r_1 \dot{Q}_\phi = 0 \qquad (2.22)$$

The above equations can also be obtained by taking the derivatives of Equation (2.19) with respect to the variable P. The stress rate resultants are defined as

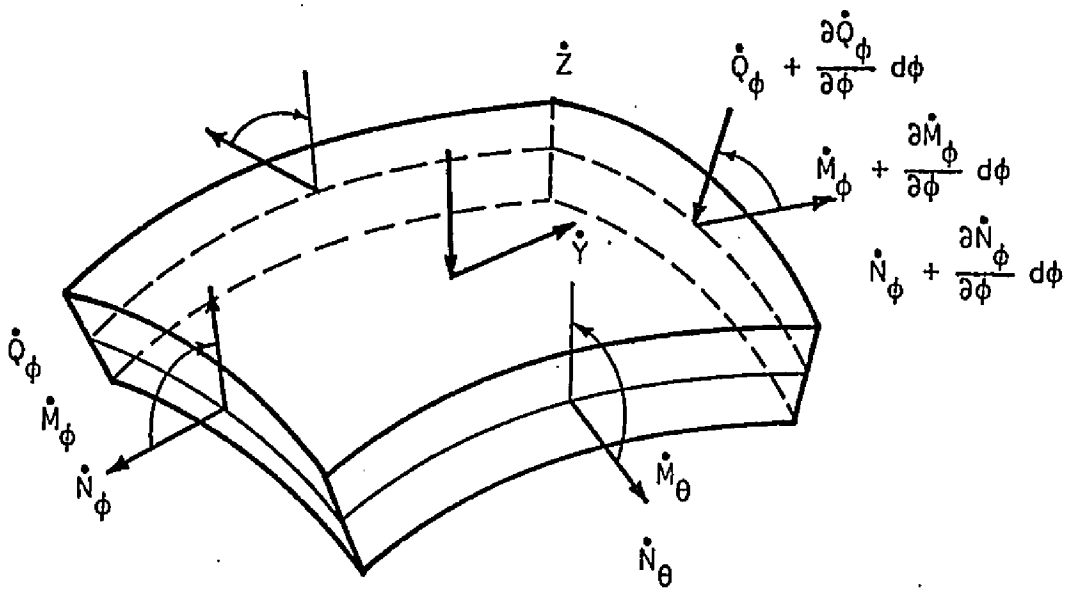

Figure 5. Stress Rate Resultants at State dP

$$\dot{N}_\phi \equiv \int_{-h/2}^{h/2} \dot{\sigma}_\phi(z)dz \qquad \dot{N}_\theta \equiv \int_{-h/2}^{h/2} \dot{\sigma}_\theta(z)dz$$

$$\dot{M}_\phi \equiv \int_{-h/2}^{h/2} \dot{\sigma}_\phi(z)zdz \qquad \dot{M}_\theta \equiv \int_{-h/2}^{h/2} \dot{\sigma}_\theta(z)zdz$$

$$\dot{Q}_\phi \equiv \int_{-h/2}^{h/2} \dot{\tau}_{\phi z}(z)dz \tag{2.23}$$

The rate force resultants have the dimensions of force per unit length per unit force, and the rate moment resultants have the dimensions of force times length per unit length per unit force.

Strain-Displacement Relations

The strain-displacement relations for thin shells are derived using the Kirchhoff assumption. It states that line elements originally normal to the middle surface remain straight and normal to the middle surface after the shell is deformed. The strain at any point in the wall thickness can be related to the strains of the middle surface and the changes in curvature using the Kirchhoff assumption. The strains at any point z are given by Equation (2.24).

$$\varepsilon_\phi = \varepsilon_{\phi_0} - z\chi_\phi \qquad \varepsilon_\theta = \varepsilon_{\theta_0} - z\chi_\theta \tag{2.24}$$

The middle surface strains are denoted by ε_{ϕ_0} and ε_{θ_0}, and the changes in curvature are denoted by χ_ϕ and χ_θ.

The strains written in terms of the displacements (Timoshenko and Woinowsky-Krieger 1959, Flugge 1966, Kraus 1967) are

$$\varepsilon_\phi = \frac{1}{r_1}\frac{dv}{d\phi} - \frac{w}{r_1} - \frac{z}{r_1}\frac{d\beta}{d\phi}$$

$$\varepsilon_\theta = \frac{v\cot\phi}{r_2} - \frac{w}{r_2} - \frac{z\beta\cot\phi}{r_2} \tag{2.25}$$

where

$$\beta = \frac{v}{r_1} + \frac{1}{r_1}\frac{dw}{d\phi} \tag{2.26}$$

The tangential displacement, v, and the normal displacement, w, are measured at the middle surface. Displacements are positive in the directions of the positive y and z axes. The rotation of a tangent to the middle surface is denoted by β. Figure 6 shows the positive displacements of the shell. Equations (2.25) and (2.26) are the total strains written in terms of the total displacements and their derivatives.

The relationships between rates of strains and rates of displacements are needed for strain-hardening material idealization. These relationships can be derived by considering two states of loading, P and P + dP, and proceeding in the same manner as in the development of the equations of equilibrium. The relationships can also be obtained by differentiating Equations (2.25) and (2.26) with respect to the variable P. The results are

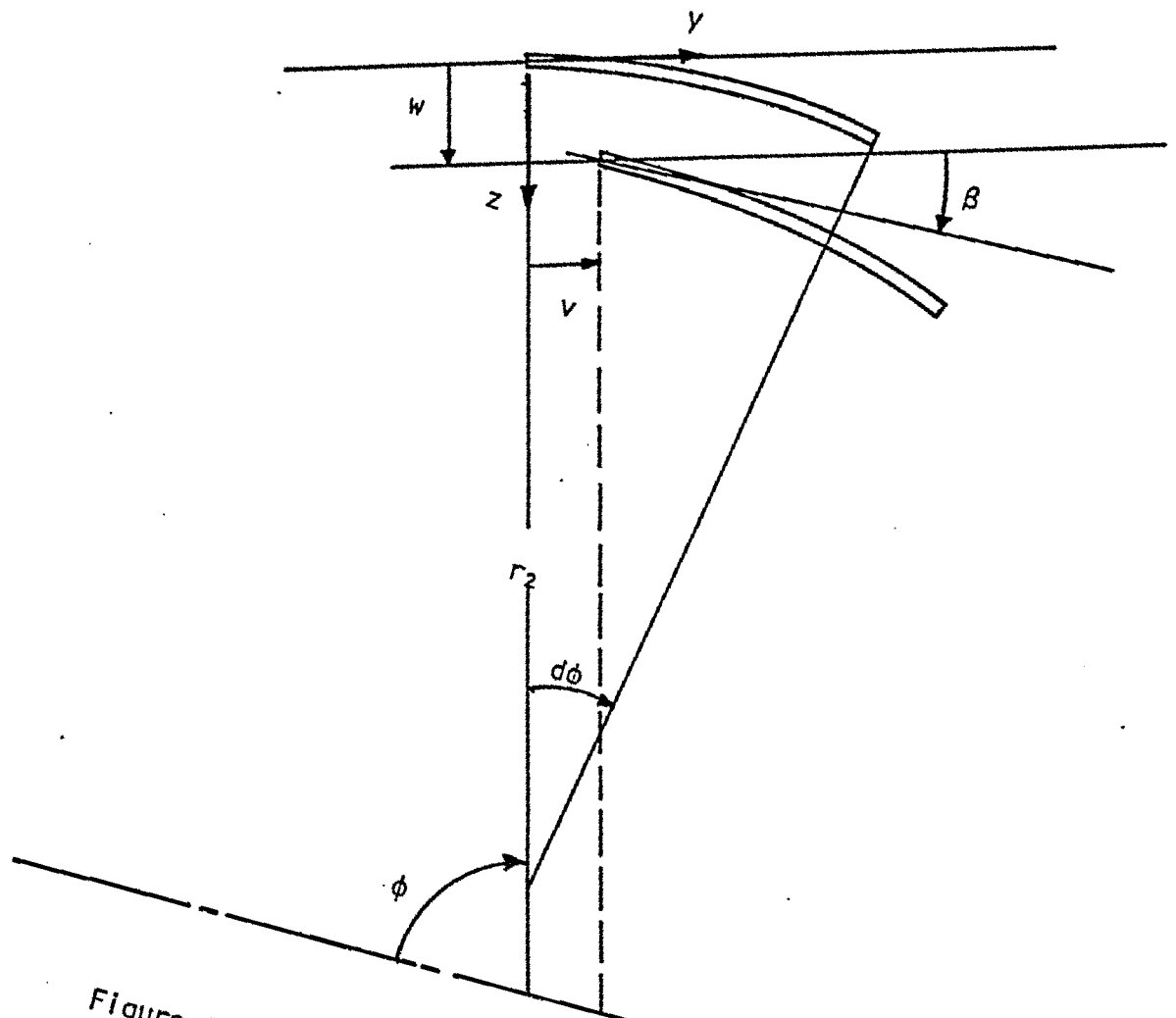

Figure 6. Displacement Sign Convention - Positive Values

$$\dot{\varepsilon}_\phi = \frac{1}{r_1}\frac{d\dot{v}}{d\phi} - \frac{\dot{w}}{r_1} - \frac{z}{r_1}\frac{d\dot{\beta}}{d\phi}$$

$$\dot{\varepsilon}_\theta = \frac{\dot{v}\cot\phi}{r_2} - \frac{\dot{w}}{r_2} - \frac{z\,\dot{\beta}\cot\phi}{r_2} \qquad (2.27)$$

where

$$\dot{\beta} = \frac{\dot{v}}{r_1} + \frac{1}{r_1}\frac{d\dot{w}}{d\phi} \qquad (2.28)$$

Stress Resultant-Displacement Relations

The stress and strain rates change throughout the thickness of the shell. How the stress rates vary depends on the material properties and the existing stresses, while the strain rates are assumed to vary in a linear manner. The stress rate resultants are determined by integrating the stress rates through the thickness. For convenience, the stress and strain rate relationships are written as

$$\dot{\sigma}_\phi(z) = k_{11}(z)\dot{\varepsilon}_\phi(z) + k_{12}(z)\dot{\varepsilon}_\theta(z)$$

$$\dot{\sigma}_\theta(z) = k_{21}(z)\dot{\varepsilon}_\phi(z) + k_{22}(z)\dot{\varepsilon}_\theta(z) \qquad (2.29)$$

where the k's are also functions of the material properties and the existing stresses. The k's are referred to as material stiffness terms.

The stress rate resultant $\dot{N}_\phi$ is defined as

$$\dot{N}_\phi \equiv \int_{-h/2}^{h/2} \dot{\sigma}_\phi(z)dz \qquad (2.30)$$

Substituting Equation (2.29) into Equation (2.30) yields

$$\dot{N}_\phi = \int_{-h/2}^{h/2} \{k_{11}(z)\dot{\varepsilon}_\phi + k_{12}(z)\dot{\varepsilon}_\theta\}\, dz \tag{2.31}$$

Replacing the values of the strain rates by Equation (2.27) gives the following result.

$$\dot{N}_\phi = \int_{-h/2}^{h/2} \{k_{11}(z)\,\frac{1}{r_1}\frac{d\dot{v}}{d\phi} - k_{11}\,\frac{\dot{w}}{r_1} - k_{11}(z)z\,\frac{1}{r_1}\frac{d\dot{\beta}}{d\phi} + k_{12}(z)\,\frac{\dot{v}\cot\phi}{r_2} - k_{12}(z)\,\frac{\dot{w}}{r_2} - k_{12}(z)z\,\frac{\dot{\beta}\cot\phi}{r_2}\}\, dz \tag{2.32}$$

The integrals in Equation (2.32) are defined as

$$\int_{-h/2}^{h/2} k_{11}(z)dz \equiv K_{11}$$

$$\int_{-h/2}^{h/2} k_{12}(z)dz \equiv K_{12}$$

$$\int_{-h/2}^{h/2} k_{11}(z)zdz \equiv B_{11}$$

$$\int_{-h/2}^{h/2} k_{12}(z)zdz \equiv B_{12} \tag{2.33}$$

By using the above definitions, $\dot{N}_\phi$ may be written as

$$\dot{N}_\phi = \frac{K_{11}}{r_1}\frac{d\dot{v}}{d\phi} - \frac{K_{11}\dot{w}}{r_1} - \frac{B_{11}}{r_1}\frac{d\dot{\beta}}{d\phi} + \frac{K_{12}\dot{v}\cot\phi}{r_2} - \frac{K_{12}\dot{w}}{r_2} - \frac{B_{12}\dot{\beta}\cot\phi}{r_2} \tag{2.34}$$

The stress rate resultants $\dot{N}_\theta$, $\dot{M}_\phi$, and $\dot{M}_\theta$ are determined in the same manner as $\dot{N}_\phi$, and the results are presented below.

$$\dot{N}_\theta = \frac{K_{21}}{r_1}\frac{d\dot{v}}{d\phi} - \frac{K_{21}\dot{w}}{r_1} - \frac{B_{21}}{r_1}\frac{d\dot{\beta}}{d\phi} + \frac{K_{22}\dot{v}\cot\phi}{r_2} - \frac{K_{22}\dot{w}}{r_2} - \frac{B_{22}\dot{\beta}\cot\phi}{r_2} \tag{2.35}$$

$$\dot{M}_\phi = \frac{B_{11}}{r_1}\frac{d\dot{v}}{d\phi} - \frac{B_{11}\dot{w}}{r_1} - \frac{D_{11}}{r_1}\frac{d\dot{\beta}}{d\phi} + \frac{B_{12}\dot{v}\cot\phi}{r_2} - \frac{B_{12}\dot{w}}{r_2} - \frac{D_{12}\dot{\beta}\cot\phi}{r_2} \tag{2.36}$$

$$\dot{M}_\theta = \frac{B_{21}}{r_1}\frac{d\dot{v}}{d\phi} - \frac{B_{21}\dot{w}}{r_1} - \frac{D_{21}}{r_1}\frac{d\dot{\beta}}{d\phi} + \frac{B_{22}\dot{v}\cot\phi}{r_2} - \frac{B_{22}\dot{w}}{r_2} - \frac{D_{22}\dot{\beta}\cot\phi}{r_2} \tag{2.37}$$

where

$$\int_{-h/2}^{h/2} k_{21}(z)dz \equiv K_{21} \equiv K_{12}$$

$$\int_{-h/2}^{h/2} k_{21}(z)z dz \equiv B_{21} \equiv B_{12}$$

$$\int_{-h/2}^{h/2} k_{22}(z)dz \equiv K_{22}$$

$$\int_{-h/2}^{h/2} k_{22}(z)z\,dz \equiv B_{22}$$

$$\int_{-h/2}^{h/2} k_{11}(z)z^2\,dz \equiv D_{11}$$

$$\int_{-h/2}^{h/2} k_{12}(z)z^2\,dz \equiv D_{12}$$

$$\int_{-h/2}^{h/2} k_{21}(z)z^2\,dz \equiv D_{21} \equiv D_{12}$$

$$\int_{-h/2}^{h/2} k_{22}(z)z^2\,dz \equiv D_{22} \qquad (2.38)$$

The K, B, and D's are referred to as stiffness terms or quantities.

The stress resultants for linearly elastic shells may be obtained by replacing the rate quantities in Equations (2.34) through (2.36) by the total quantities (N_ϕ, N_θ, Q_ϕ, M_ϕ, M_θ, v, w, and β) and redefining the Equations (2.33) and (2.38) to be total stiffness quantities instead of rate stiffness quantities. The stiffness quantities for linearly elastic isotropic materials are

$$K_{11} = K_{22} = \frac{Eh}{(1 - \nu^2)}$$

$$K_{12} = K_{21} = \frac{\nu E h}{(1 - \nu^2)}$$

$$B_{11} = B_{12} = B_{21} = B_{22} = 0$$

$$D_{11} = D_{22} = \frac{E h^3}{12(1 - \nu^2)}$$

$$D_{12} = D_{21} = \frac{\nu E h^3}{12(1 - \nu^2)}$$

The stiffness terms can also be derived for orthotropic materials and for composite materials (Dong 1966).

Governing Differential Equations

The eight unknown quantities $\dot{N}_\phi$, $\dot{N}_\theta$, $\dot{Q}_\phi$, $\dot{M}_\phi$, $\dot{M}_\theta$, $\dot{v}$, $\dot{w}$, and $\dot{\beta}$ are related by three equations of equilibrium, four stress rate resultant equations, and one displacement-rotation relationship. The eight equations may be combined in several ways. One way of combining these equations is to eliminate $\dot{\beta}$ from the stress rate resultant equations, and then to eliminate $\dot{N}_\phi$, $\dot{N}_\theta$, $\dot{M}_\phi$, and $\dot{M}_\theta$ from the equilibrium equations, which leaves three differential equations in $\dot{v}$, $\dot{w}$, and $\dot{Q}_\phi$. The quantity $\dot{Q}_\phi$ may be eliminated leaving two differential equations in $\dot{v}$ and $\dot{w}$, their derivatives, and the stiffness terms, K, B, and D, and their derivatives. The approach used here is to rewrite the eight equations as six first order differential equations and two algebraic equations. The four stress rate resultant equations, the displacement-rotation relationship, and the three rate equations of

equllibrium may be written as

$$\frac{d\dot{v}}{d\phi} = \frac{\dot{N}_\phi r_1}{A_{11}K_{11}} - \frac{B_{11}\dot{M}_\phi}{A_{11}K_{11}D_{11}} - \frac{\dot{v}C_1}{A_{11}} \frac{r_1 \cot\phi}{r_2}$$

$$+ \dot{w}\left\{1. + \frac{C_1}{A_{11}} \frac{r_1}{r_2}\right\} + \frac{\dot{\beta}C_2}{A_{11}} \frac{r_1 \cot\phi}{r_2}$$

$$\frac{d\dot{w}}{d\phi} = \dot{\beta}r_1 - \dot{v}$$

$$\frac{d\dot{\beta}}{d\phi} = -\frac{\dot{M}_\phi r_1}{A_{11}D_{11}} + \frac{B_{11}\dot{N}_\phi r_1}{A_{11}K_{11}D_{11}} + \frac{\dot{v}C_3}{A_{11}} \frac{r_1 \cot\phi}{r_2}$$

$$- \frac{\dot{w}C_3}{A_{11}} \frac{r_1}{r_2} - \frac{\dot{\beta}C_4}{A_{11}} \frac{r_1 \cot\phi}{r_2}$$

$$\frac{d\dot{N}_\phi}{d\phi} = -\frac{\dot{N}_\phi}{r_0}\frac{dr_0}{d\phi} + \frac{\dot{N}_\theta r_1 \cos\phi}{r_0} + \dot{Q}_\phi - r_1\dot{Y}$$

$$\frac{d\dot{Q}_\phi}{d\phi} = -\frac{\dot{Q}_\phi}{r_0}\frac{dr_0}{d\phi} - \dot{N}_\phi - \dot{N}_\theta \frac{r_1 \sin\phi}{r_0} - r_1\dot{Z}$$

$$\frac{d\dot{M}_\phi}{d\phi} = -\frac{\dot{M}_\phi}{r_0}\frac{dr_0}{d\phi} + \frac{\dot{M}_\theta r_1 \cos\phi}{r_0} + r_1\dot{Q}_\phi \qquad (2.39)$$

where

$$\dot{N}_\theta = \frac{\dot{N}_\phi C_1}{A_{11}} + \frac{\dot{M}_\phi C_3}{A_{11}} + \frac{\dot{v}C_5 \cot\phi}{r_2} - \frac{\dot{w}C_5}{r_2} - \frac{\dot{\beta}C_6 \cot\phi}{r_2}$$

$$\dot{M}_\theta = \frac{\dot{N}_\phi C_1}{A_{11}} + \frac{\dot{M}_\phi C_3}{A_{11}} + \frac{\dot{v}C_5 \cot\phi}{r_2} - \frac{\dot{w}C_5 \cot\phi}{r_2} - \frac{\dot{\beta}C_6 \cot\phi}{r_2} \qquad (2.40)$$

and

$$A_{11} \equiv 1. - \frac{B_{11}B_{11}}{K_{11}D_{11}}$$

$$C_1 \equiv \frac{K_{12}}{K_{11}} - \frac{B_{11}B_{12}}{K_{11}D_{11}} \equiv \frac{K_{21}}{K_{11}} - \frac{B_{11}B_{21}}{K_{11}D_{11}}$$

$$C_2 \equiv \frac{B_{12}}{K_{11}} - \frac{B_{11}D_{12}}{K_{11}D_{11}} \equiv \frac{B_{21}}{K_{11}} - \frac{B_{11}D_{21}}{K_{11}D_{11}}$$

$$C_3 \equiv \frac{B_{12}}{D_{11}} - \frac{B_{11}K_{12}}{K_{11}D_{11}} \equiv \frac{B_{21}}{D_{11}} - \frac{B_{11}K_{21}}{K_{11}D_{11}}$$

$$C_4 \equiv \frac{D_{12}}{D_{11}} - \frac{B_{11}B_{12}}{K_{11}D_{11}} \equiv \frac{D_{21}}{D_{11}} - \frac{B_{11}B_{21}}{K_{11}D_{11}}$$

$$C_5 \equiv K_{22} - \frac{K_{21}C_1}{A_{11}} - \frac{B_{21}C_5}{A_{11}}$$

$$C_6 \equiv B_{22} - \frac{K_{21}C_2}{A_{11}} - \frac{B_{21}C_4}{A_{11}}$$

$$C_7 \equiv B_{22} - \frac{B_{21}C_1}{A_{11}} - \frac{D_{21}C_3}{A_{11}}$$

$$C_8 \equiv D_{22} - \frac{B_{21}C_2}{A_{11}} - \frac{D_{21}C_4}{A_{11}} \qquad (2.41)$$

Equation (2.39) is a set of six first order linear differential equations with nonconstant coefficients. The geometry, thickness, and pressures may vary in an arbitrary manner along the meridian of the

shell. Initially, the material properties at a point must be elastic and isotropic, but can vary with the shell coordinates, ϕ and z.

CHAPTER 3

SHELL EQUATIONS FOR CONSTANT CURVATURE ELEMENTS

In Chapter 2 the governing differential equations for arbitrarily-shaped shells of revolution are developed. Two constant radii of curvature shapes are chosen for the purpose of evaluating the differential equations. The two shapes are the circular arc and the straight line segment. These two shapes are selected because many shells can be adequately modeled by using combinations of the toroidal and conical elements. The toroidal and conical elements are obtained by rotating the circular arc and the straight line segment about an axis of revolution, respectively. The differential equations are specialized for these two shapes and are given below.

Toroidal Element

The circular arc has a radius a and a center at radius r_c. Figure 7 shows the toroidal element and its associated geometry. Equation (3.1) relates the terms r_0, r_1, r_2, and $dr_0/d\phi$ to the radius a, the radius r_c, and the angle ϕ.

$$r_0 = r_c + a \sin\phi \qquad r_1 = a$$

$$r_2 = \frac{r_0}{\sin\phi} \qquad \frac{dr_0}{d\phi} = a \cos\phi \tag{3.1}$$

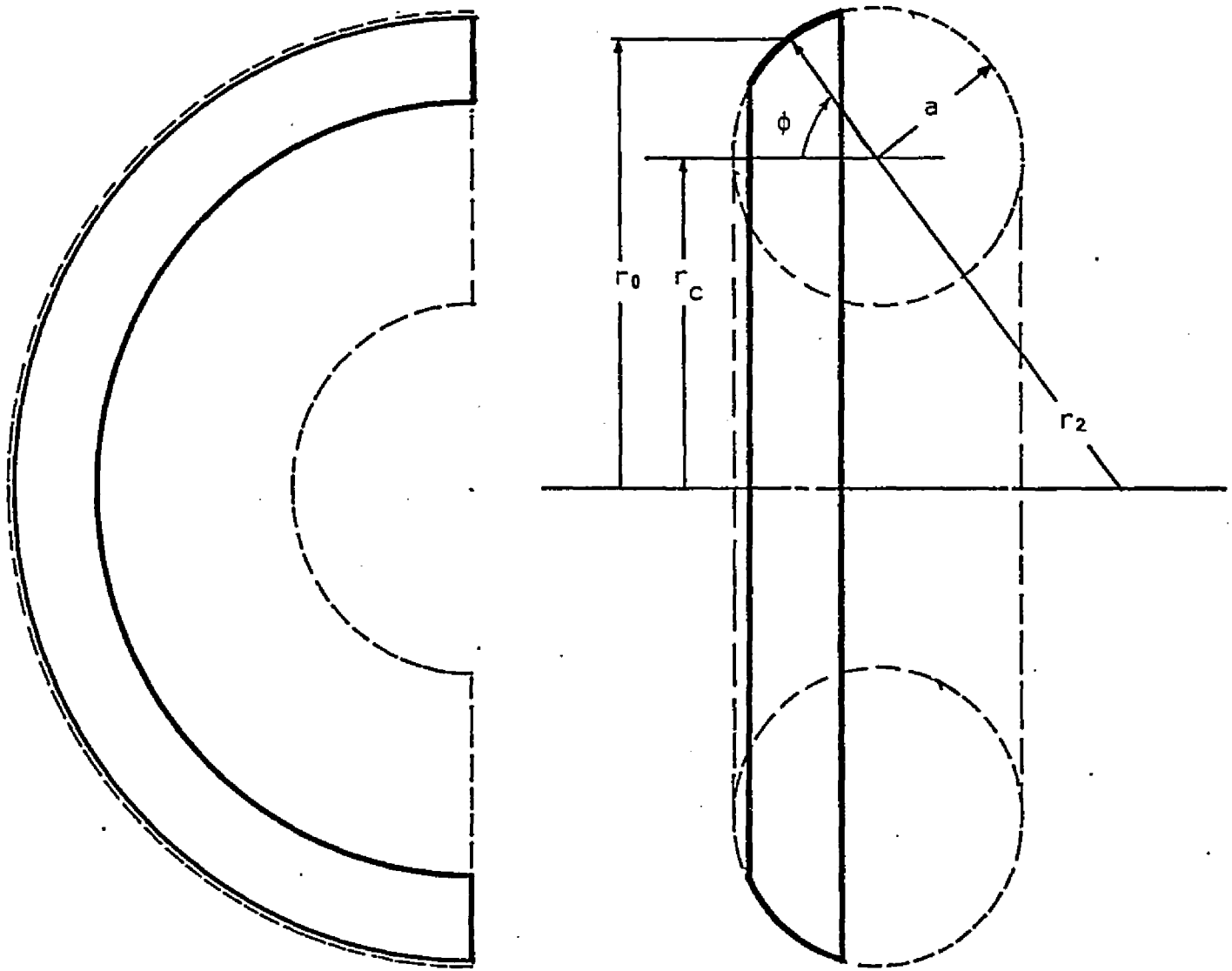

Figure 7. Toroidal Element and Associated Geometry

The angle ϕ may have any value from 0 to 2π provided that r_0 is greater than zero. Equation (2.39) is modified for the toroidal element, and the results are

$$\frac{d\dot{v}}{d\phi} = \frac{\dot{N}_\phi a}{A_{11}K_{11}} - \frac{\dot{M}_\phi a B_{11}}{A_{11}K_{11}D_{11}} - \frac{\dot{v}aC_1\cos\phi}{r_0A_{11}}$$

$$+ \dot{w}\left\{1. + \frac{aC_1\sin\phi}{r_0A_{11}}\right\} + \frac{\dot{\beta}aC_2\cos\phi}{r_0A_{11}}$$

$$\frac{d\dot{w}}{d\phi} = a\dot{\beta} - \dot{v}$$

$$\frac{d\dot{\beta}}{d\phi} = \frac{\dot{N}_\phi aB}{A_{11}K_{11}D_{11}} - \frac{\dot{M}_\phi a}{A_{11}D_{11}} + \frac{\dot{v}aC_3\cos\phi}{r_0A_{11}} - \frac{\dot{w}aC_3\sin\phi}{r_0A_{11}} - \frac{\dot{\beta}aC_4\cos\phi}{r_0A_{11}}$$

$$\frac{d\dot{N}_\phi}{d\phi} = \{-\dot{N}_\phi + \dot{N}_\theta\}\ \frac{a\cos\phi}{r_0} + \dot{Q}_\phi - a\dot{Y}$$

$$\frac{d\dot{Q}_\phi}{d\phi} = -\dot{N}_\phi - \dot{N}_\theta\ \frac{a\sin\phi}{r_0} + \frac{\dot{Q}_\phi a\cos\phi}{r_0} - a\dot{Z}$$

$$\frac{d\dot{M}_\phi}{d\phi} = \{-\dot{M}_\phi + \dot{M}_\theta\}\ \frac{a\cos\phi}{r_0} + a\dot{Q}_\phi \qquad (3.2)$$

where

$$\dot{N}_\theta = \frac{\dot{N}_\phi C_1}{A_{11}} + \frac{\dot{M}_\phi C_3}{A_{11}} + \frac{\dot{v}C_5\cos\phi}{r_0} - \frac{\dot{w}C_5\sin\phi}{r_0} - \frac{\dot{\beta}C_6\cos\phi}{r_0}$$

$$\dot{M}_\theta = \frac{\dot{N}_\phi C_2}{A_{11}} + \frac{\dot{M}_\phi C_4}{A_{11}} + \frac{\dot{v} C_7 \cos\phi}{r_0} - \frac{\dot{w} C_7 \sin\phi}{r_0} - \frac{\dot{\beta} C_8 \cos\phi}{r_0} \tag{3.3}$$

The strain-displacement relations become

$$\dot{\varepsilon}_\phi = \frac{1}{a}\frac{d\dot{v}}{d\phi} - \frac{\dot{w}}{a} - \frac{z}{a}\frac{d\dot{\beta}}{d\phi}$$

$$\dot{\varepsilon}_\theta = \frac{\dot{v}\cos\phi}{r_0} - \frac{\dot{w}\sin\phi}{r_0} - \frac{z\dot{\beta}\cos\phi}{r_0} \tag{3.4}$$

The terms C_1 through C_8 are given by Equation (2.41).

A special case of the toroidal element is the spherical element. The differential equations for the spherical element are obtained by setting the radius r_c in Equation (3.1) equal to zero, and the results are

$$\frac{d\dot{v}}{d\phi} = \frac{\dot{N}_\phi a}{A_{11}K_{11}} - \frac{\dot{M}_\phi a B_{11}}{A_{11}K_{11}D_{11}} - \frac{\dot{v} C_1 \cos\phi}{A_{11}\sin\phi}$$

$$+ \dot{w}\left\{1. + \frac{C_1}{A_{11}}\right\} + \frac{\dot{\beta} C_2 \cos\phi}{A_{11}\sin\phi}$$

$$\frac{d\dot{w}}{d\phi} = a\dot{\beta} - \dot{v}$$

$$\frac{d\dot{\beta}}{d\phi} = \frac{\dot{N}_\phi a B_{11}}{A_{11}K_{11}D_{11}} - \frac{\dot{M}_\phi a}{A_{11}D_{11}} + \frac{\dot{v} C_3 \cos\phi}{A_{11}\sin\phi} - \frac{\dot{w} C_3}{A_{11}} - \frac{\dot{\beta} C_4 \cos\phi}{A_{11}\sin\phi}$$

$$\frac{d\dot{N}_\phi}{d\phi} = \frac{\{-\dot{N}_\phi + \dot{N}_\theta\}\cos\phi}{\sin\phi} + \dot{Q}_\phi - a\dot{Y}$$

$$\frac{d\dot{Q}_\phi}{d\phi} = -\dot{N}_\phi - \dot{N}_\theta - \frac{\dot{Q}_\phi \cos\phi}{\sin\phi} - a\dot{Z}$$

$$\frac{d\dot{M}_\phi}{d\phi} = \frac{\{-\dot{M}_\phi + \dot{M}_\theta\}\cos\phi}{\sin\phi} + a\dot{Q}_\phi \qquad (3.5)$$

where

$$\dot{N}_\theta = \frac{\dot{N}_\phi C_1}{A_{11}} + \frac{\dot{M}_\phi C_3}{A_{11}} + \frac{\dot{v}C_5\cos\phi}{a\sin\phi} - \frac{\dot{w}C_5}{a} - \frac{\dot{\beta}C_6\cos\phi}{a\sin\phi}$$

$$\dot{M}_\theta = \frac{\dot{N}_\phi C_2}{A_{11}} + \frac{\dot{M}_\phi C_4}{A_{11}} + \frac{\dot{v}C_7\cos\phi}{a\sin\phi} - \frac{\dot{w}C_7}{a} - \frac{\dot{\beta}C_8\cos\phi}{a\sin\phi} \qquad (3.6)$$

The strain-displacement relations reduce to

$$\dot{\varepsilon}_\phi = \frac{1}{a}\frac{d\dot{v}}{d\phi} - \frac{\dot{w}}{a} - \frac{z}{a}\frac{d\dot{\beta}}{d\phi}$$

$$\dot{\varepsilon}_\theta = \frac{\dot{v}}{a}\frac{\cos\phi}{\sin\phi} - \frac{\dot{w}}{a} - \frac{z}{a}\frac{\dot{\beta}\cos\phi}{\sin\phi} \qquad (3.7)$$

As the angle ϕ approaches zero, many of the terms in Equations (3.5), (3.6), and (3.7) become singular. In Appendix A these equations are

examined at the apex of the sphere to determine if these singularities can be removed.

Conical Element

A conical element is generated by rotating a straight line segment about an axis. The flat plate and right circular cylinder are special cases of the conical element. A variable change is required to make the general differential equations (Equation (2.39)) applicable to conical sections. The variable ϕ is replaced by a new variable s which defines the distance from the end of the cone. The length of an infinitesimal element of a meridian is now ds instead of $r_1 d\phi$. Transformation to the new coordinate system is accomplished by replacing $\frac{1}{r_1}\frac{d}{d\phi}$ by $\frac{d}{ds}$ and letting the terms which are divided by r_1 ($r_1 \to \infty$) go to zero. The transformed differential equations contain the geometric quantities r_0, r_2, and dr_0/ds. Figure 8 shows the conical element and its associated geometry. Equation (3.8) relates the geometric quantities r_0, r_2, and dr_0/ds to the conical variables, radius r_c, the angle γ, and the variable s.

$$r_0 = r_c + s\cos\gamma$$

$$r_2 = \frac{r}{\sin\gamma} \qquad \frac{dr_0}{ds} = \cos\gamma \tag{3.8}$$

Equation (3.9) is the differential equations for the conical section.

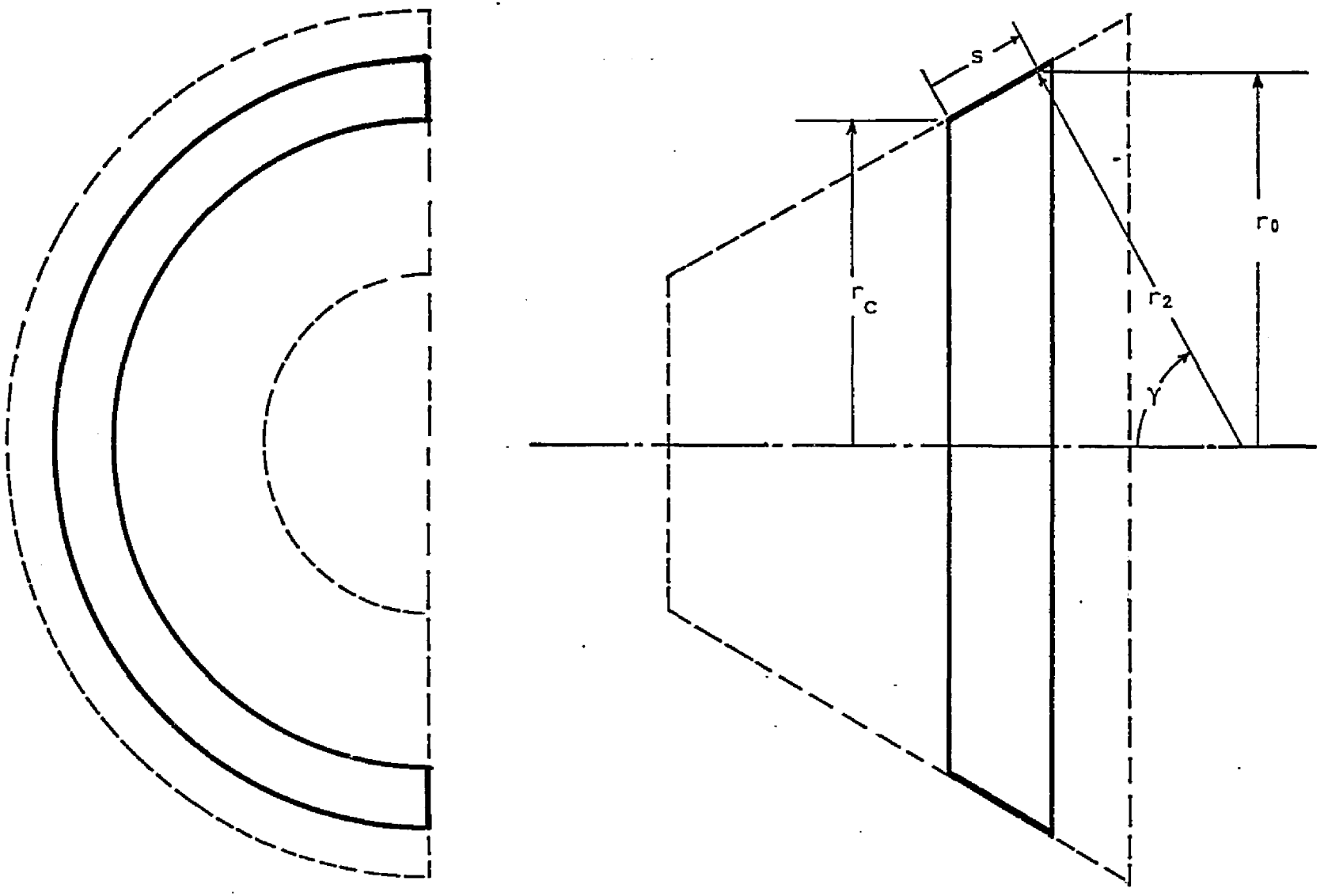

Figure 8. Conical Element and Associated Geometry

$$\frac{d\dot{v}}{ds} = \frac{\dot{N}_s}{A_{11}K_{11}} - \frac{\dot{M}_s B_{11}}{A_{11}K_{11}D_{11}} - \frac{\dot{v}C_1 \cos\gamma}{r_0 A_{11}} + \frac{\dot{w}C_1 \sin\gamma}{r_0 A_{11}} + \frac{\dot{\beta}C_2 \cos\gamma}{r_0 A_{11}}$$

$$\frac{d\dot{w}}{ds} = \dot{\beta}$$

$$\frac{d\dot{\beta}}{ds} = \frac{\dot{N}_s B_{11}}{A_{11}K_{11}D_{11}} - \frac{\dot{M}_s}{A_{11}D_{11}} + \frac{\dot{v}C_3 \cos\gamma}{r_0 A_{11}} - \frac{\dot{w}C_3 \sin\gamma}{r_0 A_{11}} - \frac{\dot{\beta}C_4 \cos\gamma}{r_0 A_{11}}$$

$$\frac{d\dot{N}_s}{ds} = \frac{\{-\dot{N}_s + \dot{N}_\theta\} \cos\gamma}{r_0} - \dot{Y}$$

$$\frac{d\dot{Q}_s}{ds} = -\frac{\dot{Q}_s \cos\gamma}{r_0} - \frac{\dot{N}_\theta \sin\gamma}{r_0} - \dot{Z}$$

$$\frac{d\dot{M}_s}{ds} = \frac{\{-\dot{M}_s + \dot{M}_\theta\} \cos\gamma}{r_0} + \dot{Q}_s \qquad (3.9)$$

where

$$\dot{N}_\theta = \frac{\dot{N}_s C_2}{A_{11}} + \frac{\dot{M}_s C_4}{A_{11}} + \frac{\dot{v}C_7 \cos\gamma}{r_0} - \frac{\dot{w}C_7 \sin\gamma}{r_0} - \frac{\dot{\beta}C_8 \cos\gamma}{r_0}$$

$$\dot{M}_\theta = \frac{\dot{N}_s C_2}{A_{11}} + \frac{\dot{M}_s C_4}{A_{11}} + \frac{\dot{v}C_7 \cos\gamma}{r_0} - \frac{\dot{w}C_7 \sin\gamma}{r_0} - \frac{\dot{\beta}C_8 \cos\gamma}{r_0} \qquad (3.10)$$

The strain-displacement relations for the conical element are

$$\dot{\varepsilon}_s = \frac{d\dot{v}}{ds} - \frac{zd\dot{\beta}}{ds}$$

$$\dot{\varepsilon}_\theta = \frac{\dot{v}\cos\gamma}{r_0} - \frac{\dot{w}\sin\gamma}{r_0} - \frac{z\dot{\beta}\cos\gamma}{r_0} \qquad (3.11)$$

In the above equations, r_0 must be greater than zero.

The flat plate is a special case of the conical element. Differential equations for the flat plate are obtained by setting the angle γ equal to zero, replacing ds by dr and r_0 by r in Equations (3.9), (3.10), and (3.11), and the results are

$$\frac{d\dot{v}}{dr} = \frac{\dot{N}_r}{A_{11}K_{11}} - \frac{\dot{M}_r B_{11}}{A_{11}K_{11}D_{11}} - \frac{\dot{v}C_1}{r\,A_{11}} + \frac{\dot{\beta}C_2}{rA_{11}}$$

$$\frac{d\dot{w}}{dr} = \dot{\beta}$$

$$\frac{d\dot{\beta}}{dr} = \frac{\dot{N}_r B_{11}}{A_{11}K_{11}D_{11}} - \frac{\dot{M}_r}{A_{11}D_{11}} + \frac{\dot{v}C_3}{rA_{11}} + \frac{\dot{\beta}C_3}{rA_{11}}$$

$$\frac{d\dot{N}_r}{dr} = \frac{\{-\dot{N}_r + \dot{N}_\theta\}}{r} - \dot{Y}$$

$$\frac{d\dot{Q}_r}{dr} = -\frac{\dot{Q}_r}{r} - \dot{Z}$$

$$\frac{d\dot{M}_r}{dr} = \frac{\{-\dot{M}_r + \dot{M}_\theta\}}{r} + \dot{Q}_r \qquad (3.12)$$

where

$$\dot{N}_\theta = \frac{\dot{N}_r C_1}{A_{11}} - \frac{\dot{M}_r C_3}{A_{11}} + \frac{\dot{v} C_5}{r} - \frac{\dot{\beta} C_6}{r}$$

$$\dot{M}_\theta = \frac{\dot{N}_r C_2}{A_{11}} + \frac{\dot{M}_r C_4}{A_{11}} + \frac{\dot{v} C_7}{r} - \frac{\dot{\beta} C_8}{r} \qquad (3.13)$$

The strain-displacement relations become

$$\dot{\varepsilon}_r = \frac{d\dot{v}}{dr} - \frac{z d\dot{\beta}}{dr}$$

and

$$\dot{\varepsilon}_\theta = \frac{\dot{v}}{r} - \frac{z\dot{\beta}}{r} \qquad (3.14)$$

As the radius r approaches zero, many of the terms in Equations (3.12), (3.13), and (3.14) become singular. In Appendix A these equations are examined at the center of the flat plate to determine if these singularities can be removed.

CHAPTER 4

METHOD OF SOLUTION

Two well known matrix methods for analyzing linear structural systems are the force and displacement methods. These methods have been extended to the analysis of nonlinear structural systems by utilizing a differential point of view and are referred to as the differential force method (Richard and Goldberg 1965) and the differential displacement method (Goldberg and Richard 1963). Both differential methods can be used to analyze the shell structures considered in this study. However, only the differential displacement method is used, and it is presented in the next section. In the following discussions only information which is pertinent to the shell structures considered here is included.

The differential displacement method requires that the shell be divided into a finite number of elements or sections. Two constant curvature elements, the toroidal and conical sections, are used to model the shell. Shells (or portions of) which are formed by rotating a continuous curve (continuous slopes) about the axis of revolution are approximated by joining constant curvature elements together so that the normals to adjacent element surfaces coincide at the element intersections.

The ends of the element are called nodal points. Each nodal point has three degrees of freedom, two displacements and a rotation.

Equation (4.1) defines the degrees of freedom of a typical nodal point k.

$$\underline{d}_k = \begin{bmatrix} \Delta_{xk} \\ \Delta_{yk} \\ \theta_{zk} \end{bmatrix} \qquad \dot{\underline{d}}_k = \begin{bmatrix} \dot{\Delta}_{xk} \\ \dot{\Delta}_{yk} \\ \dot{\theta}_{zk} \end{bmatrix} \tag{4.1}$$

The matrix $\underline{d}_k$ is a (3 x 1) column vector of nodal point displacements, and $\dot{\underline{d}}_k$ is a (3 x 1) column vector of nodal point rate displacements. Positive directions of the degrees of freedom are determined by the right-hand rule. The line under a letter is used to identify a matrix.

Differential Displacement Method

The differential displacement method is derived in the literature (Goldberg and Richard 1963, Callabresi 1970) and is not rederived here. However, the mechanics of formulating the equations is discussed. For this discussion the loading rates and the element differential stiffness matrices are assumed to be known with respect to the reference coordinate system. The development of the element differential stiffness matrices is presented in the next section.

The equations for the differential displacement method are formed by equating the external nodal point loading rates to the element rate end forces at each nodal point. In other words, a nodal point is in equilibrium with respect to the external and internal loading rates. In order to demonstrate the mechanics of formulating

the equations, a typical nodal point k is examined. The matrix $\dot{\underline{F}}_k$ is a (3 x 1) column vector of known externally applied loading rates, and the matrix $\dot{\underline{R}}^e_k$ is a (3 x 1) column vector of element rate end forces at the k-end of element e. Equation (4.2) defines the components of the vectors $\dot{\underline{F}}_k$ and $\dot{\underline{R}}^e_k$.

$$\dot{\underline{F}}_k = \begin{bmatrix} \dot{F}_{xk} \\ \dot{F}_{yk} \\ \dot{M}_{zk} \end{bmatrix} \qquad \dot{\underline{R}}^e_k = \begin{bmatrix} \dot{R}^e_{xk} \\ \dot{R}^e_{yk} \\ \dot{M}^e_{zk} \end{bmatrix} \tag{4.2}$$

The positive direction of the components of $\dot{\underline{F}}_k$ are determined by the right-hand rule. Figure 9 shows the positive rate end forces and the positive rate end displacements of element e in the xyz reference coordinate system.

The rate equilibrium conditions are established by equating $\dot{\underline{F}}_k$ to the sum of the rate end forces of all the elements attached to nodal point k.

$$\dot{\underline{F}}_k = \sum_{e=1}^{m} \dot{\underline{R}}^e_k \tag{4.3}$$

In Equation (4.3) the symbol m refers to the number of elements attached to nodal point k.

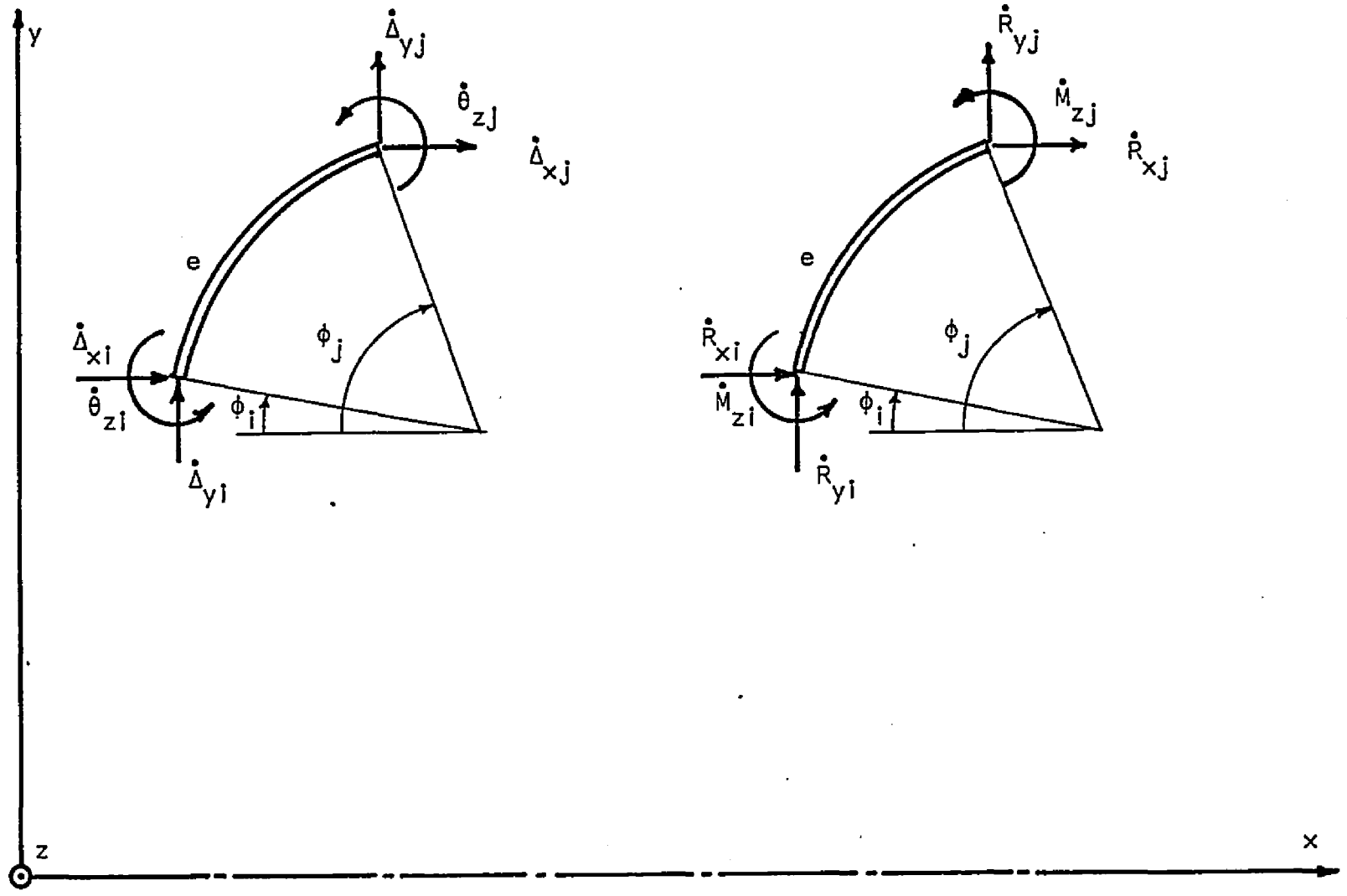

Figure 9. Positive Element End Forces and Displacements - Reference Coordinate System

The rate end forces of an element at the k-end are related to the rate end displacements in Equation (4.4)

$$\underline{\dot{R}}_k^e = \underline{\dot{R}}_{fk}^e + \underline{\overline{k}}_{kk}^e \underline{\dot{d}}_k^e + \underline{\overline{k}}_{kl}^e \underline{\dot{d}}_l^e \tag{4.4}$$

The subscript l refers to the nodal point number at the other end of element e. The quantities $\underline{\overline{k}}_{kk}^e$ and $\underline{\overline{k}}_{kl}^e$ are (3 x 3) matrices of differential stiffness relations, the quantities $\underline{\dot{d}}_k^e$ and $\underline{\dot{d}}_l^e$ are (3 x 1) column vectors of element rate end deformations, and the quantity $\underline{\dot{R}}_{fk}^e$ is a (3 x 1) column vector of rate fixed end forces. Combining Equations (4.3) and (4.4) yields

$$\underline{\dot{F}}_k = \sum_{e=1}^{m} \underline{\dot{R}}_{fk} + \sum_{e=1}^{m} \underline{\overline{k}}_{kk}^e \underline{\dot{d}}_k^e + \sum_{e=1}^{m} \underline{\overline{k}}_{kl} \underline{\dot{d}}_l^e \tag{4.5}$$

Equation (4.5) represents the rate equilibrium equations for nodal point k. The equations for the other nodal points are determined by summing k over all the nodal points, n.

$$\sum_{k=1}^{n} \underline{\dot{F}}_k = \sum_{k=1}^{n} \sum_{e=1}^{m} \underline{\dot{R}}_{fk}^e + \sum_{k=1}^{n} \sum_{e=1}^{m} \underline{\overline{k}}_{kk}^e \underline{\dot{d}}_k^e + \sum_{k=1}^{n} \sum_{e=1}^{m} \underline{\overline{k}}_{kl}^e \underline{\dot{d}}_l^e \tag{4.6}$$

In matrix notation Equation (4.6) is

$$\underline{\dot{F}} = \underline{\dot{R}} + \underline{\overline{K}}\,\underline{\dot{d}} \tag{4.7}$$

where $\underline{\dot{F}}$ is a (3n x 1) column vector of known nodal point rate forces, $\underline{\dot{R}}$ is a (3n x 1) column vector of rate fixed end forces, $\overline{K}$ is a (3n x 3n) master differential stiffness matrix, and $\underline{\dot{d}}$ is a (3n x 1) column vector of unknown nodal point rate displacements. Equation (4.7) represents the rate equilibrium equations for an unsupported shell structure, and by introducing equations of constraint, it may be written as

$$\underline{\dot{F}}_r = \underline{\dot{R}}_r + \overline{K}_r \underline{\dot{d}}_r \tag{4.8}$$

The subscript r indicates that Equation (4.7) is modified by the constraint equations. Equation (4.8) can be solved for $\underline{\dot{d}}_r$ (and $\underline{\dot{d}}$) and the results are

$$\underline{\dot{d}}_r = \overline{K}_r^{-1} \{\underline{\dot{F}}_r - \underline{\dot{R}}_r\} \tag{4.9}$$

The quantity $\{\underline{\dot{F}}_r - \underline{\dot{R}}_r\}$ is a column vector of resultant nodal point forces. The matrix $\overline{K}_r^{-1}$ is the inverse of $\overline{K}_r$. Equation (4.9) symbolizes a set of first order nonlinear ordinary differential equations which, when integrated, yield the displacements of the shell structure at the nodal points.

The master differential stiffness matrix, $\overline{K}$, can only be explicitly formed for very simple structures consisting of one dimensional elements. For the more complicated structures (frames and shells), the

matrix $\underline{\overline{K}}$ must be formed numerically. In this study, Equation (4.9) is solved by the fourth-order Runge-Kutta numerical integrating procedure (Ince 1926, McCracken 1962).

Differential Element Stiffness Matrix

Birchler, Callabresi, and Murray (1968) presented a method for calculating the stiffness matrix of sections of thin elastic shells of revolution, and their method is used here. The differential element stiffness matrix is needed for the shell elements considered in this study. The definition of a column of the differential element stiffness matrix is a vector of rate end forces which deform the element so that all the rate end displacements are zero except for the rate end displacement associated with the column which has the value of unity. The deformed shape of the element between the ends is described by the governing differential equations without the load terms (Equations (3.2), (3.5), (3.9), and (3.12)). For the rest of this discussion, the differential element stiffness matrix is referred to as the stiffness matrix, and the element rate end forces and the element rate end displacements are referred to as the end forces and end displacements, respectively.

The element has six end displacements and six end forces, three of each at both ends. Figure 10 shows the positive element end forces and end displacements in the element coordinate system. The ends of the element are referred to as the i and j ends. For the toroidal element, the i-end has the smaller value of ϕ and the j-end has the

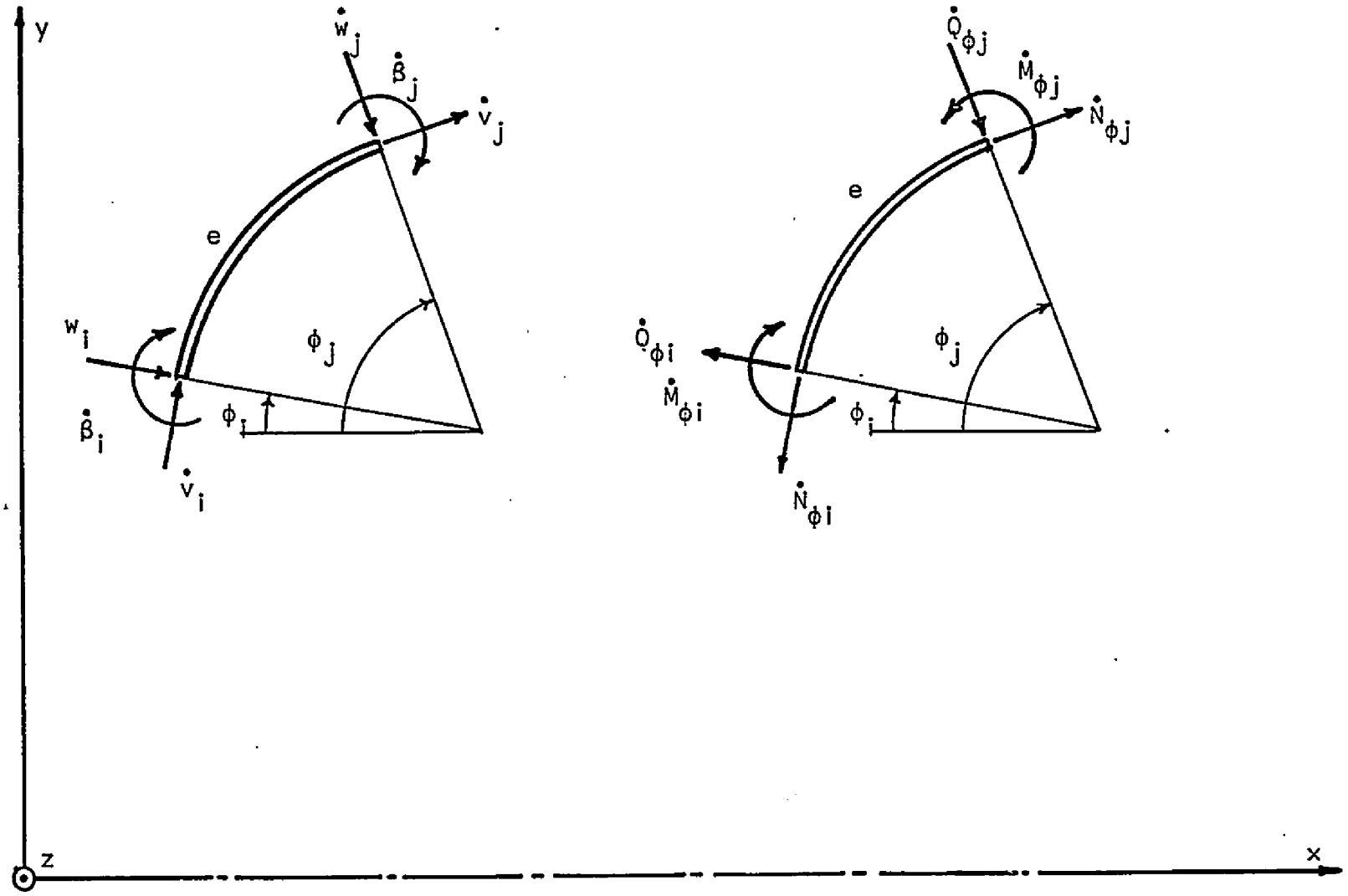

Figure 10. Positive Element End Forces and Displacements – Local Coordinate System

larger value of ϕ. The i-end for the conical element is where the variable s is zero. The end forces and end displacements are

$$\dot{\underline{N}}^e = \begin{bmatrix} \dot{N}_{\phi i}^e \\ \dot{Q}_{\phi i}^e \\ \dot{M}_{\phi i}^e \\ \dot{N}_{\phi j}^e \\ \dot{Q}_{\phi j}^e \\ \dot{M}_{\phi j}^e \end{bmatrix} \qquad \dot{\underline{v}}^e = \begin{bmatrix} \dot{v}_i^e \\ \dot{w}_i^e \\ \dot{\beta}_i^e \\ \dot{v}_j^e \\ \dot{w}_j^e \\ \dot{\beta}_j^e \end{bmatrix} \tag{4.10}$$

The end forces are related to the end displacements by a (6 x 6) square matrix of differential stiffness coefficients, $\overline{\underline{K}}^e$, and a (6 x 1) column vector of rate fixed end forces, $\dot{\underline{N}}_f^e$.

$$\dot{\underline{N}}^e = \dot{\underline{N}}_f^e + \overline{\underline{K}}^e \, \dot{\underline{v}}^e \tag{4.11}$$

The stiffness matrix is not symmetric but can be made symmetric. Positive fixed end forces have the same directions as the positive end forces shown in Figure 10.

The deformed shape and the internal forces of an element are governed by six first order differential equations and six initial conditions. The initial conditions are the end forces and end displacements at the i-end; the final conditions are the forces and

displacements at the j-end. Only three of the initial conditions are known, the displacements. The three initial forces are unknown and must be determined from the known displacements at the j-end. The procedure presented by Birchler, Callabresi, and Murray (1968) for calculating a column of the stiffness matrix is as follows.

A set of initial forces, $\dot{N}_{\phi i}^{(1)}$, $\dot{Q}_{\phi i}^{(1)}$, and $\dot{M}_{\phi i}^{(1)}$, is assumed and using the known displacements, $\dot{v}_i^{(k)}$, $\dot{w}_i^{(k)}$, and $\dot{\beta}_i^{(k)}$, the six differential equations without the load terms are solved for the displacements, $\dot{v}_j^{(1)}$, $\dot{w}_j^{(1)}$, and $\dot{\beta}_j^{(1)}$, at the j-end. The differential equations are solved numerically by the fourth-order Runge-Kutta integrating procedure. A second set of initial forces, $\dot{N}_{\phi i}^{(2)}$, $\dot{Q}_{\phi i}^{(2)}$, and $\dot{M}_{\phi i}^{(2)}$, is assumed.

where

$$\dot{N}_{\phi i}^{(2)} = \dot{N}_{\phi i}^{(1)} + \Delta\dot{N}_{\phi i}$$

$$\dot{Q}_{\phi i}^{(2)} = \dot{Q}_{\phi i}^{(1)}$$

$$\dot{M}_{\phi i}^{(2)} = \dot{M}_{\phi i}^{(1)}$$

The equations are solved for the final displacements, $\dot{v}_j^{(2)}$, $\dot{w}_j^{(2)}$, and $\dot{\beta}_j^{(2)}$, using the second set of assumed initial forces and the known initial displacements. A third and fourth set of initial forces, $\dot{N}_{\phi i}^{(3)}$, $\dot{Q}_{\phi i}^{(3)}$, and $\dot{M}_{\phi i}^{(3)}$, and $\dot{N}_{\phi i}^{(4)}$, $\dot{Q}_{\phi i}^{(4)}$, and $\dot{M}_{\phi i}^{(4)}$, are assumed

where

$$\dot{N}_{\phi i}^{(3)} = \dot{N}_{\phi i}^{(1)}$$

$$\dot{Q}_{\phi i}^{(3)} = \dot{Q}_{\phi i}^{(1)} + \Delta\dot{Q}_{\phi i}$$

$$\dot{M}_{\phi i}^{(3)} = \dot{M}_{\phi i}^{(1)}$$

and

$$\dot{N}_{\phi i}^{(4)} = \dot{N}_{\phi i}^{(1)}$$

$$\dot{Q}_{\phi i}^{(4)} = \dot{Q}_{\phi i}^{(1)}$$

$$\dot{M}_{\phi i}^{(4)} = \dot{M}_{\phi i}^{(1)} + \Delta\dot{M}_{\phi i}$$

The equations are solved two more times using the third and fourth sets of assumed initial forces for $\dot{v}_j^{(3)}$, $\dot{w}_j^{(3)}$, and $\dot{\beta}_j^{(3)}$, and for $\dot{v}_j^{(4)}$, $\dot{w}_j^{(4)}$, and $\dot{\beta}_j^{(4)}$.

A set of algebraic equations which relates the change in the j-end displacements to the unit change in the i-end forces can be established from the assumed initial forces at the i-end and the calculated displacements at the j-end. Specifically, the ratio

$$\frac{\{\dot{v}_j^{(2)} - \dot{v}_j^{(1)}\}}{\Delta\dot{N}_{\phi i}} \equiv \frac{\delta\dot{v}_j}{\delta N_{\phi i}} \qquad (4.12)$$

is the change in the $\dot{v}$ displacement at the j-end due to a unit change in $\dot{N}_{\phi i}$ at the i-end. Eight other ratios are defined in a similar

manner. The algebraic equations are

$$\begin{bmatrix} \delta\dot{v}_j \\ \delta\dot{w}_j \\ \delta\dot{\beta}_j \end{bmatrix} = \begin{bmatrix} \frac{\delta\dot{v}_j}{\delta\dot{N}_{\phi i}} & \frac{\delta\dot{v}_j}{\delta\dot{Q}_{\phi i}} & \frac{\delta\dot{v}_j}{\delta\dot{M}_{\phi i}} \\ \frac{\delta\dot{w}_j}{\delta\dot{N}_{\phi i}} & \frac{\delta\dot{w}_j}{\delta\dot{Q}_{\phi i}} & \frac{\delta\dot{w}_j}{\delta\dot{M}_{\phi i}} \\ \frac{\delta\dot{\beta}_j}{\delta\dot{N}_{\phi i}} & \frac{\delta\dot{\beta}_j}{\delta\dot{Q}_{\phi i}} & \frac{\delta\dot{\beta}_j}{\delta\dot{M}_{\phi i}} \end{bmatrix} \begin{bmatrix} \delta\dot{N}_{\phi i} \\ \delta\dot{Q}_{\phi i} \\ \delta\dot{M}_{\phi i} \end{bmatrix} \qquad (4.13)$$

where $\delta\dot{v}_j$, $\delta\dot{w}_j$, and $\delta\dot{\beta}_j$ are the changes required in $\dot{v}_j^{(1)}$, $\dot{w}_j^{(1)}$, and $\dot{\beta}_j^{(1)}$ to obtain the final known displacements, $\dot{v}_j^{(k)}$, $\dot{w}_j^{(k)}$, and $\dot{\beta}_j^{(k)}$. Equation (4.13) is solved for $\delta\dot{N}_{\phi i}$, $\delta\dot{Q}_{\phi i}$, and $\delta\dot{M}_{\phi i}$ and these are added to $\dot{N}_{\phi i}^{(1)}$, $\dot{Q}_{\phi i}^{(1)}$, and $\dot{M}_{\phi i}^{(1)}$ to obtain the true initial forces, $\dot{N}_{\phi i}$, $\dot{Q}_{\phi i}$, and $\dot{M}_{\phi i}$. The six differential equations are solved again using the six known initial conditions for the forces, $\dot{N}_{\phi j}$, $\dot{Q}_{\phi j}$, and $\dot{M}_{\phi j}$, at the j-end. Since the six differential equations are linear in the rate terms, the displacements at the j-end are $\dot{v}_j^{(k)}$, $\dot{w}_j^{(k)}$, and $\dot{\beta}_j^{(k)}$. The forces $\dot{N}_{\phi i}$, $\dot{Q}_{\phi i}$, $\dot{M}_{\phi i}$, $\dot{N}_{\phi j}$, $\dot{Q}_{\phi j}$, and $\dot{M}_{\phi j}$ form one column of the stiffness matrix. The remaining columns of the stiffness matrix are formed in the same manner.

Element Fixed End Forces

In the displacement method, all the forces must be applied at the nodal points. The concept of fixed end forces is used to handle the distributed loads on an element. The same procedure is used to calculate the fixed end forces that is used to calculate a column of the stiffness matrix except that the known displacements, $\overset{\bullet}{v}_i^{(k)}$, $\overset{\bullet}{w}_i^{(k)}$, $\overset{\bullet}{\beta}_i^{(k)}$, $\overset{\bullet}{v}_j^{(k)}$, $\overset{\bullet}{w}_j^{(k)}$, and $\overset{\bullet}{\beta}_j^{(k)}$, are all equal to zero (fixed ends) and the differential equations are solved using the load terms.

Coordinate Transformations

The element end forces, fixed end forces, and end displacements defined in the previous two sections are in a local element coordinate system. These quantities must be transformed into a reference coordinate system as required by the displacement method. Two transformations are required: one to transform the element end forces, $\underline{\overset{\bullet}{N}}^e$, from the local coordinate system to the reference coordinate system and another to transform the element end displacements, $\underline{\overset{\bullet}{d}}^e$, from the reference coordinate system to the local coordinate system. In matrix notation the transformations are

$$\underline{\overset{\bullet}{R}}^e = \underline{\overset{\bullet}{T}}^e \, \underline{\overset{\bullet}{N}}^e \qquad\qquad \underline{\overset{\bullet}{v}}^e = \underline{\overset{\bullet}{S}}^e \, \underline{\overset{\bullet}{d}}^e \tag{4.14}$$

The quantities $\underline{T}^e$ and $\underline{S}^e$ are (6 x 6) square matrices.

The transformation of element end forces from the local coordinate system to the reference coordinate system is obtained by combining Equations (4.11) and (4.14).

$$\dot{\underline{R}}^e = \underline{T}^e \dot{\underline{N}}^e = \underline{T}^e \dot{\underline{N}}_f^e + \underline{T}^e \overline{\underline{K}}^e \underline{S}^e \dot{\underline{d}}^e \tag{4.15}$$

The matrix $\underline{T}^e \overline{\underline{K}}^e \underline{S}^e$, the element stiffness matrix, and the matrix $\underline{T}^e \underline{N}_f^e$, the element fixed end forces, are in the xyz reference coordinate system.

The matrices $\underline{T}^e$ and $\underline{S}^e$ for the toroidal elements can be obtained from Figures 9 and 10, and the results are given below.

$$\underline{T}^e = \begin{bmatrix} -\sin\phi_i & -\cos\phi_i & 0 & 0 & 0 & 0 \\ -\cos\phi_i & \sin\phi_i & 0 & 0 & 0 & 0 \\ 0 & 0 & -1. & 0 & 0 & 0 \\ 0 & 0 & 0 & \sin\phi_j & \cos\phi_j & 0 \\ 0 & 0 & 0 & \cos\phi_j & -\sin\phi_j & 0 \\ 0 & 0 & 0 & 0 & 0 & 1. \end{bmatrix}$$

$$\underline{S}^e = \begin{bmatrix} \sin\phi_i & \cos\phi_i & 0 & 0 & 0 & 0 \\ \cos\phi_i & -\sin\phi_i & 0 & 0 & 0 & 0 \\ 0 & 0 & -1. & 0 & 0 & 0 \\ 0 & 0 & 0 & \sin\phi_j & \cos\phi_j & 0 \\ 0 & 0 & 0 & \cos\phi_j & -\sin\phi_j & 0 \\ 0 & 0 & 0 & 0 & 0 & -1. \end{bmatrix}$$

The matrices $\underline{T}^e$ and $\underline{S}^e$ for the conical element are obtained from the above matrices by setting $\gamma = \phi_i = \phi_j$.

Stiffness Terms

The stiffness terms, K, B, and D, must be evaluated along the meridian of an element and the only practical way to evaluate these terms is numerically. This is accomplished by maintaining a table of the material stiffness terms, k_{11}, k_{12}, and k_{22}, at points through the thickness and at stations along the meridian. The stiffness terms are determined at each station by integrating Equations (2.33) and (2.38) with Simpson's one-third rule. Only an odd number of points through the thickness is used.

The fourth-order Runge-Kutta integrating procedure requires four evaluations of the first derivatives per interval: once at the beginning, twice in the middle, and once at the end. An interval is the distance between two adjacent stations along the meridian. In this study, the table of material stiffness terms, k, is maintained only at the stations; therefore, the stiffness terms can only be determined at the stations. The values of the stiffness terms at the middle of an interval are taken to be the average of the two end point values. If an element has a variable thickness, a more elaborate scheme would have to be employed to determine the values at the middle of an interval.

Numerical Methods

In the previous sections, the major calculations are described and here the calculations of the stresses, strains, displacements, and the internal forces within the element are discussed. The element is initially free of residual stresses and strains; therefore, the initial

values of the previously mentioned quantities are zero. The subscript k is used to refer to a station along the meridian, and the subscript l refers to a point in the thickness at station k.

The strains at station k and point l are obtained by integrating the strain rates with respect to the loading parameter, P.

$$\varepsilon_{\phi kl} = \int_0^P \dot{\varepsilon}_{\phi kl}\, dP \qquad \varepsilon_{\theta kl} = \int_0^P \dot{\varepsilon}_{\theta kl}\, dP$$

The strain rates are known in terms of the displacement rates and their derivatives. Specifically, the strain rates for the toroidal element are

$$\dot{\varepsilon}_{\phi kl} = \left\{ \frac{1}{a}\frac{d\dot{v}}{d\phi} - \frac{\dot{w}}{a} - \frac{z}{a}\frac{d\dot{\beta}}{d\phi} \right\}_{kl}$$

and

$$\dot{\varepsilon}_{\theta kl} = \left\{ \frac{\dot{v}\cos\phi}{r_0} - \frac{\dot{w}\sin\phi}{r_0} - \frac{z\dot{\beta}\cos\phi}{r_0} \right\}_{kl}$$

The stresses are determined by integrating the stress rates with respect to the applied loading parameter, P,

$$\sigma_{\phi kl} = \int_0^P \dot{\sigma}_{\phi kl}\, dP \qquad \sigma_{\theta kl} = \int_0^P \dot{\sigma}_{\theta kl}\, dP$$

and the stress rates are obtained from the plastic stress-strain relations

$$\dot{\sigma}_{\phi kl} = k_{11_{kl}} \dot{\varepsilon}_{\phi kl} + k_{12_{kl}} \dot{\varepsilon}_{\theta kl}$$

and

$$\dot{\sigma}_{\theta kl} = k_{21_{kl}} \dot{\varepsilon}_{\phi kl} + k_{22_{kl}} \dot{\varepsilon}_{\theta kl}$$

Five internal forces, N_ϕ, N_θ, Q_ϕ, M_ϕ, and M_θ, exist at each station within the element, and these forces are determined by integrating them with respect to the loading parameter, P.

For example,

$$Q_{\phi k} = \int_0^P \dot{Q}_{\phi k} \, dP$$

where

$$\dot{Q}_{\phi k} = \int_{\phi_i}^{\phi_k} \{ \frac{d\dot{Q}_\phi}{d\phi} \} \, d\phi$$

where ϕ_i is the initial value of ϕ and ϕ_k is the value of ϕ at station k. The other forces are found in the same manner.

The three displacements, v, w, and β, are determined in the same manner as the forces.

For example,

$$w_k = \int_0^P \dot{w}_k \, dP$$

where

$$\dot{w}_k = \int_{\phi_i}^{\phi_k} \{ \frac{d\dot{w}}{d\phi} \} \, d\phi$$

where ϕ_i and ϕ_k are as defined above. The integrals with respect to dP are numerically evaluated with the fourth-order Runge-Kutta procedure.

CHAPTER 5

NUMERICAL RESULTS

Several example problems are presented to verify the equations and the method of solution presented in Chapters 2, 3, and 4. A Fortran IV computer language program is used to evaluate the method of solution, and the results presented are from this program.

Empirical Equation for Uniaxial Stress-Strain Curve

In Chapter 2 a function $H(\varepsilon_e^p)$, which relates the effective plastic strain to the effective stress, is defined and used. The function H is shown to be a uniaxial stress-strain diagram with the elastic strains removed. In the example problems presented here, the nonlinear material is represented by a three parameter stress-strain curve developed by Richard (1961). This empirical relation may be written as

$$\sigma = \frac{E\varepsilon}{\{1. + \left|\frac{\varepsilon}{\varepsilon_0}\right|^n\}^{1/n}} \tag{5.1}$$

or

$$\varepsilon = \frac{\varepsilon}{E\{1. - \left|\frac{\sigma}{\sigma_0}\right|^n\}^{1/n}} \tag{5.2}$$

where E is the initial linear relationship between σ and ε, ε_0 is the linear strain associated with the ultimate stress, σ_0, and n is the nonlinear parameter which defines the shape of the curve. Figure 11 is a nondimensional plot of Equation (5.1) for several values of n. The parameters, E, σ_0, ε_0, and n, are determined from the actual nonlinear stress-strain curve. Figure 12 shows how these parameters are obtained.

The inverse of the function H is obtained by subtracting the elastic strains from the total strains as given by Equation (5.2). In terms of the effective stress, σ_e, and the effective plastic strain, ε_e^p, the inverse of H may be written as

$$H^{-1}(\sigma_e) = \varepsilon_e^p = \frac{\sigma_e}{E\left[1. - \left|\frac{\sigma_e}{\sigma_0}\right|^n\right]^{1/n}} - \frac{\sigma_e}{E} \tag{5.3}$$

The quantity actually used in the plastic stress-strain relations is the slope of the effective stress-effective plastic strain curve which can be obtained by differentiating ε_e^p with respect to σ_e. The result is

$$\{H^{-1}(\sigma_e)\}' = \frac{d\varepsilon_e^p}{d\sigma_e} = \frac{1.}{E\left[1. - \left|\frac{\sigma_e}{\sigma_0}\right|^n\right]^{\frac{n+1}{n}}} - \frac{1.}{E} \tag{5.4}$$

The absolute value of the ratio σ_e/σ_0 should always be less than unity for Equation (5.4) to be valid; however, this ratio can become greater than unity during the solution of a problem. When this

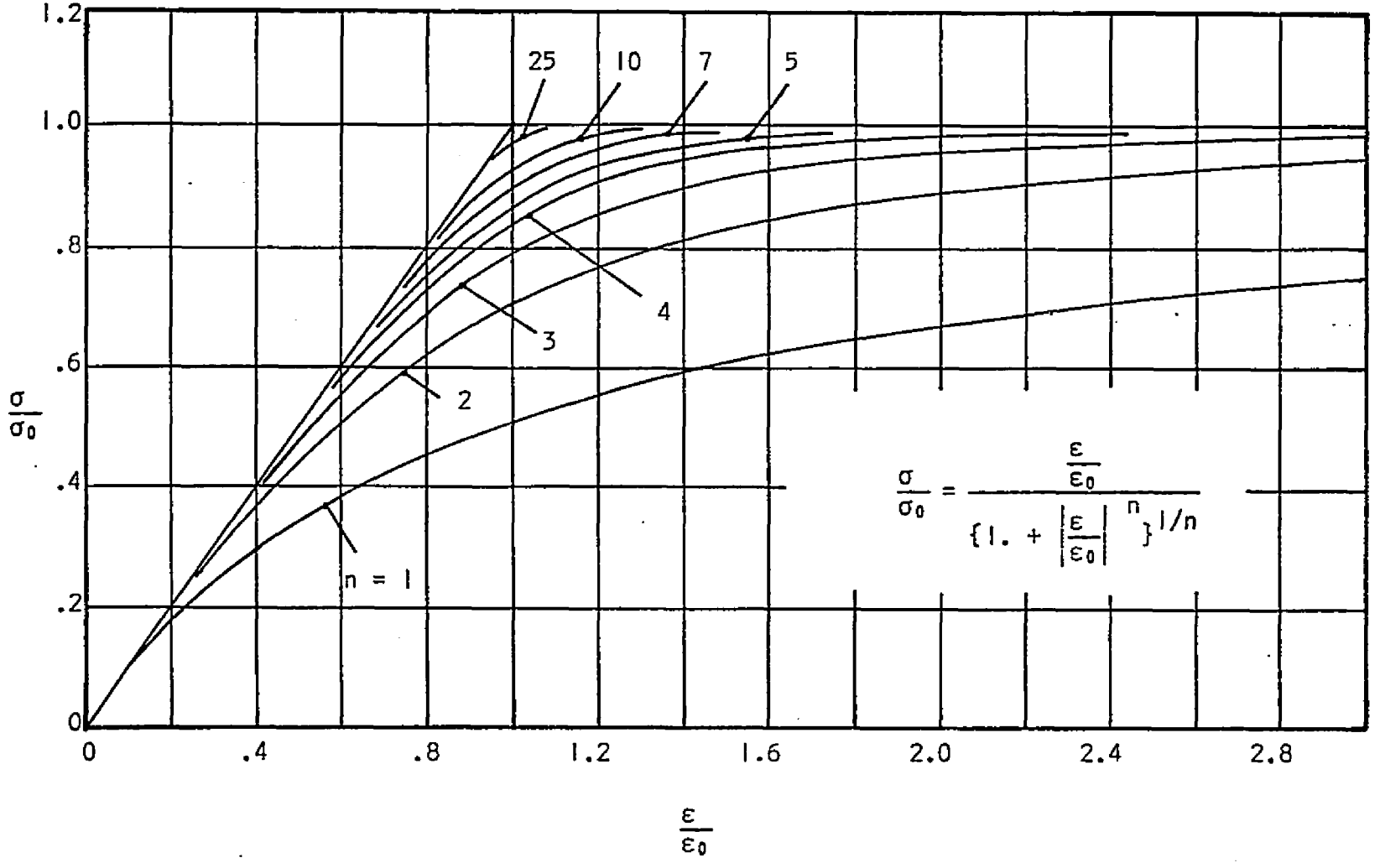

Figure 11. Nondimensional Stress-Strain Relationships

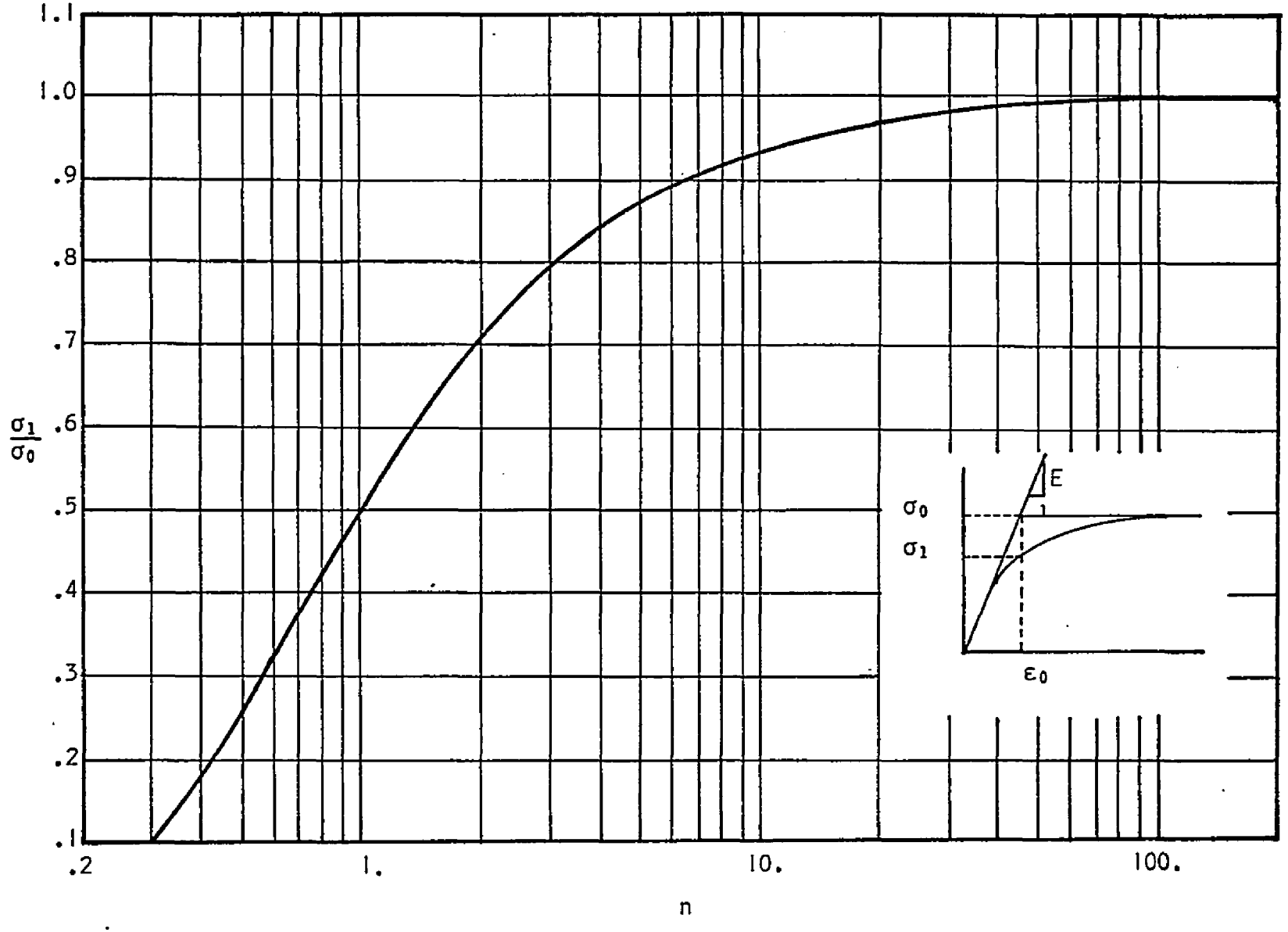

Figure 12. Nonlinear Parameter n

ratio is equal to or greater than unity, numerical difficulties arise. When σ_e/σ_0 is equal to one, an attempt is made to divide by zero. When the ratio is greater than one, an attempt is made to raise a noninteger negative number to a noninteger power. In order to avoid these numerical difficulties, a tangent line is constructed to the empirical curve (Equation (5.2)). The tangent line is used for values of σ_e greater than $.999\sigma_0$, and Equation (5.5) is used instead of Equation (5.4).

$$\{H^{-1}(\sigma_e)\}' = \frac{1.}{E\left[1. - (.999)^n\right]^{\frac{n+1}{n}}} - \frac{1.}{E} \tag{5.5}$$

Thick-Walled Cylinders

Hannon and Sidebottom (1967) presented test results for five thick-walled open-end cylinders which are pressurized internally and made from AISI 4135 steel. The dimensions of the cylinders are inside diameter, 0.624 inches; outside diameter, 1.351 inches; and length, 5.0 inches.

The cylinders are modeled by one flat plate element with sixteen points along the radius and three points through the thickness. A one inch thick section of the cylinder is used. Material properties are modulus of elasticity, 29000000 pounds per square inch; ultimate stress, 96250 pounds per square inch; and shape factor, 25.

Instead of applying an internal pressure, the inside radius is displaced outward, and the pressure necessary to cause this displacement is calculated. The maximum radial displacement is .032 inches.

Twenty loading intervals are used: the first one is 24 percent of the maximum radial displacement and the other nineteen loading intervals are each 4 percent of the maximum radial displacement.

Figure 13 shows a plot of the internal pressures to the hoop strains on the outside surface of the cylinder. Both the test results and calculated results are shown. The test results are redrawn from the work of Hannon and Sidebottom (1967) and agree with the calculated results up to about 75000 pounds per square inch. Above this value the calculated results are higher than the test results. This is because the tangent line, which is used for large values of σ_e/σ_0 in the stress-strain relation, allows the effective stresses to become greater than σ_0. As a result, the cylinder is stiffer than it should be.

Figures 14 and 15 show the radial stress and hoop stress distributions through the wall thickness of the cylinder for several values of internal pressure.

Thin-Walled Cylinder

A cylinder is analyzed using a different number of points through the wall thickness to determine the effects of these points on the stresses, strains, internal forces, and displacements. Results are obtained by using three, five, seven, and nine points. The cylinder is modeled by four conical elements as shown in Figure 16. Eleven stations are used along the meridian of each element.

The dimensions of the cylinder are length, 6 inches; radius, 6 inches; and wall thickness, 0.4 inches. The material properties

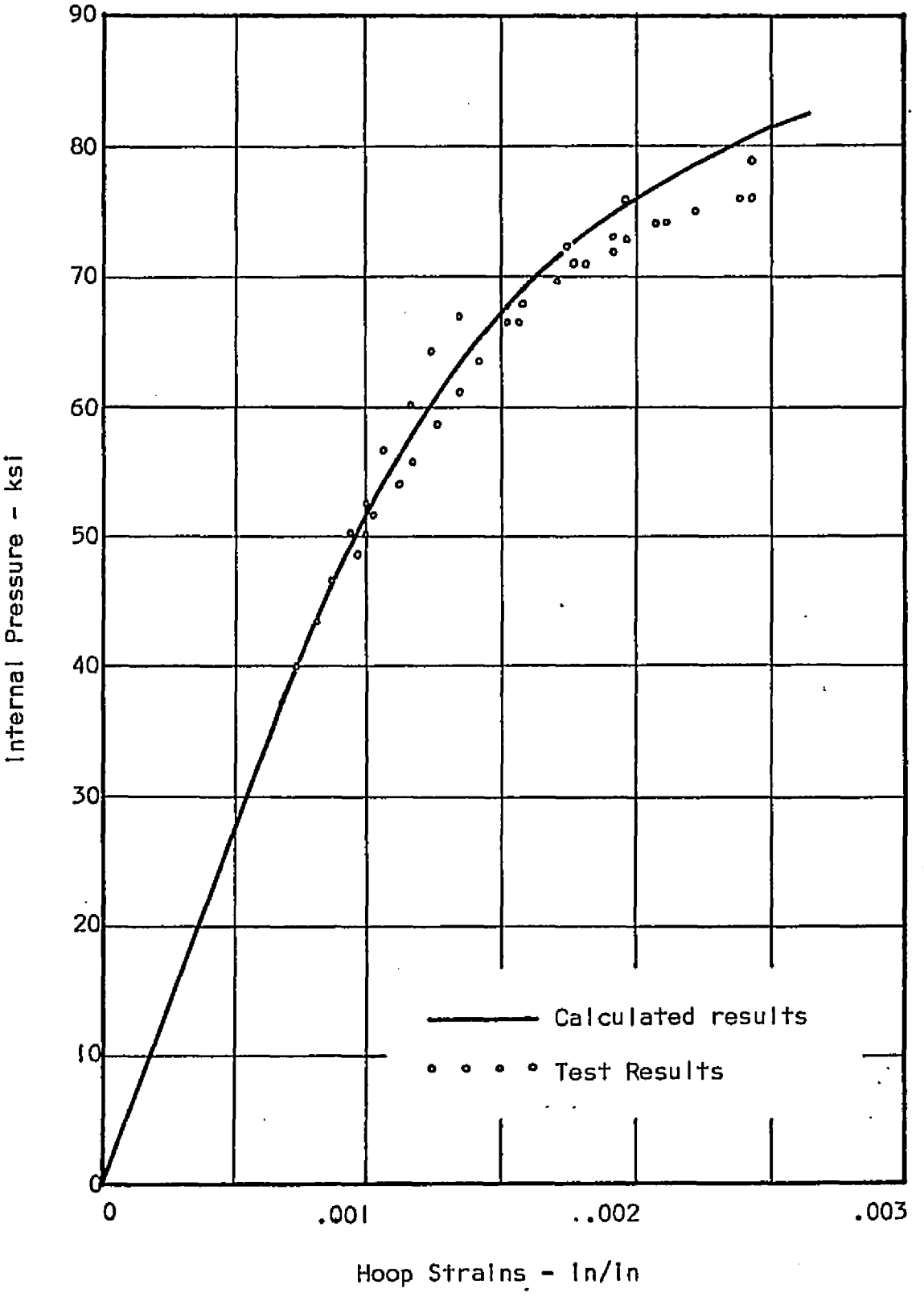

Figure 13. Thick-Walled Cylinder - Hoop Strains on Outside Surface

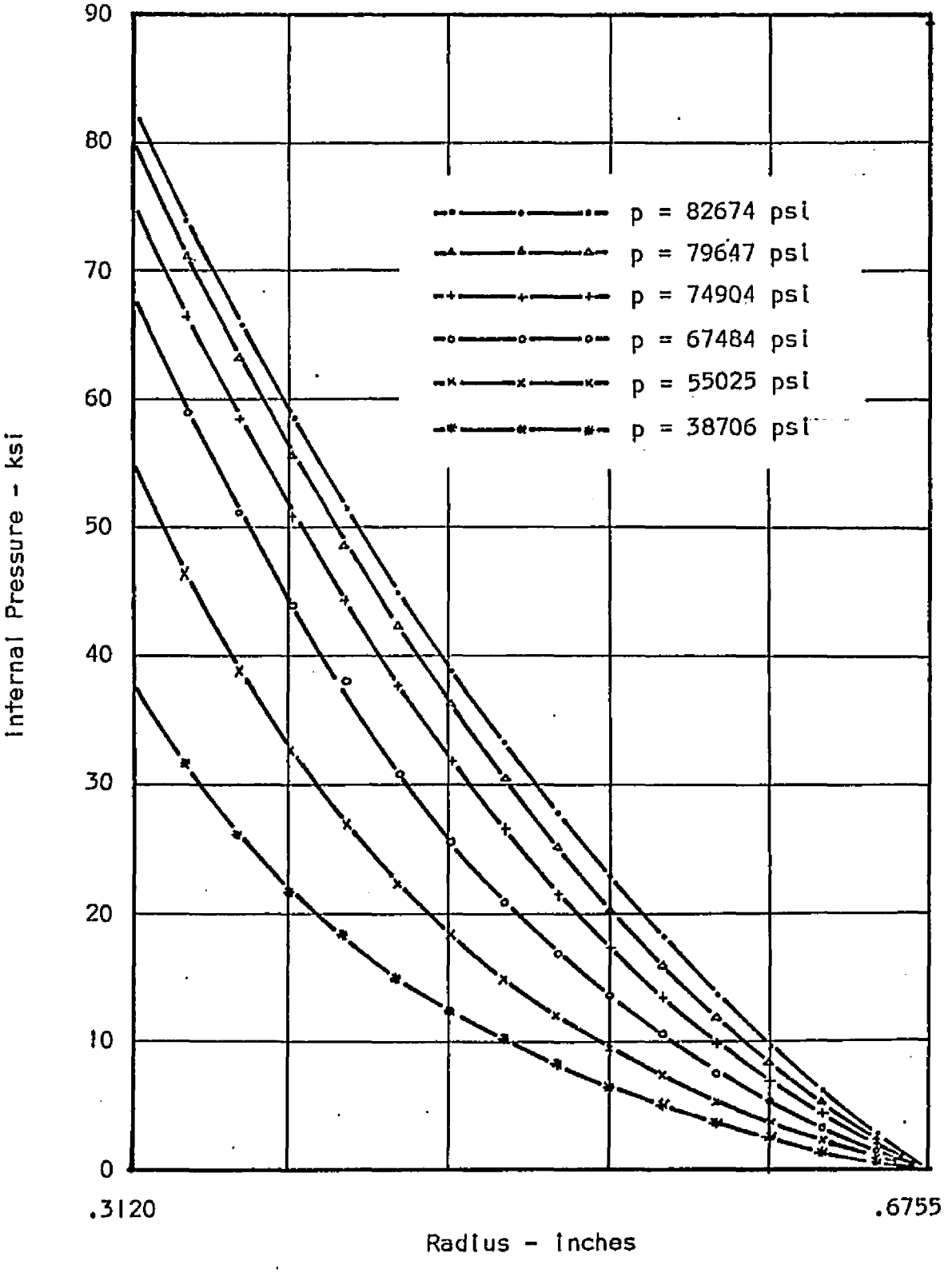

Figure 14. Thick-Walled Cylinder - Radial Stress Distributions

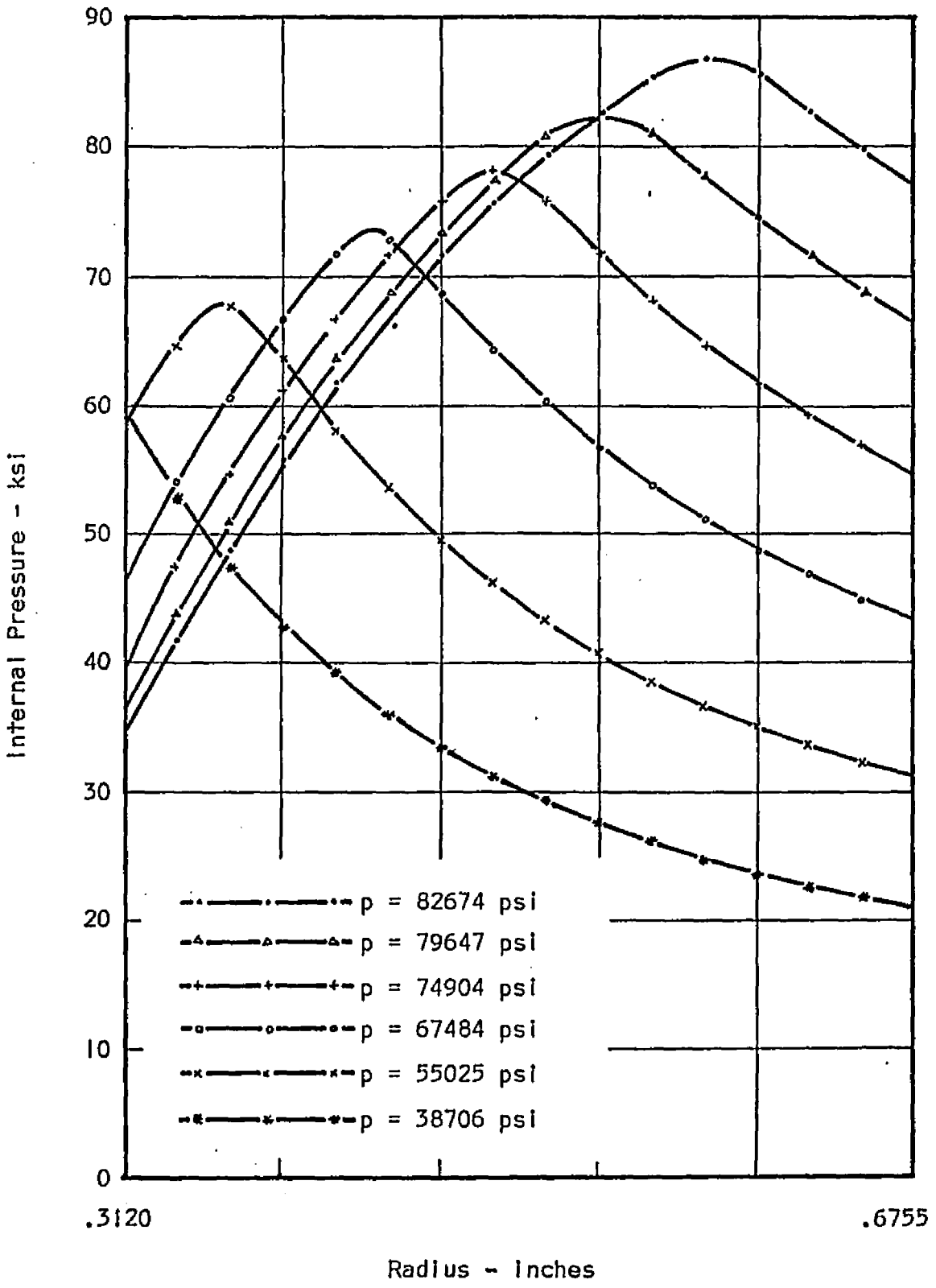

Figure 15. Thick-Walled Cylinder - Hoop Stress Distributions

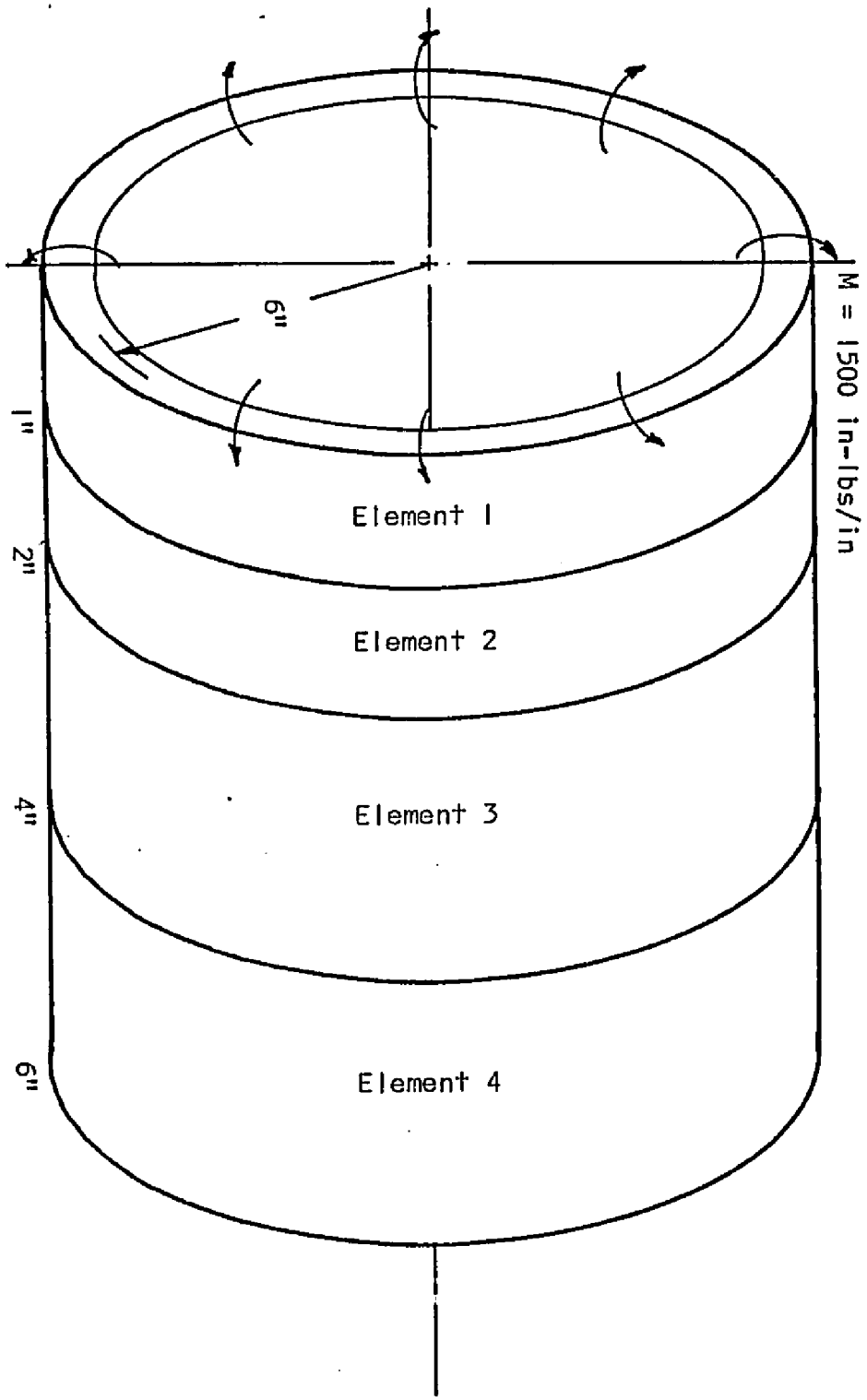

Figure 16. Thin-Walled Cylinder

of the cylinder are modulus of elasticity, 30000000 pounds per square inch; Poisson's ratio, 0.25; ultimate stress, 50000 pounds per square inch; and shape factor, 3.

An applied moment of 1500 inch-pounds per inch is applied to one end of the cylinder as shown in Figure 16. Four loading increments, 40 percent, 30 percent, 20 percent, and 10 percent of the applied moment, are used in the order given.

Table I shows a comparison of six variables at 100 percent of the reference load at five stations along the meridian. The stresses, σ_{xo} and $\sigma_{\theta o}$, are on the outside surface of the cylinder. A study of Table I shows that the results from the three point solution are inadequate. The results from the other three solutions agree within one half of one percent, except for the normal displacement at x = 1.0 inches and the meridional stress at x = 0.0 inches in the five point solution. Results from the seven and nine point solutions are almost identical. As a result of this study, the conclusion is reached that seven is the minimum number of points that should be used when both bending and membrane forces are present.

Flat Circular Plate

A flat circular plate with a hole in the center and loaded with a uniform pressure is analyzed for the stresses, strains, internal forces, and displacements. The inside radius is 10 inches and the outside radius is 12.4 inches. The material properties are modulus of elasticity, 30000000 pounds per square inch; Poisson's ratio, 0.25; ultimate stress, 50000 pounds per square inch; and shape factor, 3.

Table 1. Comparison of Results

	x	3-points	5-points	7-points	9-points
w	0.0	-.008204	-.007182	-.007172	-.007171
	0.5	-.002618	-.002453	-.002455	-.002455
	1.0	.000016	.000051	.000047	.000047
	1.5	.001092	.001099	.001097	.001096
	2.0	.001300	.001297	.001297	.001297
M_x	0.0	1500.0	1500.0	1500.0	1500.0
	0.5	1322.8	1318.7	1319.0	1319.0
	1.0	949.98	943.76	944.40	944.42
	1.5	569.35	563.99	564.71	564.74
	2.0	272.97	269.34	269.93	269.96
M_θ	0.0	679.67	568.99	566.42	565.94
	0.5	459.99	387.03	386.54	386.57
	1.0	260.98	247.30	246.64	246.58
	1.5	146.10	143.23	143.29	143.28
	2.0	68.77	67.72	67.86	67.87
N_θ	0.0	10500.4	10846.2	10833.2	10830.8
	0.5	4592.6	4486.6	4483.1	4483.4
	1.0	-25.51	-96.90	-88.37	-88.18
	1.5	-2163.7	-2182.0	-2177.1	-2176.9
	2.0	-2595.0	-2590.6	-2589.2	-2589.1
σ_{xo}	0.0	-55820.6	-46742.3	-46687.4	-46692.6
	0.5	-48430.8	-44000.7	-43896.9	-43893.1
	1.0	-35626.5	-34249.3	-34176.1	-34167.4
	1.5	-24107.9	-21069.9	-21080.0	-21078.9
	2.0	-10248.6	-10101.8	-10123.1	-10124.0
$\sigma_{\theta o}$	0.0	-17451.6	770.76	835.02	825.79
	0.5	-8531.54	-4910.93	-4824.65	-4823.10
	1.0	-9816.84	-9509.09	-9464.32	-9460.94
	1.5	-10809.6	-10755.4	-10745.9	-10745.0
	2.0	-9052.7	-9004.06	-9005.81	-9005.83

One element is used to model the plate. Twenty-five stations are used along the radius, and eleven points are used through the thickness. The inside radius has a fixed support, and the outside radius has a pin support. Rotations and normal displacements are both prevented from moving at a fixed support, and the normal displacements are prevented from moving at a pin support.

Nine pressure increments consisting of 2400, 960, 480, 480, 240, 240, 240, 120, and 120 pounds per square inch are applied to the plate in the order given. The sum of these nine pressure increments is 5280 pounds per square inch.

The normal displacements, the radial moment distributions, and the hoop moment distributions for several values of pressure are shown in Figures 17, 18, and 19, respectively. The radial moment curves in Figure 18 show the zero position of the curves shifting towards the inside radius as the pressure is increased. This shifting is taking place because a plastic hinge is forming at the inside radius, and the support condition is changing from a fixed support to a pin support.

Figure 20 shows the radial and hoop moments at the inside radius and the radial moment, hoop moment, and normal displacement at a radius equal to 11.5 inches changing with applied pressure. The tangent lines shown in the figure are the corresponding linear values.

The stress distributions at radii 10.0 and 11.5 inches are shown in Figures 21 and 22, respectively.

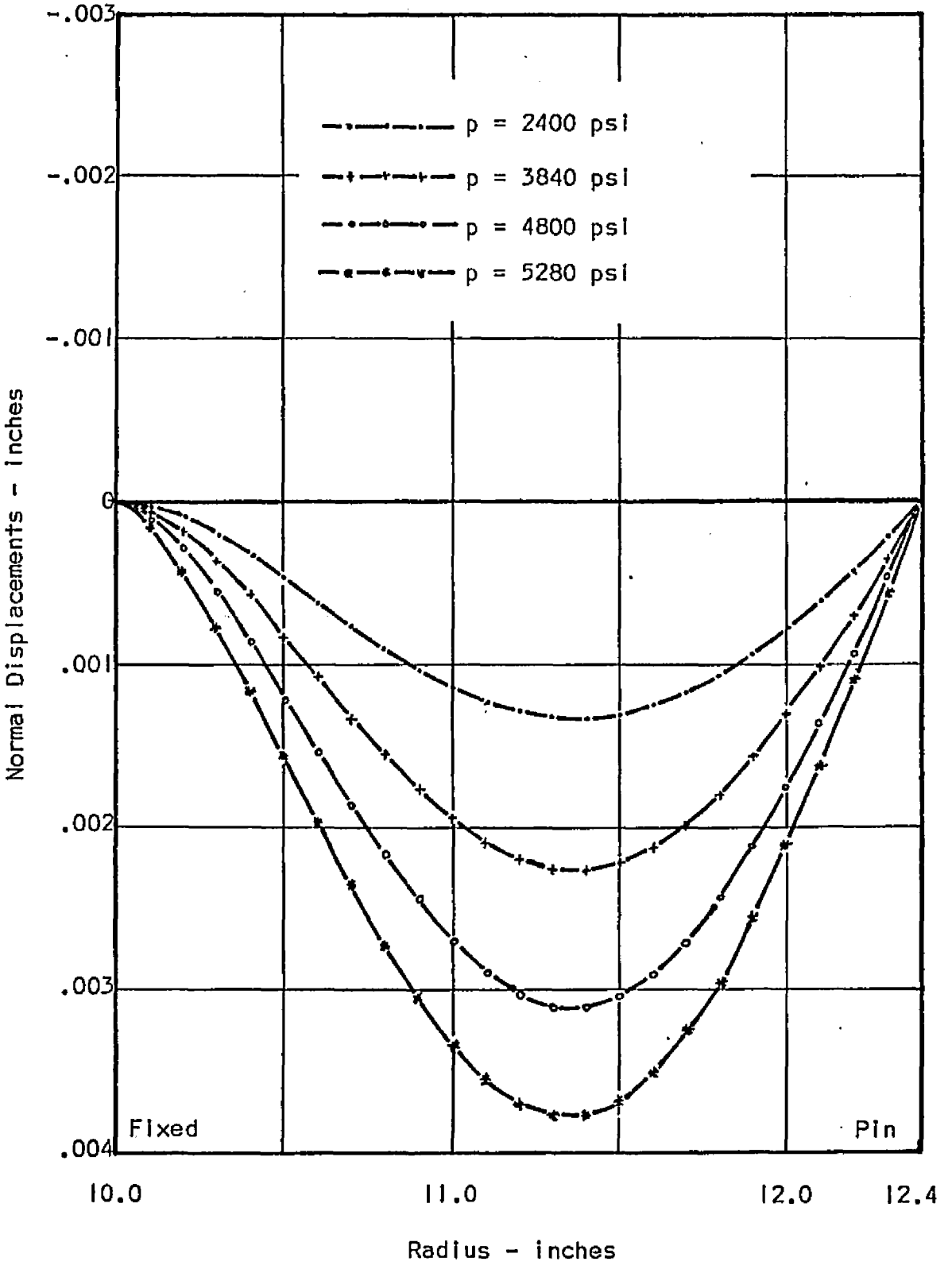

Figure 17. Flat Plate - Normal Displacements

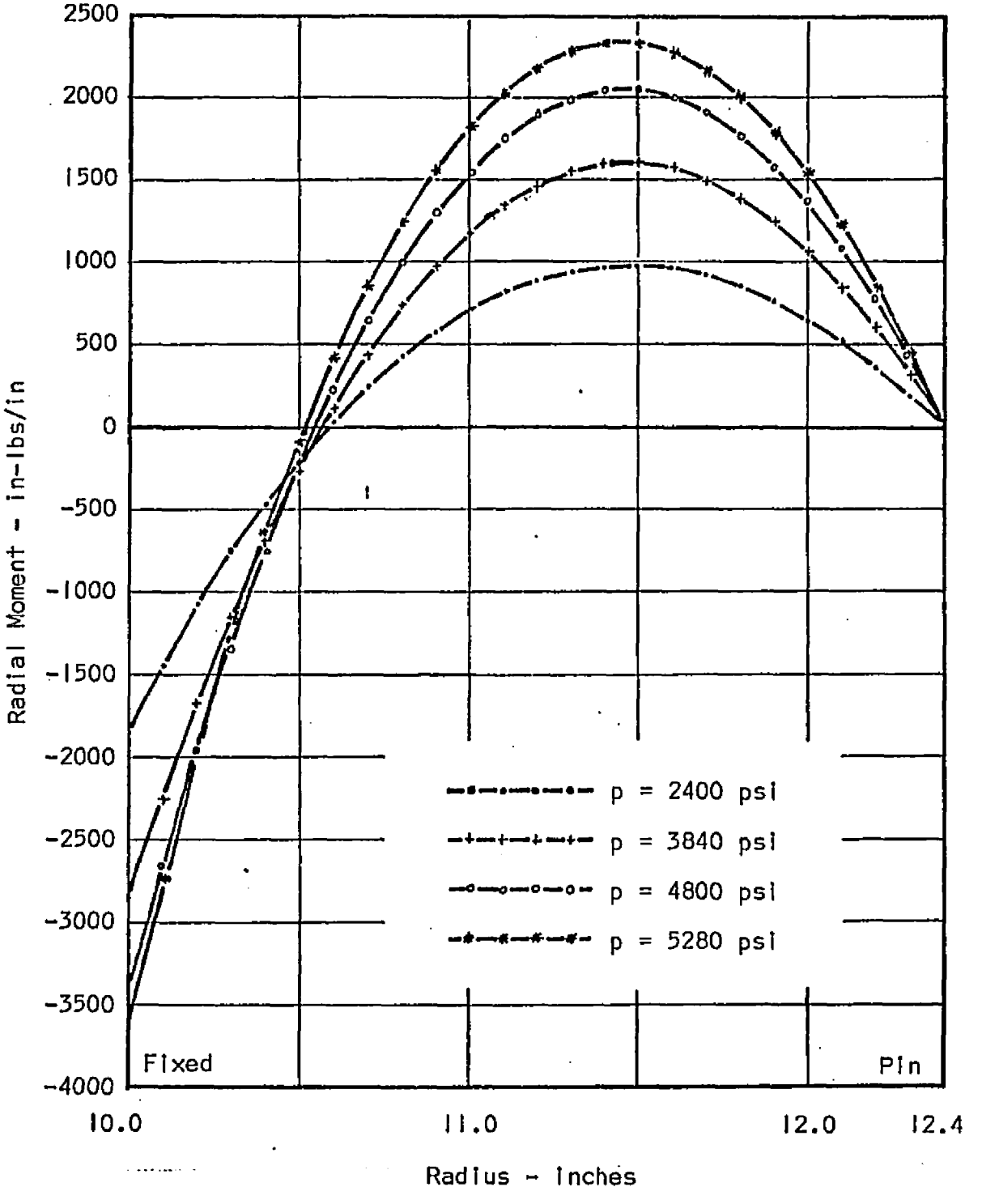

Figure 18. Flat Plate - Radial Moment Distributions

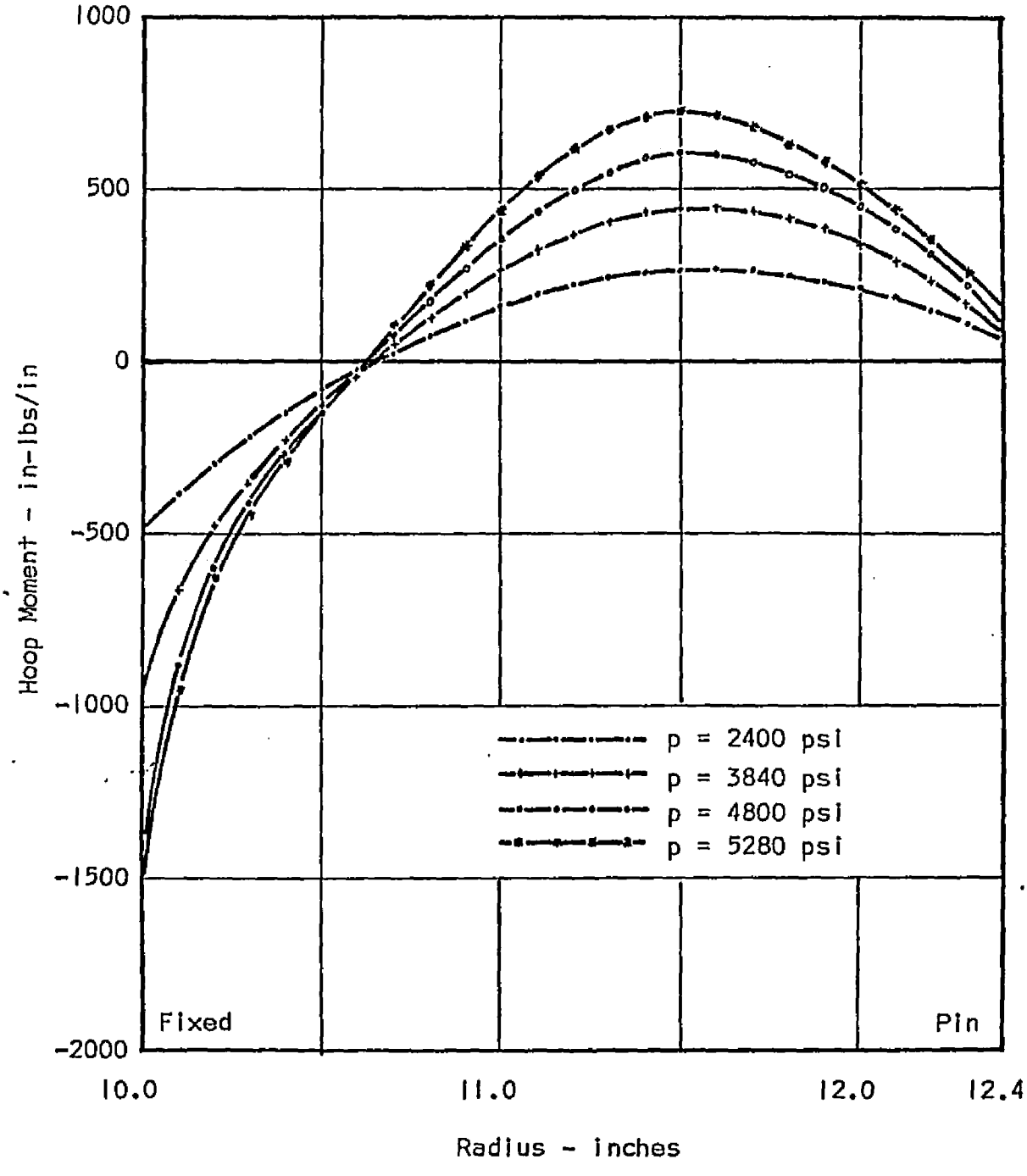

Figure 19. Flat Plate - Hoop Moment Distributions

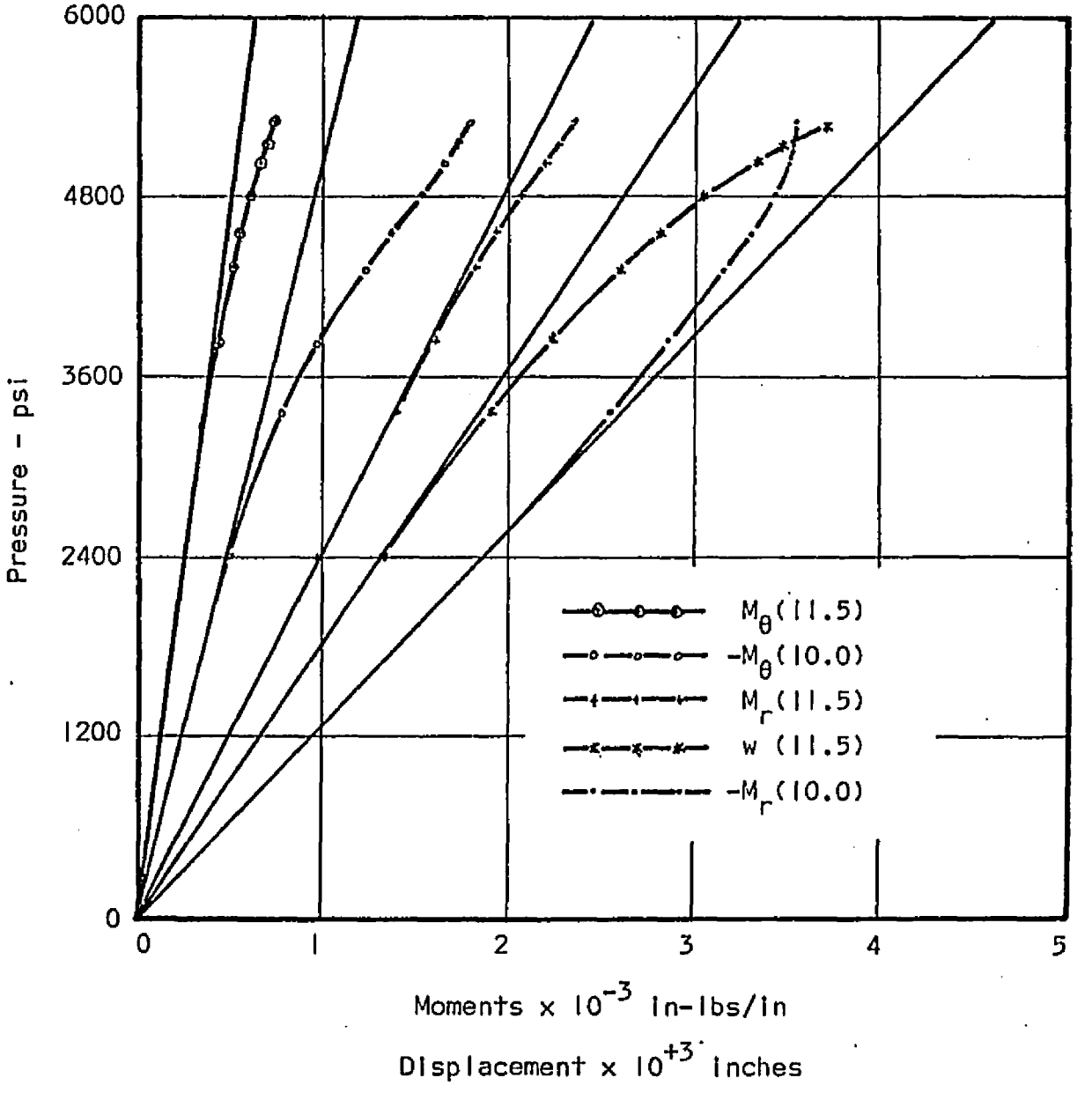

Figure 20. Flat Plate - Variables Changing with Pressure

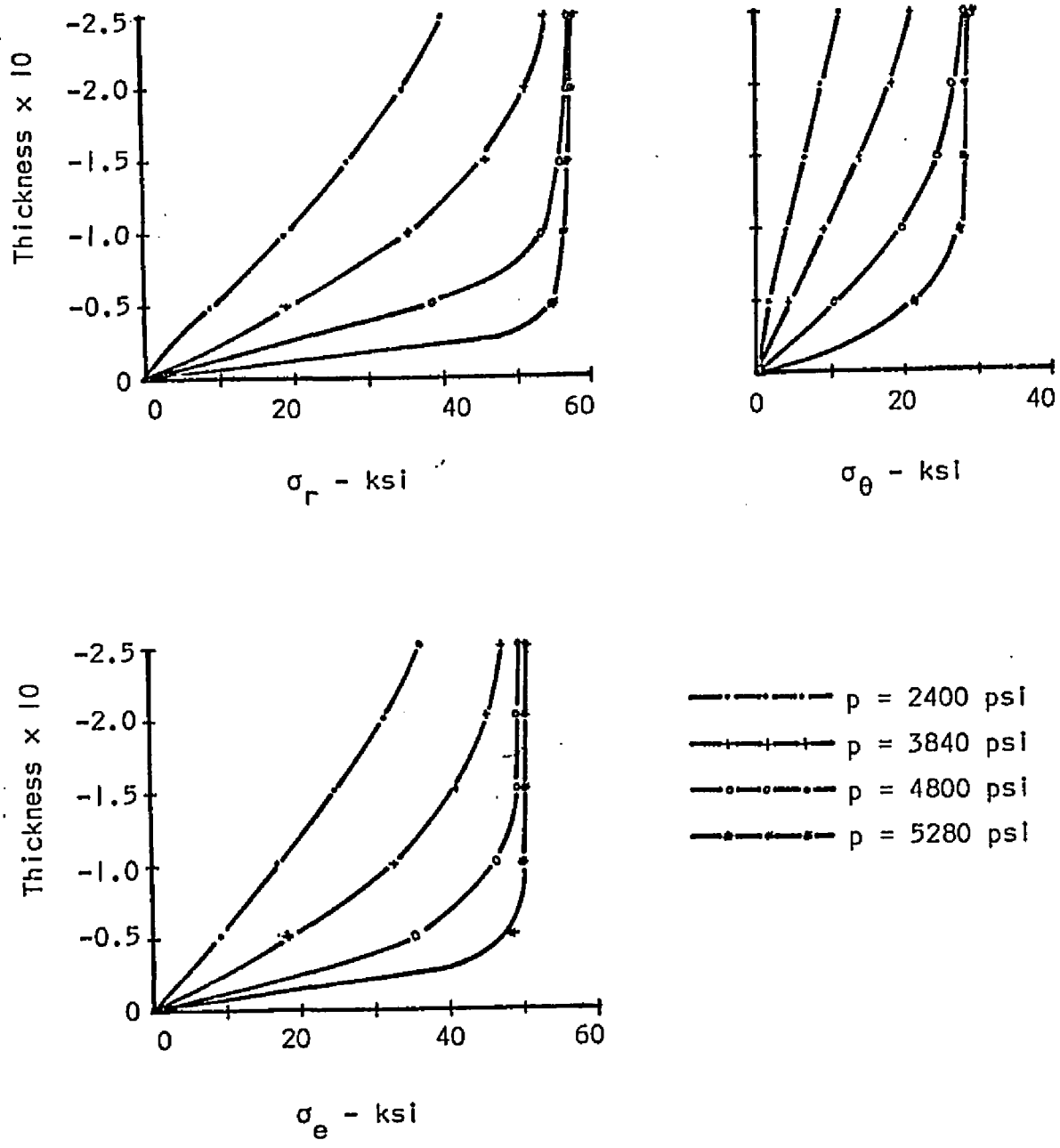

Figure 21. Flat Plate - Stress Distributions at 10.0 Inches

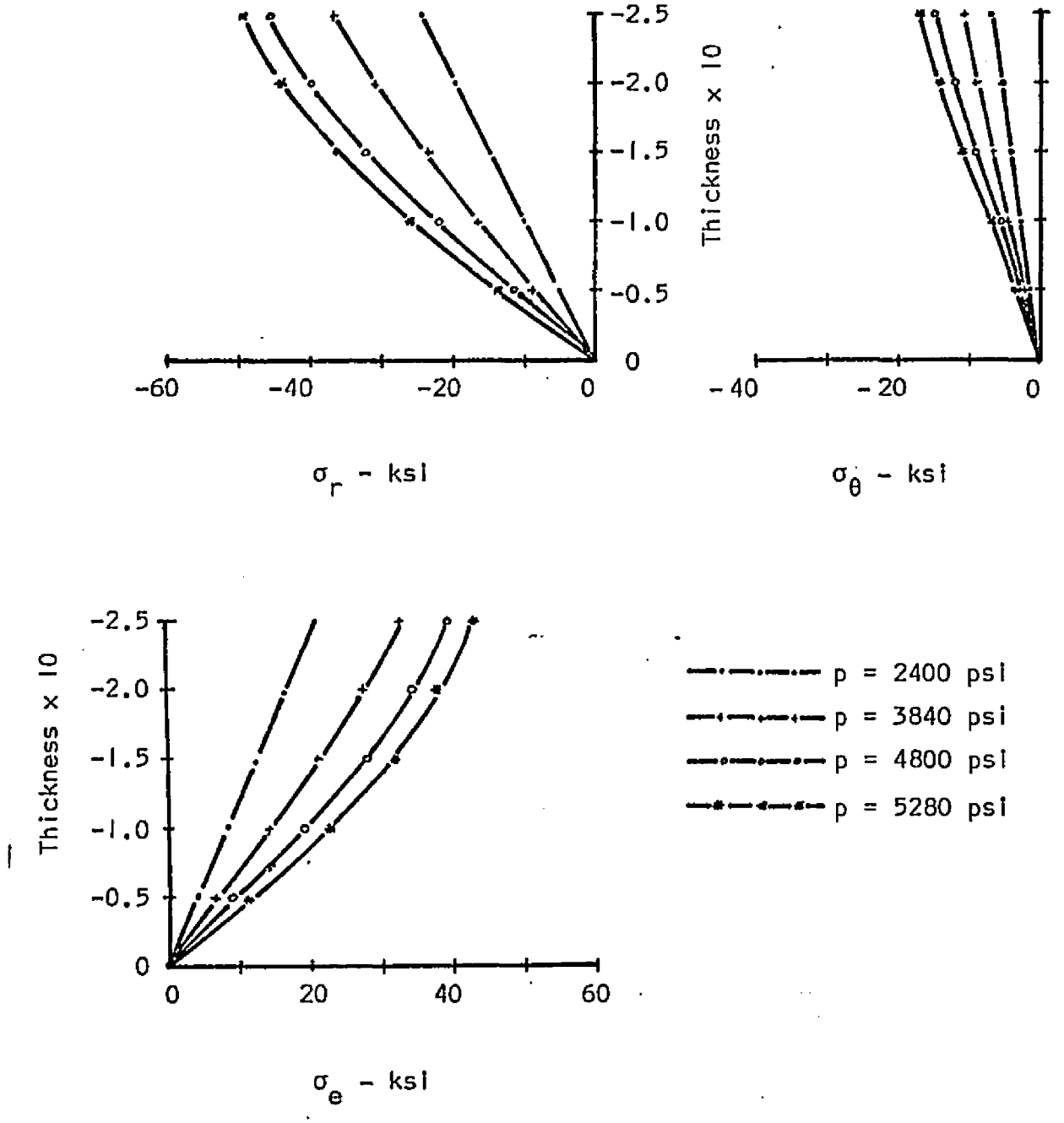

Figure 22. Flat Plate - Stress Distributions at 11.5 Inches

Torispherical Shell

Khojesteh-Bakht and Popov (1970) analyzed a torispherical shell using an incremental tangent stiffness finite element method. The model used by Khojesteh-Bakht and Popov consisted of forty-seven elements: twenty for the spherical section, sixteen for the toroidal section, and eleven for the cylinder. Twenty layers are used through the thickness.

Figure 23 shows the geometry of the shell which has a thickness of 0.04 inches. The material properties are modulus of elasticity, 30000000 pounds per square inch; Poisson's ratio, 0.3; and ultimate stress, 30000 pounds per square inch. The material is assumed to be elastic-perfectly plastic.

This shell is analyzed here using the method developed in this dissertation. In addition to the geometry, Figure 23 shows the eight elements used to model the shell; three for the spherical section, two for the toroidal section, and three for the cylinder. Twenty-five stations are used along the meridian of each element. Five points are used through the thickness of element numbers 1, 2, 7, and 8 (see Figure 23) and eleven points are used for the other four elements. Five points can be used for element numbers 1, 2, 7, and 8 because the portions of the shell modeled by these elements remain elastic. A nonlinear shape factor of ten is used to represent the elastic-perfectly plastic material.

Figure 24 shows the normal displacement of the apex of the sphere versus applied internal pressure for both methods of analysis.

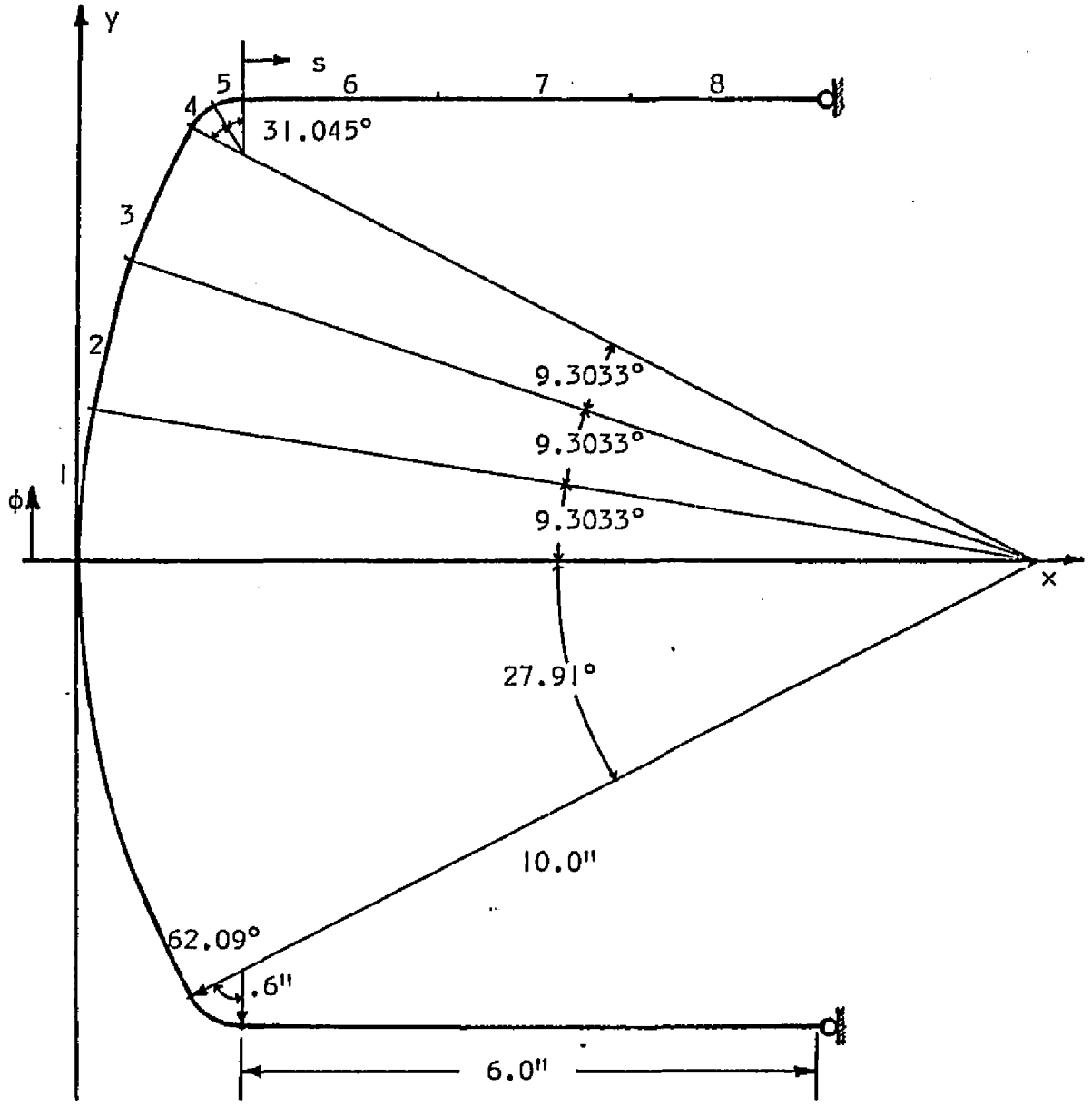

1 - Spherical Element Number

2, 3, 4, 5 - Toroidal Element Numbers

6, 7, 8 - Conical Element Numbers

Figure 23. Torispherical Shell - Geometry and Elements

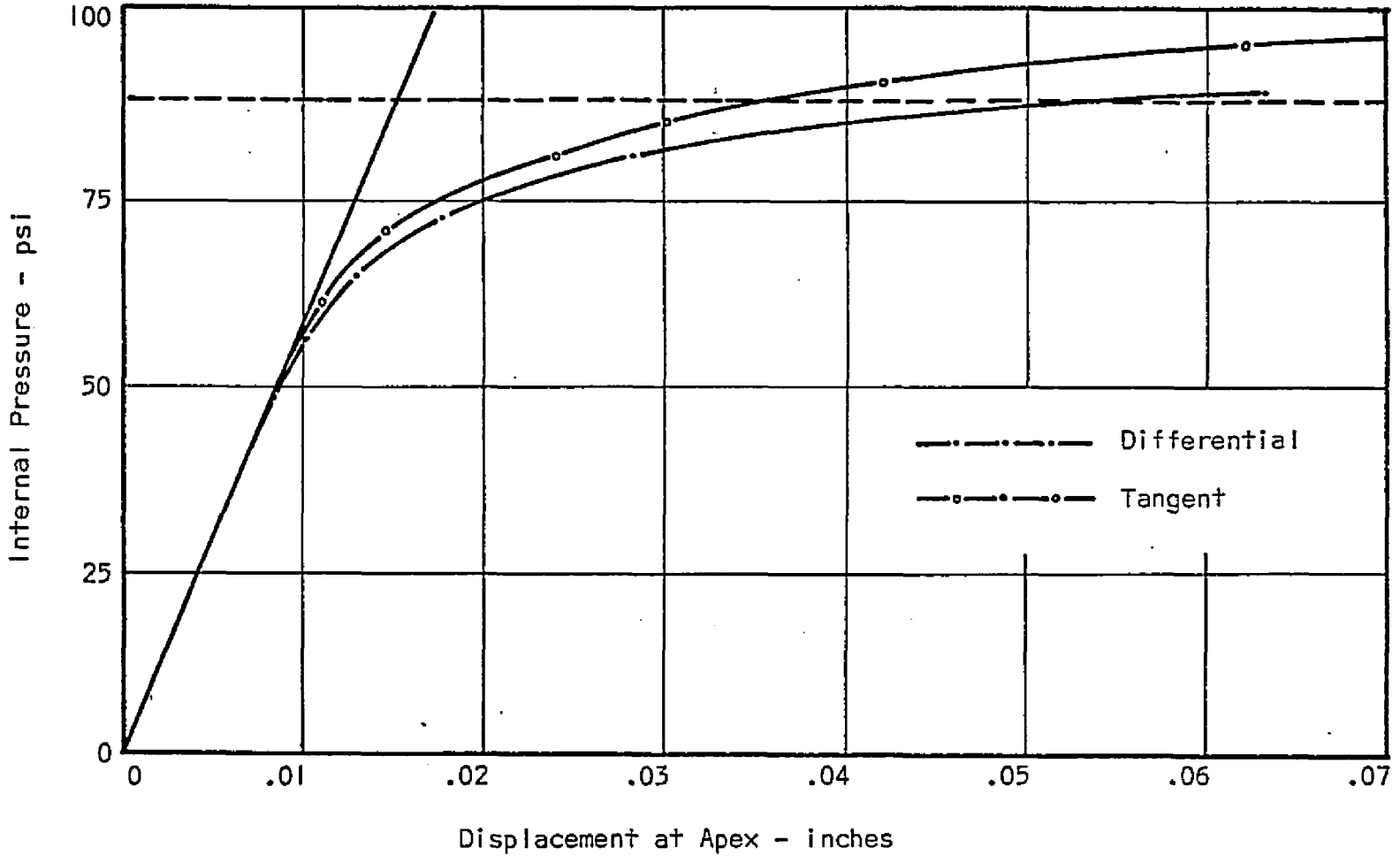

Figure 24. Torispherical Shell - Displacement at Apex

In the tangent stiffness method, the pressure increments are 1.5 pounds per square inch, and in the differential method used here, pressure increments of 8 pounds per square inch are used. The horizontal dashed line at approximately 87.5 pounds per square inch is the collapse load calculated by Khojesteh-Bakht and Popov (1970) using the limit analysis solution for torispherical shells presented by Drucker and Shield (1959). The results from the differential method indicate that the collapse is close to 88 pounds per square inch.

Figures 25, 26, and 27 show the normal displacements, the meridional moment distribution, and the hoop force distributions of element numbers 3, 4, 5, and 6 for several values of internal pressure. The other four elements are, for all practical purposes, in an elastic membrane state of stress.

Figure 28 shows the stress paths of several points on the shell as the pressure is increased. All the paths start at the origin and move outward. Seven points are plotted for each curve at internal pressures of 32, 40, 48, 56, 64, 72, and 80 pounds per square inch. Some of the points are outside of the ellipse because the yield surface is allowed to expand beyond the 30000 pounds per square inch value. These curves show that the loading is not proportional.

Figures 29 and 30 show the stress and strain distributions through the thickness of two stations.

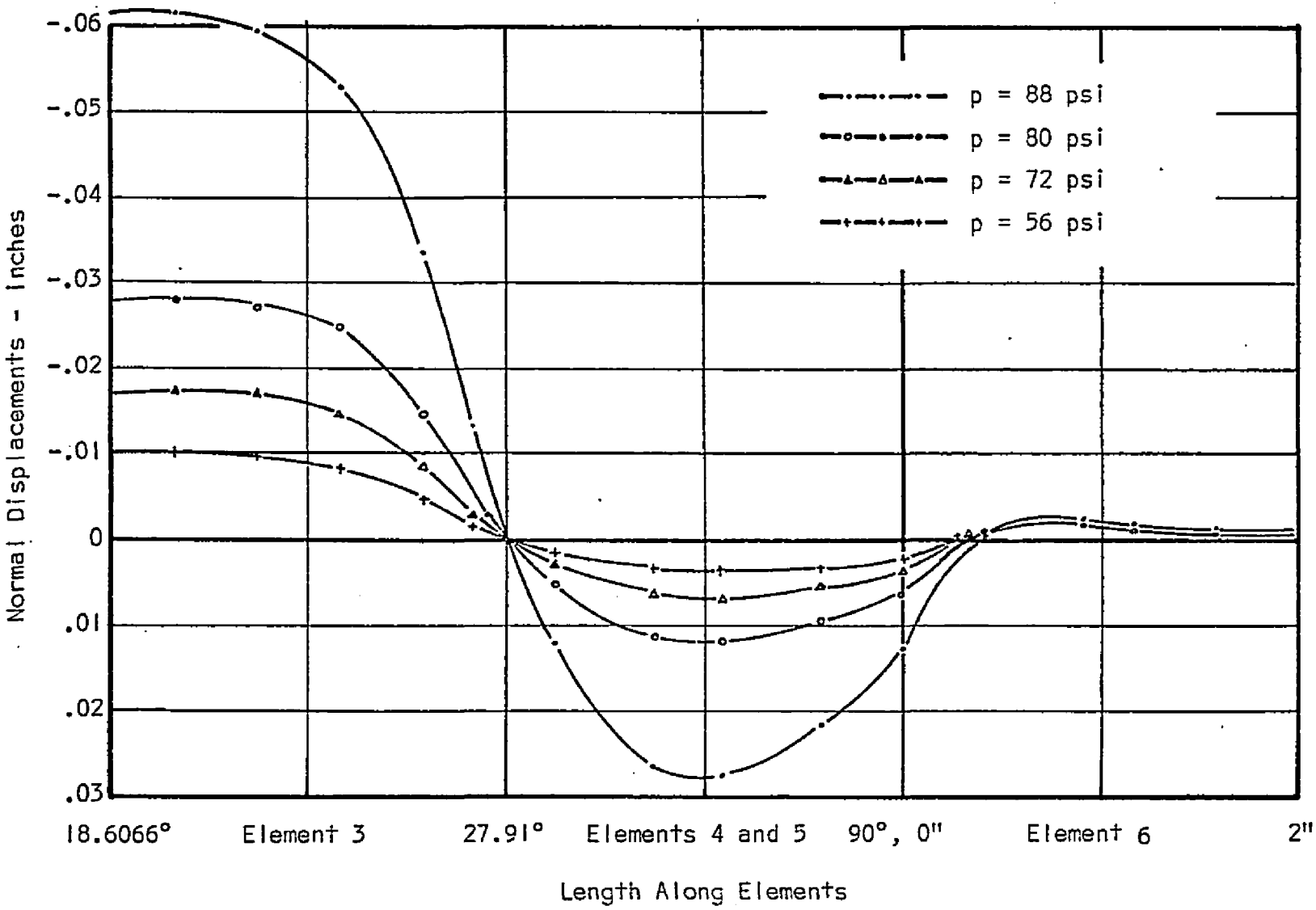

Figure 25. Torispherical Shell - Normal Displacements

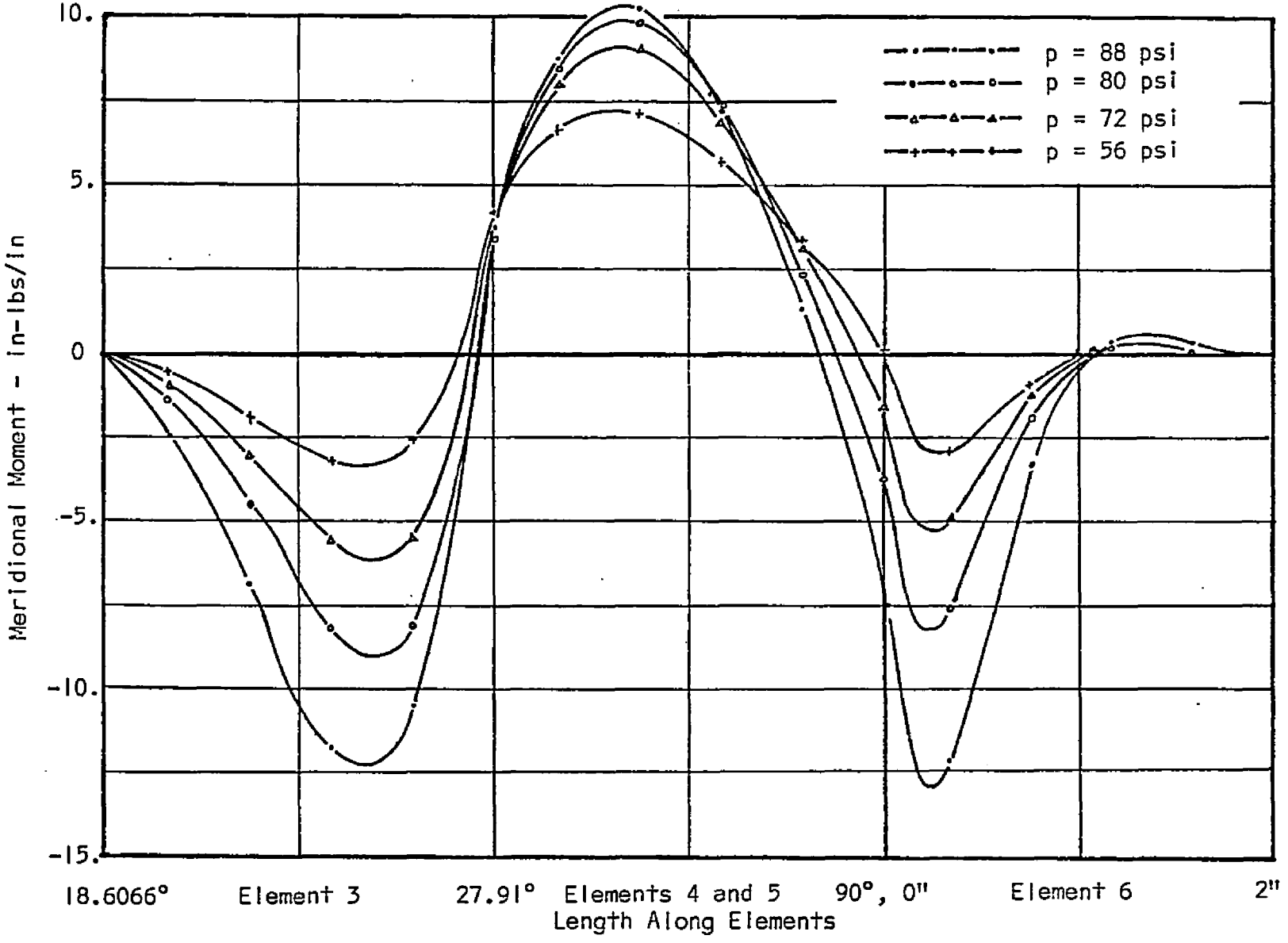

Figure 26. Torispherical Shell - Meridional Moment Distributions

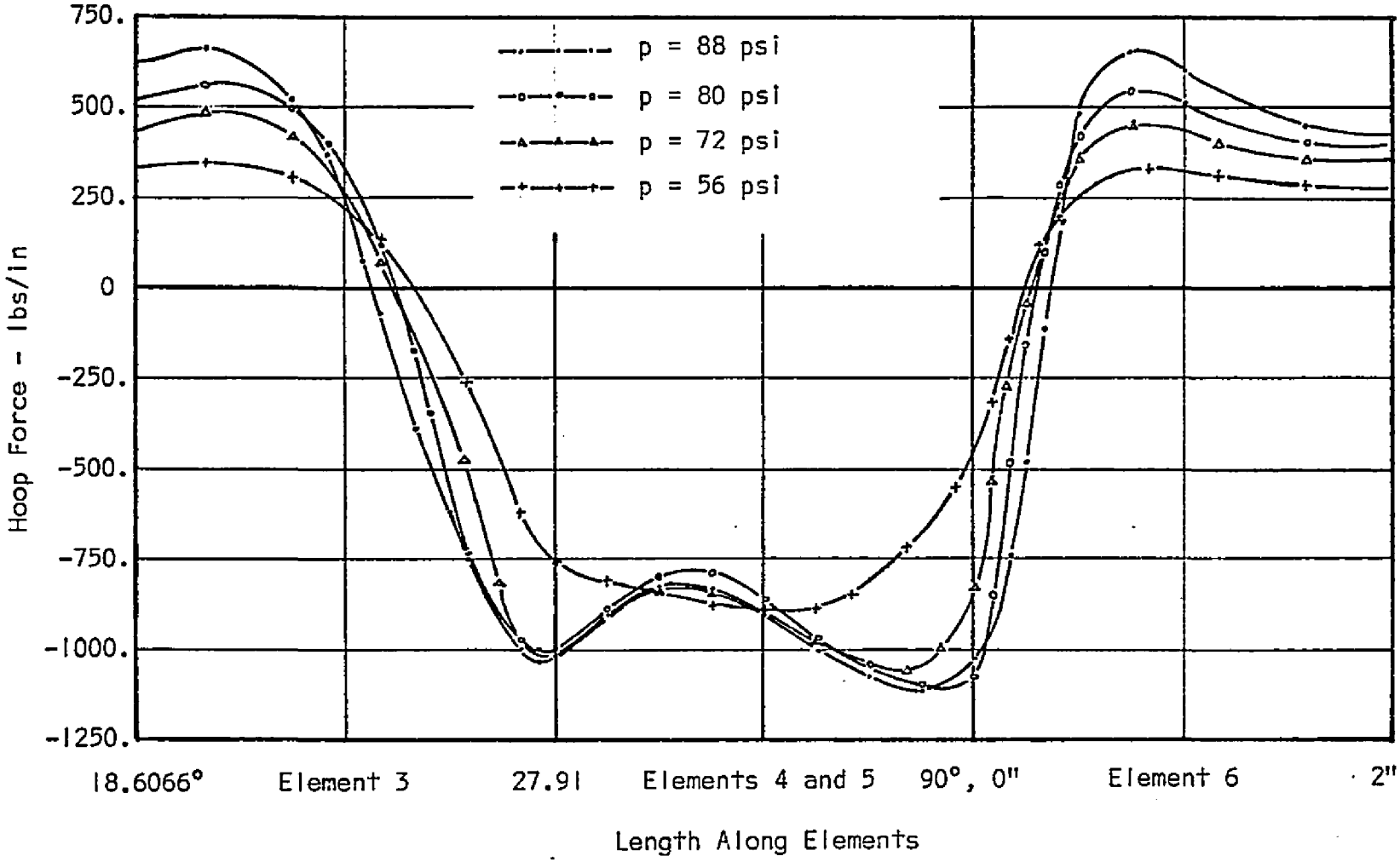

Figure 27. Torispherical Shell - Hoop Force Distributions

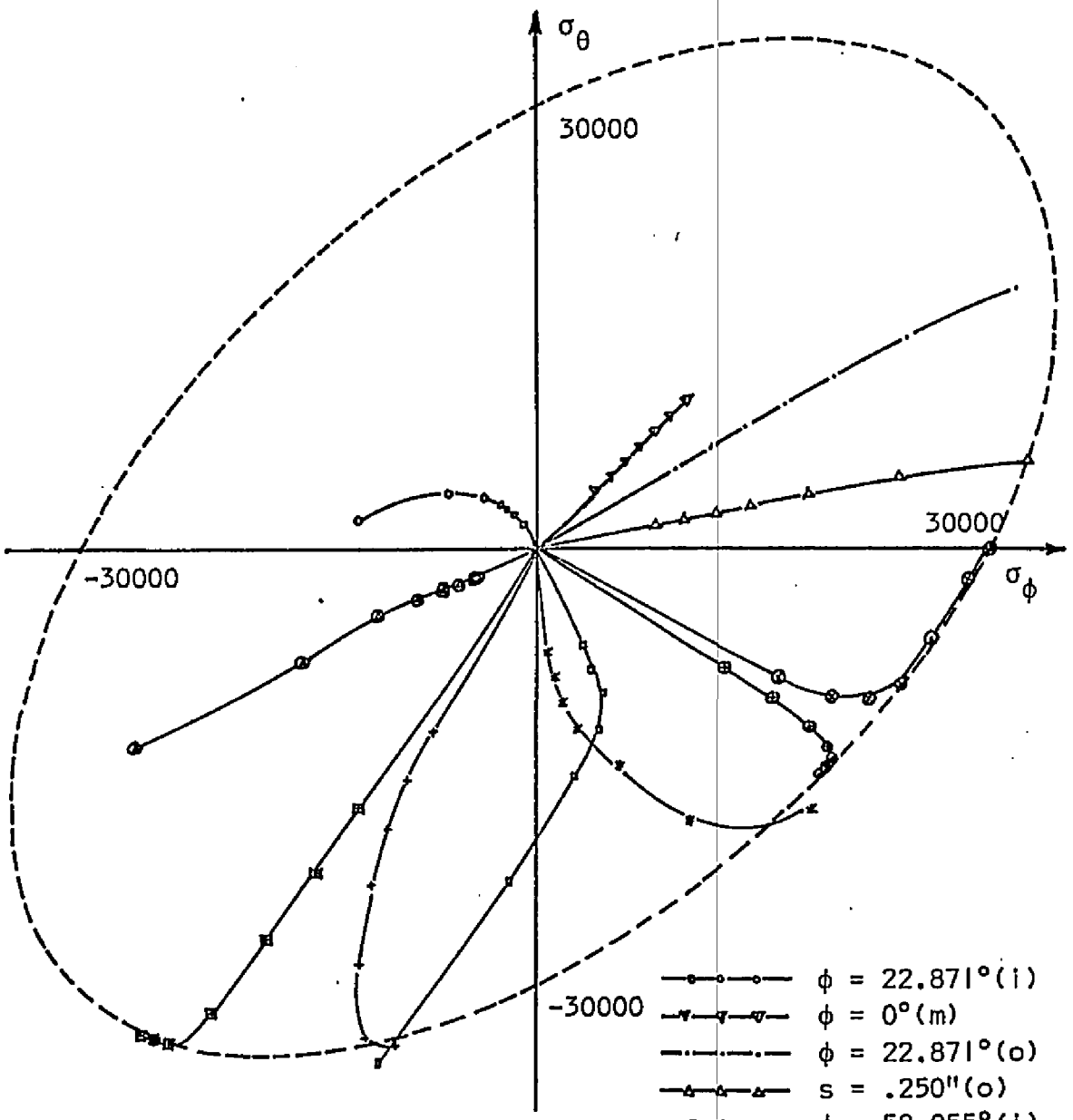

Figure 28. Torispherical Shell - Stress Paths

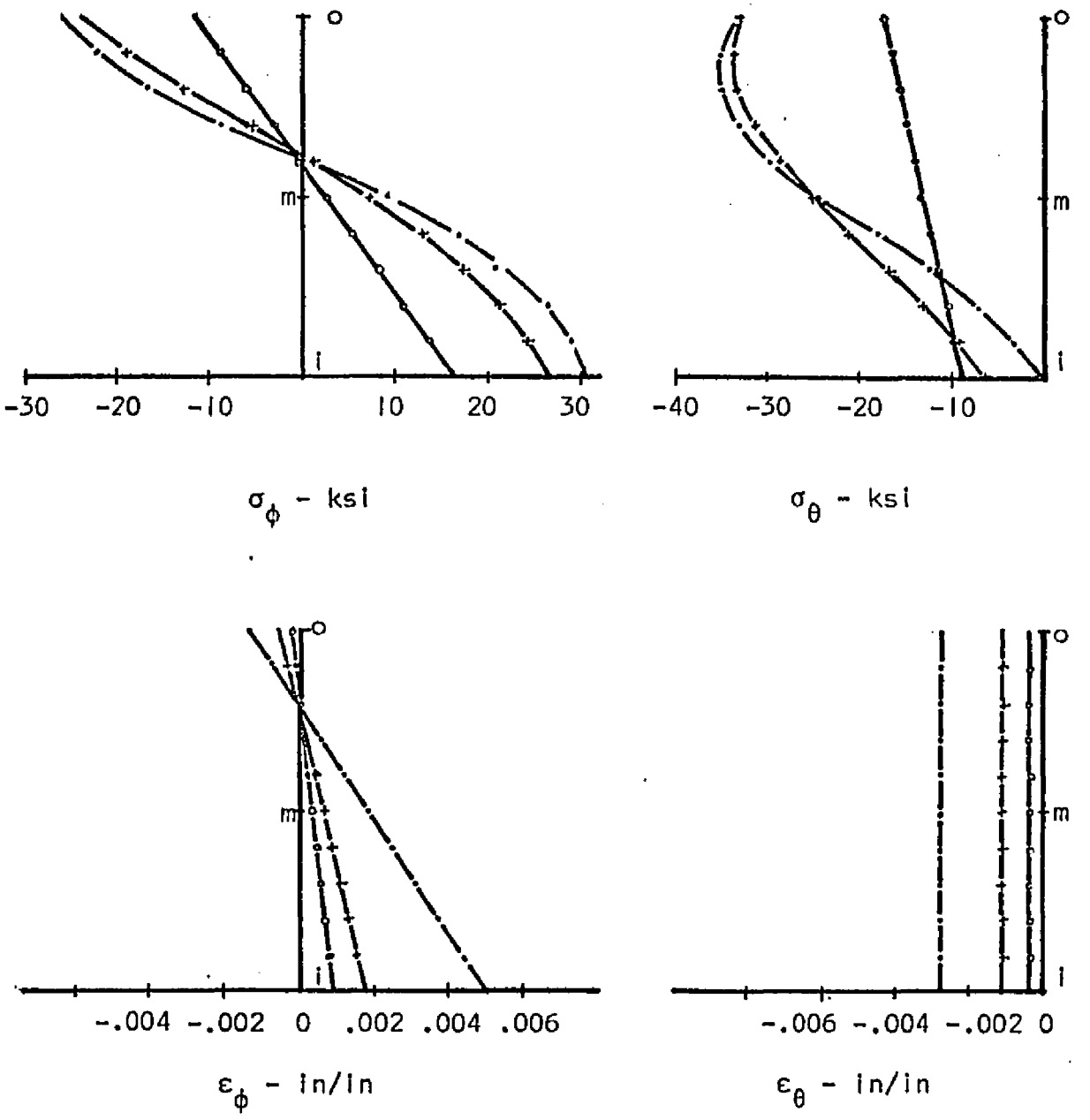

Figure 29. Torispherical Shell - Stress and Strain Distributions at $\phi = 58.955°$

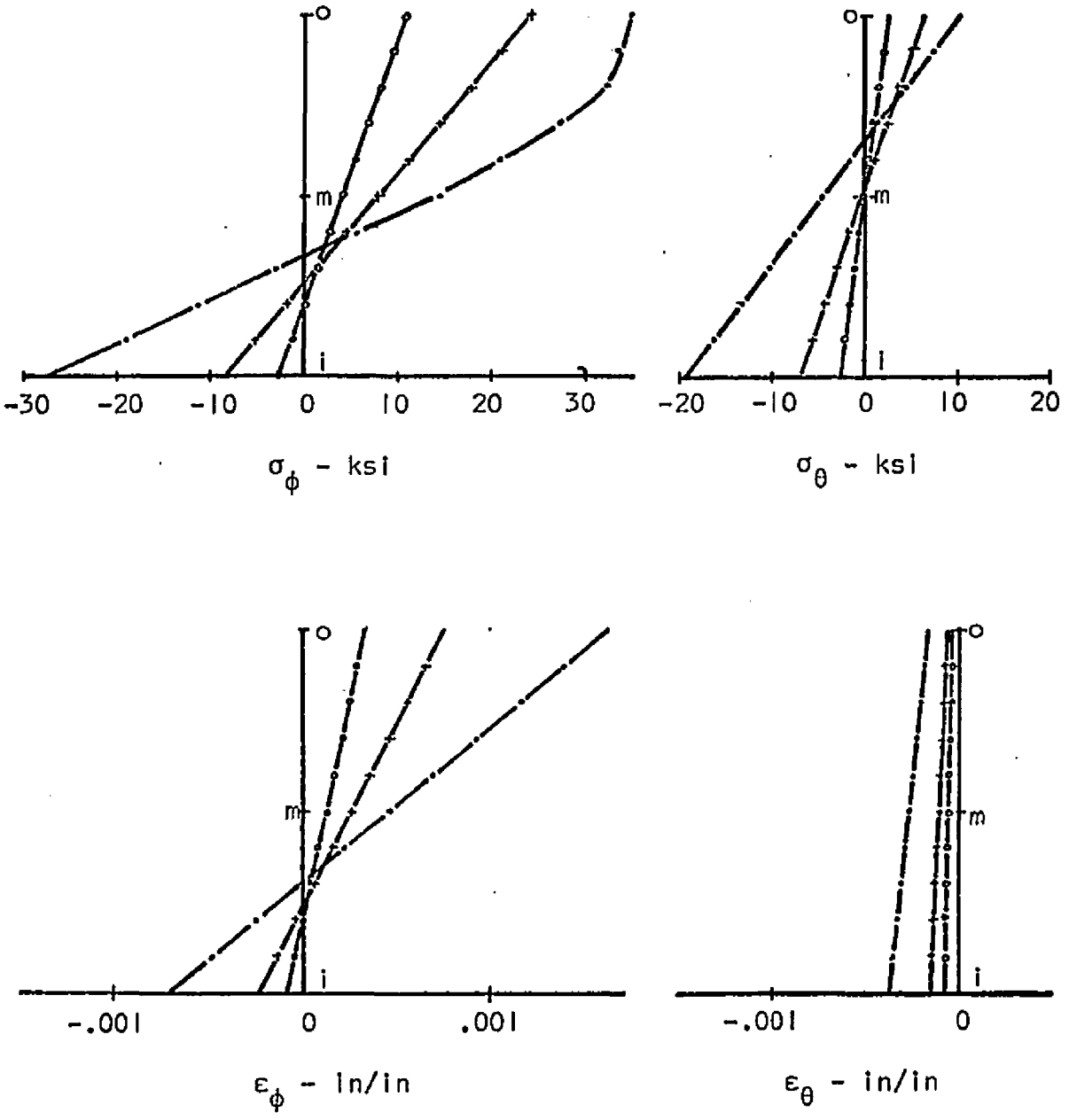

Figure 30. Torispherical Shell - Stress and Strain Distributions at $\phi = 25.186°$

CHAPTER 6

SUMMARY AND CONCLUSION

A direct numerical method for analyzing arbitrarily-shaped shells of revolution loaded beyond the yield point of the material is developed and presented. The development is based on an incremental theory of plasticity for strain-hardening materials. Plastic stress-strain relations for strain-hardening materials are differential (rate) equations. Since the stress-strain relations are in a differential (rate) form, the conclusion is reached that the equilibrium equations, the strain-displacement relations, and the stress resultants must also be in a differential form. By considering two loading states, the equilibrium equations and the strain-displacement relations can be written in differential form. The stress rate resultants are determined by integrating the stress rates through the thickness. After considerable algebra, the rate equilibrium equations, the rate strain-displacement relations, and the stress rate resultants may be written as six first order linear differential equations (in terms of the rate variables) with nonconstant coefficients.

The shell structure is divided into a finite number of elements, and a procedure for determining the differential stiffness matrices of these elements is presented. The differential displacement method for analyzing nonlinear structural systems is used to determine the nodal point rate displacements. These displacements and the

element stiffness matrices are used to determine the initial values at the I-end of each element. Using these initial values, the shell equations are numerically integrated along the meridian to determine the internal rate forces and the rate displacements at the element stations. The stresses, strains, internal forces, and displacements are obtained by integrating the corresponding rate quantities with respect to the applied loading condition. A fourth-order Runge-Kutta numerical integrating procedure is used throughout.

The shell equations presented in this dissertation are derived from the basic definitions of the nonlinear (material) shell variables. All the assumptions and restrictions needed to derive these equations are discussed in detail. A special effort is made to insure that the physical quantities are properly interpreted mathematically, and as a result, the shell equations are both mathematically and physically sound and can be used with confidence to analyze shell structures made from strain-hardening materials.

APPENDIX A

AN EXAMINATION OF THE SINGULAR TERMS

In Chapter 3 the equations are presented for the spherical and flat plate elements. These equations have many singular terms where ϕ and r are equal to zero. In this appendix these equations are examined to determine if the singularities can be removed. The reason for removing these singularities at the origin is to obtain solutions for closed shells. Many special conditions exist at the origin. For example, the quantities $\dot{v}$ and $\dot{\beta}$ are zero by symmetry. The stress rate resultants, $\dot{N}_\phi$, $\dot{N}_\theta$, $\dot{M}_\phi$, $\dot{M}_\theta$, and $\dot{Q}_\phi$, the rate displacement quantities, $\dot{v}$, $\dot{w}$, and $\dot{\beta}$, the stress rates, $\dot{\sigma}_\phi$ and $\dot{\sigma}_\theta$, and the strain rates, $\dot{\varepsilon}_\phi$ and $\dot{\varepsilon}_\theta$, are assumed to be continuous functions of ϕ (or r) and can be differentiated as required.

Spherical Element

The strain-displacement relations, Equation (3.4), are the first functions to be evaluated at the origin. The hoop strain rate, $\dot{\varepsilon}_\theta(z, \phi)$, has two terms which have the indeterminate form of 0/0 as ϕ approaches zero.

$$\dot{\varepsilon}_\theta(z, \phi)\Big|_{\phi \to 0} = \frac{l}{a}\left\{\frac{0}{0}\right\} - \frac{w}{a} - \frac{z}{a}\left\{\frac{0}{0}\right\}$$

L'Hospital's rule is used to evaluate these terms. The hoop strain rate becomes

$$\dot{\varepsilon}_\theta(z, \phi)\Big|_{\phi \to 0} = \left[\frac{\frac{d\dot{v}}{d\phi}\cos\phi - \dot{v}\sin\phi}{a\cos\phi} - \frac{\dot{w}}{a} - \frac{z}{a}\frac{\{\frac{d\dot{\beta}}{d\phi}\cos\phi - \dot{\beta}\sin\phi\}}{a\cos\phi}\right]$$

$$= \left[\frac{1}{a}\frac{d\dot{v}}{d\phi} - \frac{\dot{w}}{a} - \frac{z}{a}\frac{d\dot{\beta}}{d\phi}\right]_{\phi \to 0} \qquad (A.1)$$

which is identical to the meridional strain rate, $\dot{\varepsilon}_\phi(z, \phi)$, evaluated at the origin.

In order to determine the relationship between the stress rates, $\dot{\sigma}_\phi(z, \phi)$ and $\dot{\sigma}_\theta(z, \phi)$, at the origin, the plastic stress-strain relations must be examined. The material is initially isotropic and homogeneous, and the initial relationship between the terms of the plastic stress-strain relations are

$$k_{11} = k_{22} \qquad k_{12} = k_{21}$$

The initial relationship between the stress rates is determined from the relations between the k's and the equality of the strain rates. Initially the stress rates are found to be equal

$$\dot{\sigma}_\phi = \dot{\sigma}_\theta$$

Since the stresses, σ_ϕ and σ_θ, are determined from the stress rates, the initial values of the stresses are equal.

$$\sigma_\phi = \sigma_\theta$$

The terms k_{11}, k_{12}, k_{21}, and k_{22} are functions of the stresses (and other quantities), and since the initial values of the stresses have been shown to be equal, the subsequent relationships between the k's must be the same as given above. Also, the subsequent relationships between the stress rates and the stresses are the same as the ones given above. Therefore, the stress rates are equal at the origin.

The relationships between the stiffness terms, K, B, and D, are established from the relationships between the k's and Equations (2.33) and (2.38). The relationships are

$$K_{11} = K_{22} \qquad K_{12} = K_{21}$$

$$B_{11} = B_{22} \qquad B_{12} = B_{21}$$

$$D_{11} = D_{22} \qquad D_{12} = D_{21} \tag{A.2}$$

The stress rate resultants are the next functions to be considered. Since the stress rates are equal at the origin, a reasonable assumption might be that the stress rate resultants are also equal (i.e., $\dot{N}_\phi = \dot{N}_\theta$ and $\dot{M}_\phi = \dot{M}_\theta$). However, to show that the stress rate resultants are, in fact, equal, Equations (2.34), (2.35), (2.36), and (2.37) are modified for the geometry of the spherical element and are evaluated at the apex of the sphere. The modified stress rate resultants are

$$\dot{N}_\phi = \frac{K_{11}}{a}\frac{d\dot{v}}{d\phi} - \frac{K_{11}\dot{w}}{a} - \frac{B_{11}}{a}\frac{d\dot{\beta}}{d\phi} + \frac{K_{12}\dot{v}\cos\phi}{a\sin\phi} - \frac{K_{12}\dot{w}}{a} - \frac{B_{12}\dot{\beta}\cos\phi}{a\sin\phi}$$

$$\dot{N}_\theta = \frac{K_{21}}{a}\frac{d\dot{v}}{d\phi} - \frac{K_{21}\dot{w}}{a} - \frac{B_{21}}{a}\frac{d\dot{\beta}}{d\phi} + \frac{K_{22}\dot{v}\cos\phi}{a\sin\phi} - \frac{K_{22}\dot{w}}{a} - \frac{B_{22}\dot{\beta}\cos\phi}{a\sin\phi}$$

$$\dot{M}_\phi = \frac{B_{11}}{a}\frac{d\dot{v}}{d\phi} - \frac{B_{11}\dot{w}}{a} - \frac{D_{11}}{a}\frac{d\dot{\beta}}{d\phi} + \frac{B_{12}\dot{v}\cos\phi}{a\sin\phi} - \frac{B_{12}\dot{w}}{a} - \frac{D_{12}\dot{\beta}\cos\phi}{a\sin\phi}$$

$$\dot{M}_\theta = \frac{B_{21}}{a}\frac{d\dot{v}}{d\phi} - \frac{B_{21}\dot{w}}{a} - \frac{D_{21}}{a}\frac{d\dot{\beta}}{d\phi} + \frac{B_{22}\dot{v}\cos\phi}{a\sin\phi} - \frac{B_{22}\dot{w}}{a} - \frac{D_{22}\dot{\beta}\cos\phi}{a\sin\phi} \qquad (A.3)$$

The terms containing the quantities $\dot{v}/\sin\phi$ and $\dot{\beta}/\sin\phi$ in the above equations have the indeterminate form of 0/0 as ϕ approaches zero. L'Hospital's rule is used to evaluate these terms, and the results are

$$\dot{N}_\phi\Big|_{\phi \to 0} = \left[\frac{K_{11}}{a}\frac{d\dot{v}}{d\phi} - \frac{K_{11}\dot{w}}{a} - \frac{B_{11}}{a}\frac{d\dot{\beta}}{d\phi} + \frac{K_{12}}{a}\frac{d\dot{v}}{d\phi} - \frac{K_{12}\dot{w}}{a} - \frac{B_{12}}{a}\frac{d\dot{\beta}}{d\phi}\right]_{\phi \to 0}$$

$$\dot{N}_\theta\Big|_{\phi \to 0} = \left[\frac{K_{21}}{a}\frac{d\dot{v}}{d\phi} - \frac{K_{21}\dot{w}}{a} - \frac{B_{21}}{a}\frac{d\dot{\beta}}{d\phi} + \frac{K_{22}}{a}\frac{d\dot{v}}{d\phi} - \frac{K_{22}\dot{w}}{a} - \frac{B_{22}}{a}\frac{d\dot{\beta}}{d\phi}\right]_{\phi \to 0}$$

$$\dot{M}_\phi\Big|_{\phi \to 0} = \left[\frac{B_{11}}{a}\frac{d\dot{v}}{d\phi} - \frac{B_{11}\dot{w}}{a} - \frac{D_{11}}{a}\frac{d\dot{\beta}}{d\phi} + \frac{B_{12}}{a}\frac{d\dot{v}}{d\phi} - \frac{B_{12}\dot{w}}{a} - \frac{D_{12}}{a}\frac{d\dot{\beta}}{d\phi}\right]_{\phi \to 0}$$

$$\dot{M}_\theta\Big|_{\phi \to 0} = \left[\frac{B_{21}}{a}\frac{d\dot{v}}{d\phi} - \frac{B_{21}\dot{w}}{a} - \frac{D_{21}}{a}\frac{d\dot{\beta}}{d\phi} + \frac{B_{22}}{a}\frac{d\dot{v}}{d\phi} - \frac{B_{22}\dot{w}}{a} - \frac{D_{22}}{a}\frac{d\dot{\beta}}{d\phi}\right]_{\phi \to 0} \qquad (A.4)$$

The equalities of the stress rate resultants are established by substituting Equation (A.2) in the above equations.

The six first order differential equations for the spherical element (Equation 3.5) are the next functions to be examined. After considerable algebra and by employing the L'Hospital rule to evaluate the indeterminate terms, the first three differential equations evaluated at the origin become

$$\left.\frac{d\dot{v}}{d\phi}\right|_{\phi \to 0} = \left[\frac{\dot{N}_\phi a T_3}{A_{11} K_{11} T_1} - \frac{\dot{M}_\phi a T_4}{A_{11} D_{11} T_1} + \dot{w}\right]_{\phi \to 0}$$

$$\left.\frac{d\dot{w}}{d\phi}\right|_{\phi \to 0} = 0$$

$$\left.\frac{d\dot{\beta}}{d\phi}\right|_{\phi \to 0} = \left[\frac{\dot{N}_\phi a T_5}{A_{11} K_{11} T_2} - \frac{\dot{M}_\phi a T_6}{A_{11} D_{11} T_2}\right]_{\phi \to 0} \qquad \text{(A.5)}$$

where

$$T_1 = 1. + \frac{C_1}{A_{11}} - \frac{C_2 C_3}{A_{11}\{A_{11} + C_4\}} \qquad T_2 = 1. + \frac{C_4}{A_{11}} - \frac{C_2 C_3}{A_{11}\{A_{11} + C_1\}}$$

$$T_3 = 1. + \frac{C_2 B_{11}}{D_{11}\{A_{11} + C_4\}} \qquad T_4 = \frac{B_{11}}{K_{11}} + \frac{C_2}{A_{11} + C_4}$$

$$T_5 = \frac{B_{11}}{D_{11}} + \frac{C_3}{A_{11} + C_1} \qquad T_6 = 1. + \frac{C_3 B_{11}}{K_{11}\{A_{11} + C_1\}} \qquad \text{(A.6)}$$

In order to evaluate the last three differential equations, a restriction is placed on the loading. The restriction is that concentrated loads are not allowed at the origin. This restriction makes $\dot{Q}_\phi(0)$ equal to zero, and with the conditions $\dot{N}_\phi(0) = \dot{N}_\theta(0)$ and $\dot{M}_\phi(0) = \dot{M}_\theta(0)$, the last three differential equations evaluated at the origin become

$$\left.\frac{d\dot{N}_\phi}{d\phi}\right|_{\phi \to 0} = \left[\frac{1}{2}\ \frac{d\dot{N}_\theta}{d\phi} - \frac{1}{2}\ a\dot{Y}\right]_{\phi \to 0} \tag{A.7}$$

$$\left.\frac{d\dot{Q}_\phi}{d\phi}\right|_{\phi \to 0} = \left[-\frac{a\dot{Z}}{z} - \dot{N}_\phi\right]_{\phi \to 0} \tag{A.8}$$

$$\left.\frac{d\dot{M}_\phi}{d\phi}\right|_{\phi \to 0} = \frac{1}{2}\ \left.\frac{d\dot{M}_\phi}{d\phi}\right|_{\phi \to 0} \tag{A.9}$$

If $\dot{Y}(0)$ is set to equal zero, Equation (A.6) becomes

$$\left.\frac{d\dot{N}_\phi}{d\phi}\right|_{\phi \to 0} = \frac{1}{2}\ \left.\frac{d\dot{N}_\theta}{d\phi}\right|_{\phi \to 0} \tag{A.10}$$

which is of the same form as Equation (A.9)

The two derivatives which have not been shown to have specific values at the origin are $\frac{d\dot{N}_\phi}{d\phi}(0)$ and $\frac{d\dot{M}_\phi}{d\phi}(0)$. The other derivatives

In order to evaluate the last three differential equations, a restriction is placed on the loading. The restriction is that concentrated loads are not allowed at the origin. This restriction makes $\dot{Q}_\phi(0)$ equal to zero, and with the conditions $\dot{N}_\phi(0) = \dot{N}_\theta(0)$ and $\dot{M}_\phi(0) = \dot{M}_\theta(0)$, the last three differential equations evaluated at the origin become

$$\left.\frac{d\dot{N}_\phi}{d\phi}\right|_{\phi \to 0} = \left[\frac{1}{2}\ \frac{d\dot{N}_\theta}{d\phi} - \frac{1}{2}\ aY\right]_{\phi \to 0} \tag{A.7}$$

$$\left.\frac{d\dot{Q}_\phi}{d\phi}\right|_{\phi \to 0} = \left[-\frac{a\dot{Z}}{z} - \dot{N}_\phi\right]_{\phi \to 0} \tag{A.8}$$

$$\left.\frac{d\dot{M}_\phi}{d\phi}\right|_{\phi \to 0} = \frac{1}{2}\ \left.\frac{d\dot{M}_\phi}{d\phi}\right|_{\phi \to 0} \tag{A.9}$$

If $\dot{Y}(0)$ is set to equal zero, Equation (A.6) becomes

$$\left.\frac{d\dot{N}_\phi}{d\phi}\right|_{\phi \to 0} = \frac{1}{2}\ \left.\frac{d\dot{N}_\theta}{d\phi}\right|_{\phi \to 0} \tag{A.10}$$

which is of the same form as Equation (A.9)

The two derivatives which have not been shown to have specific values at the origin are $\frac{d\dot{N}_\phi}{d\phi}(0)$ and $\frac{d\dot{M}_\phi}{d\phi}(0)$. The other derivatives

are known in terms of the stress rate resultants, rate displacement quantities, and the stiffness terms. The values of $\frac{d\dot{N}_\phi}{d\phi}(0)$ and $\frac{d\dot{M}_\phi}{d\phi}(0)$ cannot be determined in the present coordinate system because of the vanishing Jacobian at the apex of the shell. With the additional restriction that the spherical element be of constant thickness, the derivatives in Equations (A.9) and (A.10) can be evaluated. The point in question is physically no different than any other in the shell structure. In general, strains (here strain rates) are assumed to have continuous derivatives. As before, $k_{11}(z, 0) = k_{22}(z, 0)$ and $k_{12}(z, 0) = k_{21}(z, 0)$ which indicates that the material (at any constant z) has the same properties along any meridian. If the material properties are assumed to change in a smooth manner, then

$$\left.\frac{dk_{11}}{d\phi}\right|_{\phi \to 0} = \left.\frac{dk_{22}}{d\phi}\right|_{\phi \to 0} = \left.\frac{dk_{12}}{d\phi}\right|_{\phi \to 0} = \left.\frac{dk_{21}}{d\phi}\right|_{\phi \to 0} \equiv 0$$

From the assumption that the strain rates change in a smooth manner, geometric symmetry implies

$$\left.\frac{d\dot{\varepsilon}_\phi}{d\phi}\right|_{\phi \to 0} = \left.\frac{d\dot{\varepsilon}_\theta}{d\phi}\right|_{\phi \to 0} \equiv 0$$

But this implies

$$\left.\frac{d\dot{\sigma}_\phi}{d\phi}\right|_{\phi \to 0} = \left.\frac{d\dot{\sigma}_\theta}{d\phi}\right|_{\phi \to 0} \equiv 0$$

Since $\frac{d\dot{N}_\phi}{d\phi}(0)$ and $\frac{d\dot{M}_\phi}{d\phi}(0)$ are defined as

$$\frac{d\dot{N}_\phi}{d\phi} = \int_{-h/2}^{h/2} \frac{d\dot{\sigma}_\phi}{d\phi}\, dz \qquad \frac{d\dot{M}_\phi}{d\phi} = \int_{-h/2}^{h/2} \frac{d\dot{\sigma}_\phi}{d\phi}\, z dz \tag{A.11}$$

the desired result must be

$$\left.\frac{d\dot{N}_\phi}{d\phi}\right|_{\phi \to 0} = \left.\frac{d\dot{N}_\theta}{d\phi}\right|_{\phi \to 0} = \left.\frac{d\dot{M}_\phi}{d\phi}\right|_{\phi \to 0} = \left.\frac{d\dot{M}_\theta}{d\phi}\right|_{\phi \to 0} \equiv 0 \tag{A.12}$$

Flat Plate Element

The values of the first derivatives and the relationships between the stress rate resultants for the flat plate element at the center can be obtained in the same manner as is done for the spherical element. However, only the results are presented here.

$$\dot{N}_r\Big|_{r \to 0} = \dot{N}_\theta\Big|_{r \to 0} \qquad \dot{M}_r\Big|_{r \to 0} = \dot{M}_\theta\Big|_{r \to 0}$$

$$\left.\frac{d\dot{v}}{d\phi}\right|_{r \to 0} = \left[\frac{\dot{N}_r T_3}{A_{11} K_{11} T_1} - \frac{\dot{M}_r T_4}{A_{11} D_{11} T_1}\right]_{r \to 0}$$

$$\left.\frac{d\dot{w}}{dr}\right|_{r \to 0} = 0$$

$$\left.\frac{d\dot{\beta}}{dr}\right|_{r \to 0} = \left[\frac{\dot{N}_r T_5}{A_{11} K_{11} T_2} - \frac{\dot{M}_r T_6}{A_{11} D_{11} T_2}\right]_{r \to 0}$$

$$\left.\frac{d\dot{N}_r}{dr}\right|_{r \to 0} = \frac{1}{2} \left.\frac{d\dot{N}_\theta}{dr}\right|_{r \to 0} = 0$$

$$\left.\frac{d\dot{Q}_r}{dr}\right|_{r \to 0} = -\frac{1}{2} \left.\dot{Z}\right|_{r \to 0}$$

$$\left.\frac{d\dot{M}_r}{dr}\right|_{r \to 0} = \frac{1}{2} \left.\frac{d\dot{M}_\theta}{dr}\right|_{r \to 0} = 0 \qquad \text{(A.13)}$$

The values of T are given in Equation (A.6), and the same restrictions are placed on the flat plate element that are placed on the spherical element.

REFERENCES

Birchler, W. D., M. L. Callabresi, and J. E. Murray, "Finite Element Models for Shells of Revolution," EES Series Report No. 21, University of Arizona, 1968.

Callabresi, M. L., "Inelastic Stress Analysis of Solids," Doctoral Dissertation, University of Arizona, 1970.

Dong, Stanley B., "Analysis of Laminated Shells of Revolution," Journal of the Engineering Mechanics Division, ASCE, Vol. 92, No. EM6, (December, 1966).

Drucker, D. C., and R. T. Shield, "Limit Analysis of Symmetrically Loaded Thin Shells of Revolution," Journal of Applied Mechanics, Vol. 26, No. 1, (March, 1959), pp. 61-68.

Ellyin, F., and A. N. Sherbourne, "Limit Analysis of Axisymmetric Intersecting Shells of Revolution," Nuclear Structural Engineering, Vol. 2, No. 1, North-Holland Publishing Company, Amsterdam, (July, 1965), pp. 86-91.

Flugge, Wilhelm, Stresses in Shells, 3rd Printing, Springer-Verlag New York Inc., 1966.

Flugge, Wilhelm, and Tsuneyoski Nakamura, "Plastic Analysis of Shells of Revolution under Axisymmetric Loads," Ingenieur-Archiv, Vol. 34, n4, 1965, pp. 238-247.

Goldberg, J. E., and R. M. Richard, "Analysis of Nonlinear Structures," Journal of the Structural Division, ASCE, Vol. 89, No. ST4, (August, 1963).

Grafton, Peter E., and Donald R. Strome, "Analysis of Axisymmetrical Shells by the Direct Stiffness Method," AIAA Journal, Vol. 1, No. 10, (October, 1963), pp. 2342-2347.

Hannon, B. M., and O. M. Sidebottom, "Plastic Behavior of Open-End and Closed-End Thick-Walled Cylinders," ASME paper - 67-WA/PVP-8, 1967.

Hill, R., The Mathematical Theory of Plasticity, Oxford at the Clarendon Press, 1950.

Hodge, P. G., Jr., Limit Analysis of Rotationally Symmetric Plates and Shells, Prentice-Hall, New Jersey, 1963.

Ince, E. L., Ordinary Differential Equations, Dover Publications, Inc., New York, 1926.

Jones, R. E., and D. R. Strome, "Direct Stiffness Method Analysis of Shells of Revolution Utilizing Curved Element," AIAA Journal, Vol. 4, No. 9, (September, 1966), pp. 1519-1525.

Khojesteh-Bakht, Mohmound, and Egor P. Popov, "Analysis of Elastic-Plastic Shells of Revolution," Journal of the Engineering Mechanics Division, ASCE, Vol. 96, No. EM3, (June, 1970), pp. 327-340.

Kraus, Harry, Thin Elastic Shells, John Wiley and Sons, Inc., New York, London, Sydney, Toronto, 1967.

Lin, T. H., Theory of Inelastic Structures, John Wiley and Sons, Inc., New York, London, Sydney, Toronto, 1968.

Marcal, P. V., and C. E. Turner, "Numerical Analysis of the Elastic-Plastic Behavior of Axisymmetrically Loaded Shells of Revolution," Journal of Mechanical Engineering Science, Vol. 5, No. 3, (September, 1963).

McCracken, D. D., A Guide to Fortran Programming, John Wiley and Sons, Inc., New York and London, 1962.

Mendelson, A., Plasticity: Theory and Application, MacMillan Company; Collier-MacMillan Ltd., London, 1968.

Mendelson, A., and S. S. Manson, "Practical Solution of Plastic Deformation Problems in Elastic-Plastic Range," NASA TR-R-28, 1959.

Olszak, W., Z. Mroz, and P. Perzyna, Recent Trends in the Development of the Theory of Plasticity, MacMillan Company, New York, 1963.

Olszak, W., and A. Sawczuk, Inelastic Behavior in Shells, P. Noordhoff Ltd., Groningen, The Netherlands, 1967.

Richard, R. M., "A Study of Structural Systems Having Conservative Nonlinear Elements," Doctoral Dissertation, Purdue University, 1961.

Richard, R. M., and J. E. Goldberg, "Analysis of Nonlinear Structures: Force Method," Journal of the Structural Division, ASCE, Vol. 91, No. ST6, (December, 1965).

Spera, David A., "Analysis of Elastic-Plastic Shells of Revolution Containing Discontinuities," AIAA Journal, Vol. 1, No. 11, (November, 1963).

Thorn, B. J., and S. L. Lee, "Linear Strain Hardening of Cylindrical Shells," Journal of the Engineering Mechanics Division, ASCE, Vol. 90, No. EM4, Proc. Paper 4007, (August, 1964), pp. 97-122.

Timoshenko, S., and S. Woinowsky-Krieger, Theory of Plates and Shells, 2nd Edition, McGraw-Hill Book Company, Inc., New York, Toronto, London, 1959.